Use of joint trace data to evaluate stability of mining excavations, and validation against underground observations

Edgar Nezomba

A dissertation submitted to the Faculty of Engineering and the Built Environment, University of the Witwatersrand, Johannesburg, in fulfilment of the requirements for the degree of Master of Science in Engineering.

Johannesburg, 2012

Declaration

I declare that this dissertation is my own unaided work. It is being submitted for the Degree of Master in Science in Engineering to the University of the Witwatersrand, Johannesburg. It has not been submitted before for any degree or examination to any other University.

....

(Signature of Candidate)

...16th... day of ...APRIL..... (Year) ..2012..

at ...PERTH, WESTERN AUSTRALIA...

Abstract

Mining is a sensitive business that yields high returns and at the same time is associated with high risk of injuries/fatalities and potential losses of revenue. There is increasing intolerance for injuries and fatalities by governments and the other stakeholders involved in the mining business often resulting in mine closures and revenue loss. Chief among the mining risks is the occurrence of rockfalls where people work and access. The rockfalls are bound mainly by joints that intersect the rockmass thereby forming rock blocks that may fall once an excavation has been created.

There are many methods that have been used over time to predict the occurrence of rockfalls. More recently probabilistic methods have gained more ground over deterministic methods. The properties of the joints that are identifiable on exposed excavations are the main inputs used in simulating rockfalls. To date there has been little work that has been done to compare predicted rockfalls to actual rockfalls.

This dissertation presents a practical method for collecting rockfall and joint data in the stope hangiwall at two mines in the Bushveld Complex. The joint data has been used in simulating rockfalls using JBlock (a probabilistic keyblock stability programme). A comparison between simulated rockfalls and mapped rockfalls has been presented. Based on this comparison, a number of iterations were done to calibrate the JBlock results until near realistic rockfalls were achieved.

Three case studies have been conducted to investigate the effectiveness of different stope support systems in reducing rockfall. The potential losses and injury risk associated with the different support systems have been quantified for all the individual rockfalls. In general the rockfall frequency is directly proportional to the risks associated with the rockfalls.

Through this research it has been demonstrated that it is possible to use joint data found on excavation surfaces to statistically predict the occurrence of potential rockfalls in similar ground conditions. The optimum support system that has minimum injury and cost risk can also be selected from a comparison of a number of support systems. Armed with this information, rock engineers can now make strategic decisions versus the existing common tactical approach.

Acknowledgements

I would like to express my gratitude and appreciation to the following people and organisations for their invaluable assistance and support in this research:

Professor T.R. Stacey for his guidance, support and patience. His talent to motivate and inspire also helped me to accomplish this work.

William Joughin for his critique, desire and drive to make this research a success

SRK Consulting for affording me the opportunity to participate in this research and using their resources on this research.

SIMRAC for providing funding for this research

Jonas Machake from CSIR and former SRK colleagues Chistopher Nyoni and Felix Joel, with whom I spent time doing the underground mapping of joints and rockfalls

The two mining companies for allowing the mapping exercise to be done on their mines

Steve Donovan from CSIR for his work on the RiskEval programme

Anthony Jaeger for critical review of the mapping exercise

All other SRK employees who contributed to the success of this work

Table of contents

List of Figures

List of tables

1 Introduction

1.1 Background

For centuries mining has been known for its ability to generate wealth, which makes it an important part of the economies of many countries the world over. In comparison with other industries, mining has had a very poor safety record throughout its history. Some of the worst fatalities have occurred in the coal mining industry as a result of methane gas explosions. For example, the worst ever recorded accident in mining history, in which 1 549 people were killed on April 26 1942, was at the Honkeiko Colliery in China (www.epicdisasters.com). In South Africa the Coalbrook disaster of 21 January 1960 claimed 437 lives when a three square kilometre section of the mine collapsed. Today mining is safer than it was fifty years ago, but it is still a high-risk occupation, as evidenced by frequent news headlines of mining related fatalities.

South Africa is a country endowed with huge reserves of gold and platinum group minerals as well as other mineral commodities. This places the country amongst leading mining countries in the world, creating employment and wealth for economic growth, but at the same time exposing thousands of employees to mining-related hazards. In 2003, stakeholders in the mining industry comprising government, labour and the South African Chamber of Mines, agreed that, by 2013, mine fatality occurrences should be comparable with international benchmarks, as represented by Australia, Canada and the United States. This has placed focus on improving safety related strategies, which will eventually translate into the reduction of mining-related injuries and fatalities.

The South African mining fatality record since 2003, when the action plan to reduce mining accidents was initiated, is shown in Figure 1-1. This shows that there has been a steady decline in the number of fatalities from 270 in 2003 to 128 in 2010. The fatality figures for the year 2010 according to the Chamber of Mines of South Africa are the best in the history of mining in South Africa. In 2003, fatalities per million hours worked were 0.29, and by 2009 this statistic has improved by almost 50% to 0.15 (DME, 2010). Despite the decline in mine fatalities in 2010, the safety record in South African mines is still worse than in Australia, the USA and Canada combined. Australia reported four fatalities in 2007/08, while the US had twenty-three deaths, and Canada recorded eight mining-related fatalities in the same period.

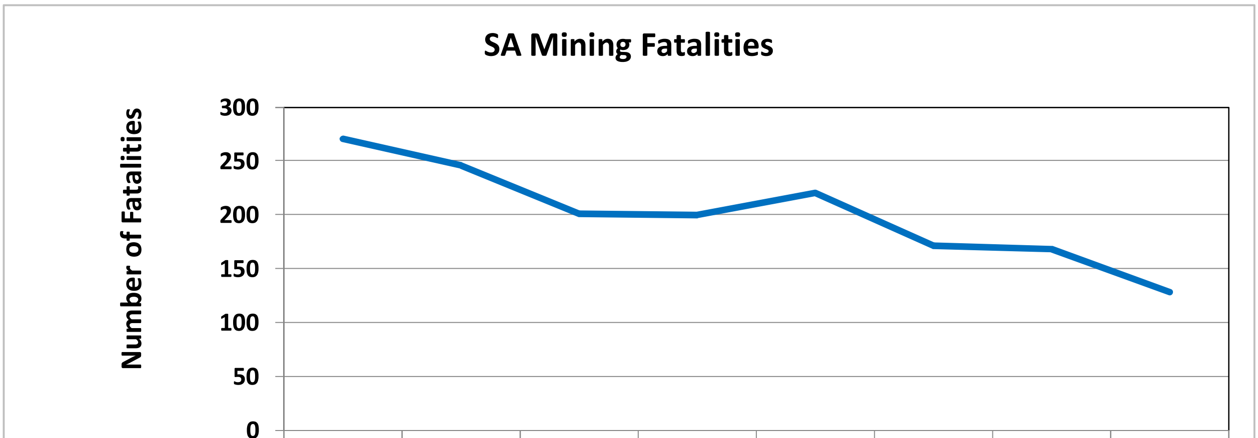

	2003	2004	2005	2006	2007	2008	2009	2010
Industry fatalities	270	246	201	200	220	171	168	128

Figure 1-1: South African Mine Accident Statistics (Chamber of Mines 2011)

In 2011, there was a reversal of these gains, as highlighted by a headline from the Business Report on 12th April 2011, "Rising SA mine deaths need urgent attention." This headline was in response to fatality statistics released by the Department of Mineral Resources for the period January 1 to March 31, 2011, by which time 38 fatalities had been recorded in the mines, in comparison with 30 for the same period in 2010. This indicates that, although there has been a marked improvement in mining-related safety statistics in recent years, more work still needs to be done in order to reduce the injury and fatality numbers.

The mine accident and fatality statistics can be grouped into different categories according to the causative agent. Chief amongst the causes is rockfall accidents, which have generally constituted the highest contributor to accidents throughout this period. An example is the period between January and December 2008 where gold and platinum mines accounted for 94% of rockfall fatalities. This observation is similar to the findings made by Adu-Acheampong (2003) when analysing mining related fatalities. In excess of 50% of all rockfall fatalities are gravity driven whilst the remainder can be attributed to seismicity.

Apart from the injuries and fatalities associated with the rockfalls, there is also financial loss associated with rockfalls (Rwodzi, 2011; Joughin, 2010). Reducing the number of rockfalls can be expected to result in improved productivity on mines by boosting morale of employees, and by reducing losses associated with each rockfall. There are many methods being used to predict and develop strategies to reduce rockfall-related incidents. The main goal of this research is to refine one of these methods to better understand, predict and reduce rockfall occurrences on mines.

1.2 Definition of the problem

South Africa is the world's largest platinum producer and hosts the world's largest platinum reserves, in the Bushveld Complex. Due to the nature of the geometry of the platinum reefs of the Bushveld Complex, the conventional underground narrow reef mining method is the main method utilised to exploit the mineral. This mining method (Figure 1-2) involves opening up about a meter of a shallow dipping reef using jackhammer drilling, and blasting, to extract ore. The hangingwall is often supported by mine poles, rockbolts, grout packs and pillars. This mining method has man access stopes and is highly labour intensive thereby exposing many people to many hazards, chief among them being blocks of rocks falling from the roof of the stope.

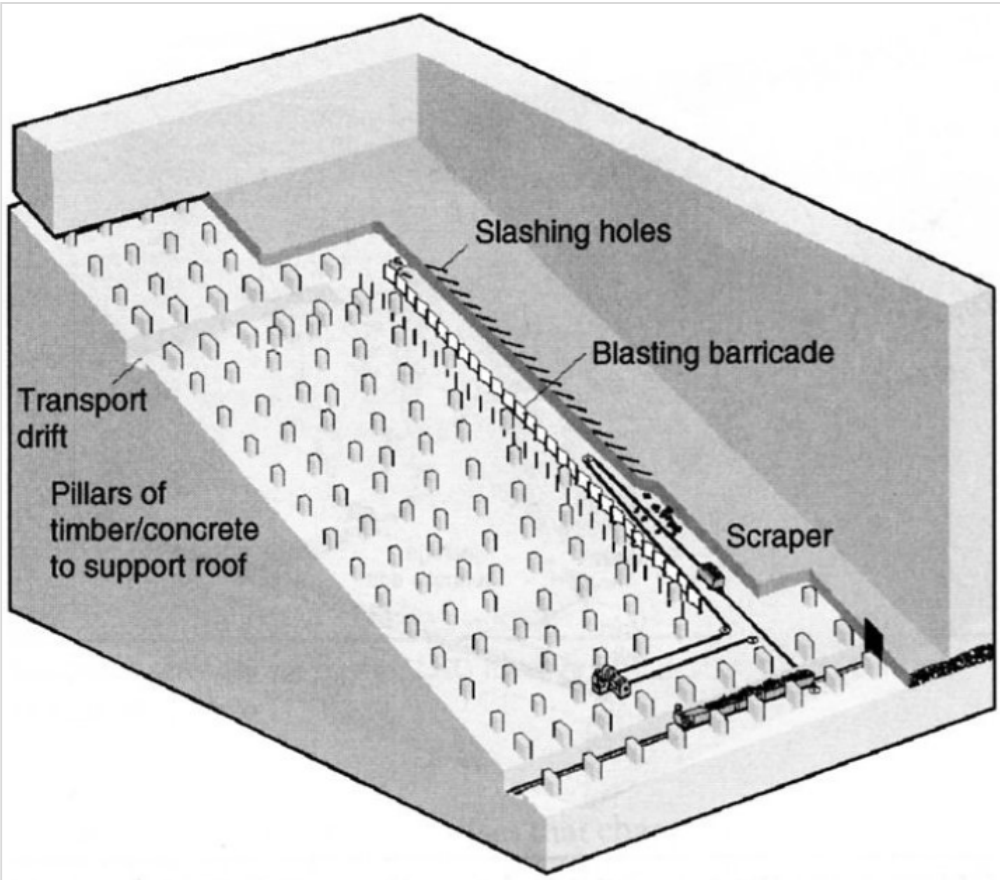

Figure 1-2: Conventional mining method used on platinum mines in South Africa (after Hustrulid, 1982)

There are many geological structures that transect the rockmass in the Bushveld Complex, including faults, dykes, potholes, domes and joints. These structures often intersect each other and the excavations created in rock, leading to the formation of rock blocks that have the potential to fall into the excavations once they are exposed. The intensity of jointing in rock is much higher than any of the other structures, and therefore, with regard to excavation stability, a lot of attention needs to be directed at joints. Joints can be identified on exposed rock surfaces as traces or lines on which no visible shear movement can be observed. At an average producing mine in this locality, hundreds, if not thousands of joints, are exposed daily where people work. Sadly, not enough is being done in terms of acquiring and using jointing information on mines in order to quantify injury and cost risk associated with rockfalls. Current support design in the mining stopes of the Bushveld Complex platinum mines is based on deterministic semi-empirical methods, in which joint properties are used implicitly (Stacey, 2007). Keyblock stability methods are not included in the complement of design tools used when choosing the optimum support systems to be used on the mine. The selection of a support system is based on recorded fallout heights, historical support used, and trial and error. There is a lack of a conscious design approach with quantifiable comparisons of different support systems. In the isolated cases where keyblock stability methods are used (Gumede, 2006), they have never been validated against actual rockfalls recorded underground. This made the approach more of a rockfall comparison tool than a predictive tool. An improved statistical rockfall prediction method will lead to improved confidence in applying such tools to design. If such a tool can be used, it would be able to demonstrate that rockfall-related fatalities and production losses can be forecasted, controlled and managed in future mining, with a certain degree of confidence.

1.3 Objectives

The objectives of this research are as follows:

- To collect data associated with rockfalls such as volume, location, orientation, and shear strength properties of weakness planes bounding rockfalls;
- To collect rock joint properties from joint traces on the jointed hangingwall of an underground stope so that statistics for these properties can be defined;
- To use rock joint statistical data in generating potential keyblocks, and simulating rockfalls, using a statistical keyblock stability method;
- To compare rockfalls observed from underground mapping with the predicted rockfalls, and hence to calibrate the statistical keyblock stability method;
- To analyse case studies, comparing the effectiveness of different support systems in reducing rockfall frequency;
- To quantify the injury and rockfall risk associated with each support system in the case studies.

1.4 Research methodology

In achieving the objectives outlined above, the following methodology was adopted:

- Conduct a review of literature related to joints and their importance when creating excavation.
- Carry out underground mapping of rockfalls and joints at a platinum mine. The Merensky and UG2 reefs were covered during this process.
- Correlate actual mapped rockfalls with predicted rockfalls from the statistical keyblock analyses for these two reefs
- Carry out joint mapping at an additional platinum mine to widen the use of the statistical keyblock stability method.
- Analyse case studies on two mines, based on actual support strategies and variations thereof, to demonstrate a reduction in the number of rockfalls with improved support of the stope hangingwalls.

Joint and rockfall mapping was carried out at two underground platinum mines to achieve these objectives. Stopes on the Merensky reef and the UG2 reef were mapped. An analysis of the joint and rockfall data then followed. Using the joint data, rockfalls were simulated using a statistical keyblock analysis package and the results were correlated and validated against recorded rockfalls. Starting off with the current support system used in each of the mapped areas, different but practical support improvements were made for comparative purposes.

1.5 Content of the dissertation

The next chapter presents a background description of joints, their properties and different methods currently being used when collecting joint information in the field. The underground mapping of joints and rockfalls will be described in Chapter 3. In the same chapter, the mapping results for both exercises will be presented and analysed. A review of design methods in blocky ground and, in particular keyblock stability methods, will be presented in Chapter 4. The potential for the occurrence of rockfalls, based on the collected joint information and the correlation between the simulated rockfalls and the mapped rockfalls, is evaluated in the same chapter. Case studies for different support scenarios in the mapped areas are presented in Chapter 5. Chapter 6 provides a discussion of the conclusions and recommendations arising from this research.

2 Review of joint properties and mapping methods

This chapter provides a review of literature relating to joints, how they are formed, their properties and the various methods that can be used to obtain joint data in the field. Joint networks and how they can be used to evaluate the stability of excavations are also discussed in this chapter.

2.1 Introduction

In nature, a rock mass is almost never a single block of uniform solid rock. Instead, it usually contains many structural weakness planes such as joints, bedding planes, veins faults, dykes, and shear zones which transect it. Joints are by far the most common and generally the most prominent geotechnical structural features in rocks. The presence of joints in rock masses makes the design of excavations, and the support systems necessary to inhibit loose rock wedges/blocks from falling into the excavation, challenging. Generally, as the number of sets of joints exceeds two, the design of an excavation and the support becomes complex. Loose rock wedges can also be formed by vein networks as observed by Brzovic and Villaescusa, (2007) at El Teniente mine, although this is not very common.

In jointed hard rock excavations at relatively shallow depths i.e. upper 300m, and in low stress environments, the most common types of failures observed in jointed rock masses involve wedges/blocks falling from the roof or sliding from the sidewalls of the openings (Piteau, 1970; Steffen et al, 1975). These wedges/blocks are formed by the intersection of the excavation surface and joints which separate the rock mass into discrete interlocked pieces. Once a free surface occurs by the creation of the excavation, the restraint from the surrounding rock is removed and these blocks are free to move into the excavation if the frictional forces resisting this movement are less than the weight of the wedge. The wedge formed with its surface exposed in the excavation, and the first to fall out from the walls or hangingwall, is called a keblock. What exacerbates the problem of keyblocks is that they may fall after little or no observable movement has occurred to warn people working in its vicinity. This poses a hazard for men working or travelling in the excavation. Further, if there are no measures put in place to stabilise the excavation and stop the movement of such wedges, the failure of these surface keyblocks may give rise to the failure of subsequent blocks. The success of supporting a jointed excavation hinges on the ability to support all keyblocks exposed in the excavation.

2.2 Joint Definition

A joint can be described as a naturally occurring fracture on which there is a rock to rock contact, and which causes the rockmass to be discontinuous and have a much lower(or zero) tensile strength than the intact rock ISRM (1978). On the other hand ISRM defines a discontinuity as being almost similar to a joint, but differentiated by the existence of a filling material in between the joint surfaces. The term joint has been adopted in this research to mean a natural fracture which renders a rock mass discontinuous, and which may contain infill material or not. A group of parallel or sub-parallel joints is called a joint set, and joint sets intersect to form a joint system.

2.3 Mechanism of Joint Formation

Joints are believed to develop at practically all ages in the history of rock formation. For this reason Price (1966) suggested that the formation of joints is highly unlikely to be due to a single mechanism. Several studies (Leith, 1923; Price, 1966; Hobbs et al, 1976; Suppe, 1985, Ivanova, 1998; Dershowitz, 1984) on the mechanisms that contribute towards joint formation individually, or as combinations of mechanisms, have suggested that joints are formed as a result of the cooling of rock, folding, contraction of sediments, earthquakes, compression and tensile stresses due to regional compression. These mechanisms result in the development of stresses that can be tensile, compressive, and shear and are often associated with faulting and folding. Joints are formed when these stresses exceed the strength of the rock and the rockmass fails along weakness planes. These joints vary in appearance, dimensions and occurrence in differing lithologies as a result of different responses to the stresses controlled by varying rock strengths across the lithologies. Other factors that influence joint formation include rock type, mineralogy, grain size and temperature.

As a result of the joints resulting from stresses acting on the rock mass, they generally form in a near parallel fashion, resulting in a joint set. Over time, stresses from more than one direction often act on a rock mass, and a number of joint sets may therefore be present (see Fig. 2). These joint sets are often different in age and the associated stress field may also differ suggesting different geological periods. The manner in which the rockmass reacts to new external forces is greatly affected by the orientation of these joint sets, because the rockmass will most likely separate at its weakest point, i.e. on the joint planes rather than in intact rock.

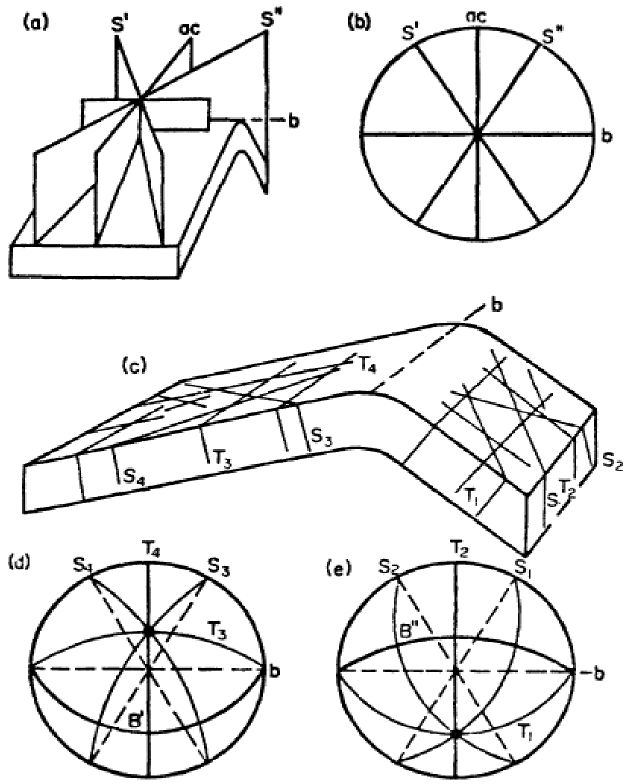

Figure 2-1: Tensional joints accompanying folding (after Price,1966).

Based on the history of their formation, structural features in rockmasses have been classified into two major types (Ivanova, 1998):

1. Tensile features (joints) which open in planes parallel to the maximum and intermediate principal stresses, σ_1 and σ_2, and orthogonal to the minimum principal stress, σ_3; and
2. Shear features (faults), which form in the plane of σ_2, and make an angle of less than 45^o with the direction of σ_1.

The distinction between joints and faults is based on their visibility, with faults being of a larger scale and more visible than joints. Due to shearing on fault formation there is also markedly a visible relative movement on fault walls. In contrast, joints are simply breaks in the continuity of a rock mass with no relative movement between the surfaces of the joint. Under normal circumstances in rock mass, the density of joints is far higher than that of faults.

2.4 Theory of Joint Data collection

In order to understand the behaviour of rock joints in a rock mass, it is vital to have a comprehensive description of the individual characteristics of the joints and their effects on stability. According to Priest and Samaniego (1983), the important properties in describing rock joints are:

- Orientation
- Spacing
- Length
- Shear strength

These properties are normally grouped for each joint set. In addition to these properties, joint shape and size is also important for a three dimensional description of joints. However, most joint measurements are done either in one dimension (oriented borehole cores) or two dimensions (outcrops) and hence these two properties are not measured in most joint surveys. Although joint properties are assumed to be the same for each set in many analyses, it has to be appreciated that each joint in reality has its own unique characteristics. The variability in jointing is approximated by statistically describing joint characteristics (Clark, 1979).

2.4.1 Joint Properties

The performance of the immediate rock surfaces of excavations created in jointed rock masses is highly influenced by the geometric characteristics of joints i.e., orientation, length and spacing, and the shear strengths of the joints and the intact rock. These properties are of important considerations when carrying out a stability analysis of a jointed rock mass. It is therefore important to understand them in order to make accurate predictions of rock mass behaviour.

The present methods of joint data collection include information from orientated drill cores and from exposed rock surfaces such as rock outcrops and tunnel walls. Table 2-1 below lists joint properties and the corresponding source of information for that particular property. These data can be one dimensional or at best two dimensional. However, since joints are three dimensional in nature, Steffen et. al (1975) suggested the use of three mutually perpendicular directions when collecting joint data on exposed surfaces. In this research, joint data was obtained by the careful mapping of underground hangingwall exposures. Attempts were made, where possible, to obtain joint data in the third dimension.

Table 2-1: Joint Property and Source

Joint Property	Source
Orientation	Oriented borehole cores, outcrops and excavation walls
Spacing	Oriented borehole cores, excavation walls, outcrops
Length	Excavation walls and outcrops
Shear Strength Properties	Excavation walls and borehole cores

Joint Orientation

Orientation or attitude of a joint in space is described by the dip of the line of maximum declination on the discontinuity surface, measured from the horizontal, and the dip direction of this line, measured clockwise from the true north (Figure 2-2). It is usual to quote orientation data in the form of dip (two digits)/dip direction (three digits) for example 46º/009º and 70º/320º. Joint dip and dip direction can usually be measured using compasses.

Orientation data can be represented on stereographic projections (Shi and Goodman, 1981, 1985; Priest, 1985). It has been noted by Priest and Samaniego (1983) that in many cases joints generally have a planar geometry and are oriented in sub-parallel groups or sets. Joint sets are identified from joint orientation information and stereographic projection software is commonly used for this purpose.

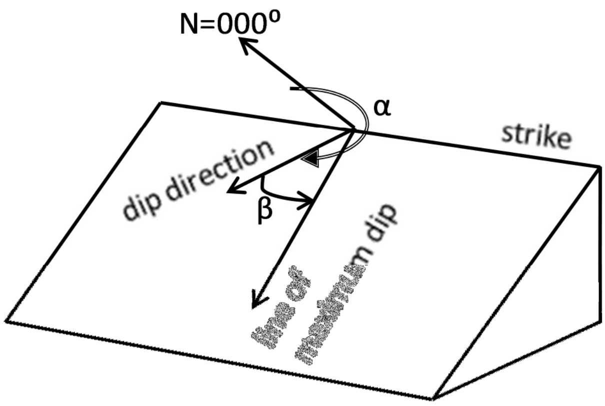

Figure 2-2: Definition of dip (β) and dip direction (α)

The shapes of blocks are determined by the mutual orientation of the joint sets. Further to this, the relative orientation of the proposed excavation to the joint sets will control the possibility of unstable conditions. The importance of joint orientation increases when the other conditions for instability are present, such as low joint shear strength, and a sufficient number of joint sets to delineate a failure mode. Orientation has been observed to follow a normal distribution (Stacey and Bartlett, 1990; Gumede, 2006; Grady, 1983). However, other researchers (Priest, 1985; 1993; Brown, 2007; Thompson, 2002) have found the Fisher distribution (Fisher, 1953) to represent the orientation distribution better. Correction for sampling bias to joint orientations has been done (Kulatilake and Wu, 1984 a) and shown to be dependent on joint shape and size. However, joint shape and size are difficult properties to measure in 2 dimensions making the correction exercise difficult.

Joint Spacing

Joint spacing is the perpendicular distance between two adjacent joints of the same set, and is often expressed as a mean spacing for a particular joint set. The spacing of joints determines the sizes of the blocks making up the rock mass. This parameter can be measured on rock exposures both on surface or underground and it can also be estimated from orientated drill cores. It should be noted though that spacing cannot be measured directly from cores when the borehole is sub-parallel to the joint surface. When measuring spacing on rock exposures, it is recommended to have a scanline length of not less than 3m and greater than ten times the estimated spacing for reliable results (ISRM, 1978). Joint spacing has been found to follow either an exponential distribution or a lognormal distribution (Hudson and Priest, 1979; Priest and Samaniego, 1983; Steffen et al, 1975; Grady, 1983; Gumede, 2006; Baecher et al, 1977; McCullagh and Lang; 1984; Pahl, 1981; Warburton, 1980).

An error in spacing calculation is often brought about by the sampling line cutting across the joint set at an angle less than 90° resulting in the overestimation of joint spacing (Terzaghi, 1965). This error is illustrated in Figure 2-3 and can be corrected as follows:

$$\mathrm{d} = \ell \sin \theta$$

Where: ℓ is the distance between successive joints of the same set

d is the true spacing distance

θ is the angle between the scanline and the mean orientation of the joint set.

In order to obtain accurately the angle (θ) between the joint and the scanline, the orientation of the scanline also needs to be known. Different scanline orientations at the same site can be used to obtain spacing information. This will reduce the error imposed by the relative angle between the scanline and the average orientation of the joint set.

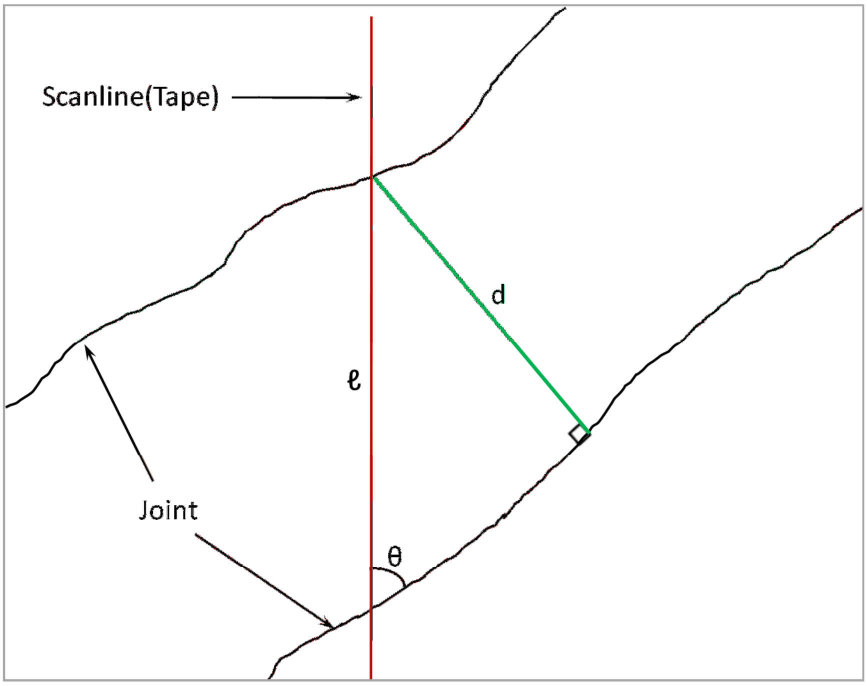

Figure 2-3: Joint spacing error correction

Length

Joint traces are lines formed by the intersections of joints with excavations in rock. The individual lengths of these traces indicate the extents of the joint within the rock mass, denoted by the straight line distance between end points of the joint. Joint length measurements can be made on natural outcrops, underground surfaces and open cut excavation walls. Persistence is an equivalent term to joint length when describing joints in three dimensions. However, frequently rock exposures are small compared with the area or length of continuous joints and persistence can only be guessed. Joint trace lengths have been found to follow lognormal or negative exponential distributions (Baecher et al, 1977; Bridges, 1976; Zhang, 2004).

Joint length measurements are often biased and difficult to determine accurately. The main reason for this bias is that joints may extend beyond the boundaries of the exposure, or that small joints are ignored. These errors are discussed in section 2.4.3. The orientation and position of the joint exposure in space can also affect the joint length because of differing points of cutting the joint plane. Kulatilake and Wu (1984b) suggested a method for correcting this bias.

Joint shear strength

In addition to joint geometry when analyzing rock block failures linked to joints, joint shear strength is also a very important property. This property is a measure of the resistance to sliding of a block on a surface. The nature of the joint walls and infill material between the walls on a joint will influence the shearing behavior. A number of models have been developed for determining the shear strength of joint surfaces. These models are among others, the Coulomb model (1776), the bilinear shear strength model (Roberds and Einstein, 1978), the Barton-Bandis model (Barton, 1973; 1976; Barton et. al, 1985; Bandis et.al, 1983), the Barton model (2002), and the Landanyi and Archambault (1969) model. The widely used models are described below:

Coulomb model

The simplest shear strength model of discontinuities is the Coulomb failure criterion. Coulomb (1776) suggested that the shear strength of a surface is made up of two components, a constant cohesion and a normal stress-dependent frictional component. This model can be represented by the following equation:

$$\tau = c_j + \sigma_n \tan \varphi_j \qquad (3)$$

Where $\tau =$ joint shear strength

c_j =joint cohesion

σ_n =effective normal stress

φ_j =internal friction angle of the joint

The weakness of this model is that it predicts a linear relationship between joint shear strength and normal stress. This assumption leads to an overestimation of the shear strength at high normal stress.

Bilinear shear strength model

In reality the shear-normal stress relationship of joints is non-linear. Patton (1966) addressed the weakness of the Coulomb model by formulating a bilinear model as shown in Figure 2-4. The shear strength of a joint at low normal stresses is given by:

$$\tau = \sigma_n \tan(\varphi_b + i)$$

Where $\tau =$ Peak shear strength

σ_n =Effective normal stress

$\varphi_b =$ Basic friction angle for a apparently smooth surface

i =Effective roughness angle of a saw tooth face

The main weakness of this model is that it is only valid at low normal stresses. At higher normal stresses, the strength of the intact material will be exceeded and the teeth will tend to break off and there is a transition from sliding along the joint to fracturing through the intact material. This then results in shear strength behaviour that is more closely related to the intact material strength than to the frictional characteristics of the surfaces as represented by the change in gradient in the second line in Figure 2-4. As a result Jaeger (1971) proposed another shear strength model to provide a curved transition between the straight lines of the Patton model.

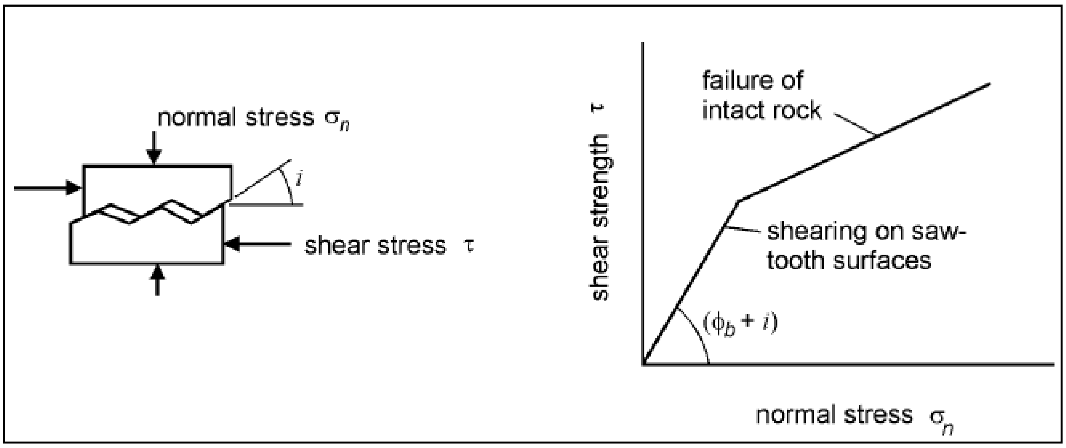

Figure 2-4: Patton's experiment on the shear strength of saw-tooth joints (Patton 1966).

<u>Barton-Bandis model</u>

This model is an improvement on Patton's approach by Barton (1973, 1976). In this case changes in shear strength with increasing normal stress are gradual rather than abrupt. Barton studied the behaviour of natural rock joints and proposed that Patton's equation could be re-written. In the Barton-Bandis model, simple measurements of joints were developed to have a practical way of evaluating the shear strength of joints (Barton, 1976; Barton and Choubey, 1977; Barton and Bandis, 1990). The joint shear strength for the Barton-Bandis model can be represented by the following equation:

$$\tau = \sigma_n \tan[\varphi_b + JRClog_{10}(\frac{JCS}{\sigma_n})]$$

Where τ = joint shear strength

σ_n = effective normal stress

φ_b = basic friction angle

JRC = Joint Roughness Coefficient in the range 0 (smooth) to 20 (rough)

JCS = Joint Wall Compressive Strength

The weakness of this model is that its focus is on expressing joint behaviour at peak shear strength. This therefore means that it cannot be relied upon when describing the pre-yield and post-yield behaviour of rock joints.

<u>Barton model</u>

Barton (2002) provided a simple method of determining friction angles as follows:

$$\varphi = \tan^{-1}\frac{J_r}{J_a}$$

where: φ is the joint friction angle

J_r is Joint roughness condition (J_r = smooth for sepentinized joints and rough undulating for calcite filled joints and joints with no fill)

J_a is the joint alteration number (J_a= unaltered for joints with no infill, non-softening sandy particles for calcite fill and clay mineral fillings of varying thicknesses for serpentinised joints)

This model has an underlying assumption that the joints are cohesionless. This is normally the case with sheared joints. This model provides an easy, cheap and intelligent field estimate of joint shear strength properties.

Other important joint properties are thickness of filled joints, type of infill and water conditions. These properties contribute towards the joint shear strength. It should be noted here that joint set properties contributing toward the shear strength cannot be described by distributions and therefore mean values will be used.

2.4.2 Joint Mapping Techniques

Since joints have a significant influence on the engineering properties of rock masses, it is vital to have adequately accurate descriptions of the properties of such joints. This can be achieved by mapping joints where they are exposed. Joint mapping is an integral component of site characterization studies in rock engineering as observed by several authors (for example, Baecher, 1983; Call and Nicholas, 1978; Adu-Acheampong 2003). The motivation for this exercise is the need to take the distributive character of joint properties into account and obtain a representative statistical distribution for each property. In mapping rock exposures, four main techniques are used. These are spot mapping, scanline mapping, area or window mapping, and photogrammetric mapping (Read and

Stacey, 2009; Priest and Hudson 1981; Windsor and Thompson 1997; Ulusay and Hudson, 2007).

Spot mapping

This is where the observer selectively samples only those discontinuities that are considered to be important (Brown, 2007). This method has an inherent weakness in that it ignores the influence of the other, unselected joints on excavation stability. The apparently non-important or random joints are known to have to have a significant influence on rock block formation.

Area or Window mapping

This technique involves selecting an exposed area of the rock face and mapping all joints within this selected area, as shown in Figure 2-5 (Brady and Brown, 2004; Read and Stacey, 2009; Pahl, 1981). The portions of the joint traces that are within the window are measured, while the portions of traces intersecting such a window, but lying outside, are ignored. This method has an advantage over spot and scanline mapping in that it reduces sampling biases for orientation and size. However, it suffers practical difficulty in application to underground operations because of limited areas of exposure. It also suffers from censoring bias for joint lengths, whereby the lengths proceeding beyond the area window are ignored.

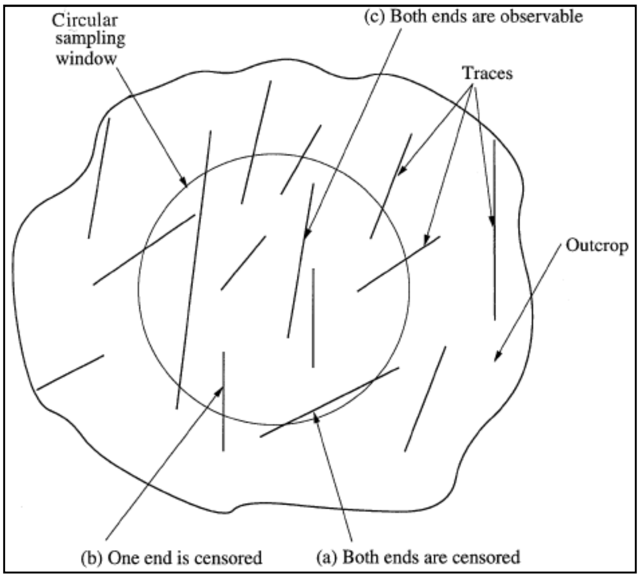

Figure 2-5: Area mapping (after Zhang and Einstein, 1998).

Photogrammetric mapping

More recently photogrammetric mapping, which makes use of high resolution cameras in mapping of joints, as shown in Figure 2-6, is being used in joint mapping. There are three steps involved in mapping joints using this method as listed below (Birch, 2006; Gaich et al, 2006):

- Using high resolution digital cameras to collect images of rock face
- Producing an oriented point cloud, and a digital 3D surface called a Digital Terrain Model (DTM) which is made of spatial data points of the face
- Analysis of the DTM to characterise the rock mass (e.g. take joint dip direction, dip, spacing measurements etc). This can be seen on the right side of Figure 2-6.

A drawback of photogrammetric mapping over traditional mapping is that hardware and software are relatively expensive. However, photogrammetric face mapping techniques far outweigh traditional methods of field data capturing (Tonon and Kettensette, 2006; Poropat, 2006). The advantages of photogrammetric face mapping techniques over traditional methods are (Tonon and Kettensette, 2006):

- The ability to analyze large areas of rock masses, including inaccessible areas, by capturing images from distances of up to 3km. Limited size and access to rock exposures for mapping had been cited by Villaescusa (1993) as a hindrance to describing joint set characteristics.

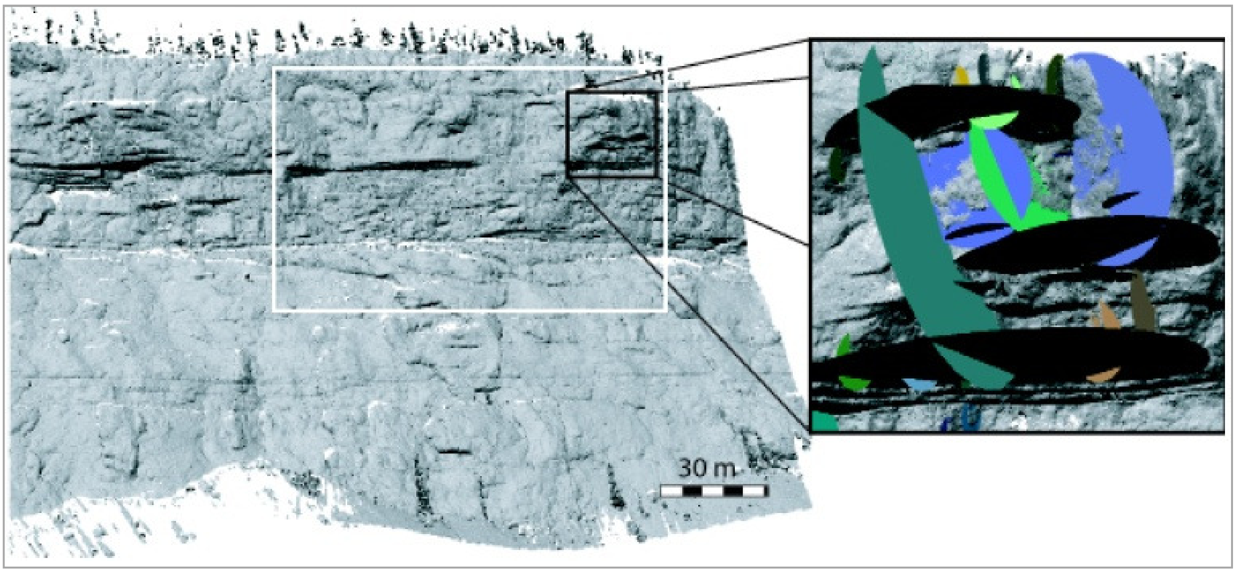

Figure 2-6: Photogrammetric mapping (from Sturzenegger and Stead, 2009)

- Large data sets can be collected resulting in a more realistic picture of fracture orientations. Joint sets that may have been missed by manual mapping are often discovered using this approach.

- Zooming in and out of the face improves the identification of structural features, such as major shears or fractures, which are otherwise not apparent when working close to the rock face.
- Despite these methods acquiring large numbers of data points, they are typically five times faster than manual data collection.
- There is permanent documentation of the rock face condition for reporting and contractual or legal issues. Data can still be processed even after the face has been shotcreted.
- Reliable three dimensional characterization of the rockmass can be done if each stage of the excavation is documented, and information on fracture persistence and fracture clustering is obtained.
- It is relatively easy of use i.e. there is no need for a photogrammetry expert, as was the case with traditional photogrammetry. This expert is now substituted for by the software adjustment capability.

Scanline mapping

This method involves setting up a line on the surface of a rockmass and mapping all joints intersecting that line as shown in Figure 2-7 (Priest and Hudson, 1976; 1981; Baecher, 1983; Steffen et al, 1975, Haines and Marker, 1992; Zhang, 2004; Goodman, 1995; Brzovic and Villaescusa, 2007). Brady and Brown (2004) suggested the use of a measuring tape pinned to the rock face with masonry nails, and chalk lines drawn on the face, as a scanline. The tape needs to be taut at all times in order to produce reliable joint spacings. To reduce orientation bias, a three dimensional view of the joint data is needed. This is achieved by using two orthorgonal scanlines (one on dip and the other on strike) in the stope hangingwall and a borehole drilled into the hangingwall. This mapping technique has been recommended when using probabilistic methods for key block analysis (Kemeny and Post, 2003). An orientated drill core is an indirect scan-line that can be used to measure orientations and joint spacings only in unexposed rock masses. Scanline mapping of outcrops and surface exposures offers the extra opportunity of measuring joint length which cannot be done on oriented drill cores. Circular scanlines are also used for joint mapping and offer an advantage of eliminating directional bias. Scanline mapping is by far the most common mapping technique in use because of its relative ease to use.

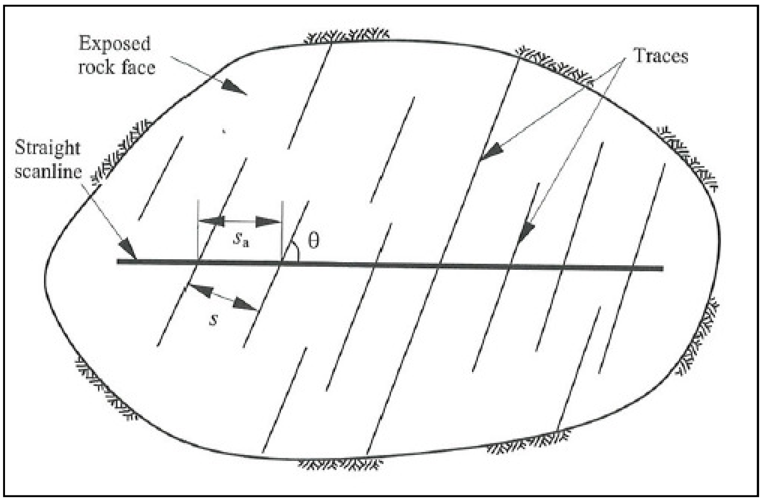

Figure 2-7: Straight scanline mapping (Zhang, 2004).

From field mapping experience, Priest (1993) suggested that 150-350 joint observations need to be made using scanline mapping techniques. The lower number and higher number are ideal for a rockmass containing three and six joint sets respectively. On the other hand, Robertson (1970) suggested that 100 observations be made per joint set in order to reduce the effect of potential errors. Savely (1972) observed that 60 joint recordings are required in order to define a set along a given sample line. According to Villaescusa (1993), at least 40 joints observations are required per set to provide a representative database of the joint set. However, Call et al (1976) have also suggested that the number of observations required be dependent on the fracture intensity and the number of sets. The scanline mapping technique is the one that was chosen and utilised in this particular research because it is comprehensive, cheap and will provide the data required for a probabilistic keyblock stability analysis. One drawback observed regarding this method is that it provides unreliable information when the mean orientation of a joint set is less than 20° from the sampling line (Baecher et al, 1977).

2.4.3 Joint Mapping Errors

The quality of the input joint information will determine the quality of the output from the probabilistic keyblock stability analysis. It is important to highlight the potential sources of errors associated with carrying out joint surveys using the scanline method. The potential sources of error in joint mapping, apart from human bias and instrumentation error, are joint size or length, orientation, censoring and truncation (Baecher and Lanney, 1978; Baecher, 1983; Einstein and Baecher, 1983; Priest and Hudson, 1981; Kulatilake and Wu, 1984a; Kulatilake and Wu, 1984b; Mauldon and Mauldon, 1997). These errors are discussed in detail below;

Joint Size

Joint size or length bias leads to non-equal sampling probabilities among traces of varying lengths in two ways:

(a) a larger discontinuity is more likely to appear in an outcrop than a smaller one; and

(b) a longer trace is more likely to appear in a sampling area than a shorter one.

Censoring

Joint censoring bias takes place when traces observed on a joint exposure run off into the rock walls and cannot be observed in their fullness. This gives a false trace length of the joint in that it reduces the effective joint trace length.

Truncation

This bias takes place when trace lengths below a cut off length are ignored in data collection. This has an effect of increasing the sample mean of the joint trace lengths. Joint spacing values are also overestimated in this case as some of the joints in the same set are omitted.

Orientation

Orientation bias is where joints sub-parallel to the rock face less chance of intersecting the rock face than joints perpendicular to the rock face (Terzaghi, 1965; Stacey and Bartlett, 1990). This usually arises from outcrops that may form along joint surfaces, resulting in a strong possibility of an entire set of joints being underestimated in the mapping results. This error can be reduced significantly by using three mutually orthogonal scanlines in the same area. An effort has been made in this research to reduce the orientation bias by using scanlines that have more than one orientation.

2.5 Joint Networks and Joint Traces

When large rock surface areas are exposed daily at an average producing mine, a large number of joints are exposed. The numbers of joints depend on the geological complexity of each site. However, due to the many joints that are exposed daily, it is impractical to map each joint and carry out a stability analysis to identify potential rockfalls. In order to enhance the joint mapping data, a suggestion was made (SRK Internal Report, 1986) to use geostatistical methods where insufficient structural data have been collected in the field. Grady (1983) conducted a geostatistical analysis on joint data obtained from the Natal Group sediments One of the main findings from the analysis was that data samples less than 300 produce poor geostatistical estimations. These weaknesses motivate for reproducing joint network models to represent the joint network using the joint properties to be described in (section 2.4.1).

Modelled joint networks have been used widely in analysing fluid flow and to predict stability of rock excavations (Dershowitz, 1984; Dershowitz and Einstein, 1988; Ivanova, 1995; Kulatilake and Wathugala, 1990; Hadjigeorgiou et al. 1998; Starzec and Andersson, 2002). The ability to properly develop a reliable joint network depends on the quality and quantity of data that describes the rock mass in the area of interest. If the exact position of each discontinuity, its geometry and strength characteristics are known in advance, then it is relatively easy to reproduce a joint network. Unfortunately these data are not available until the excavation has been made.

Several stochastic joint models have been found to be most appropriate to describe joint networks (Baecher and Lanney, 1978; Veneziano 1978, Villaescusa, 1993, Dershowitz, 1984; Dershowitz and Einstein, 1988; Ivanova 1995; Kulatilake, 1993). These models include the Orthogonal model, Baecher model, Veneziano model, Parent-Daughter model, Mosaic Block Tessellation model and the Ivanova model. Based on each of these or a hybrid of the joint models, several software packages have been developed to model rock jointing. Among these software is Fracman (Dershowitz et. al, 1998), FRACNTWK (Kulatilake, 1988), RESOBLOK (Merrien-Soukatchoff et. al, 2011), 3FLO (Billaux et. al., 2006), JointStats (Brown, 2007), and SIMBLOC (Hamdi and du Mouza 2004). In simulating joint networks, joints are assumed to be planar. This assumption is an oversimplification of joints in reality as they are not planar in all cases. When simulating joint networks in complicated geology, the rock unit is divided into structural domains having statistical homogeneity (Miller, 1983; Mahtab and Yegulap, 1984; Kulatilake, 1988; Kulatilake and Wathugala, 1990). Statistically homogeneous regions are determined by considering, rock type, number of joint sets and their orientation distributions.

Joint system models can either be 3D or 2D. However, 3D joint simulations have a weakness in that joint intensity and shape parameters are used, and these parameters are difficult to determine, since joints can rarely be viewed in three dimensions. In order for the best rock joint models to be developed, it is critical to have a system that can penetrate the rock and give a three dimensional view of the joints.

2.5.1 Joint traces and evaluation of excavation stability

The intersection of joints and planar excavations results in a 2D imprint of the joints being observed. These imprints of the joints on the excavation walls are called joint traces and can provide joint properties described in section 2.4.1. All required inputs in modelling joint networks in 2D can be obtained on joint surface exposures or in 1D from oriented borehole cores. Although joint systems are three dimensional in nature, it was observed on a number of different exposed rock surfaces that two dimensional versions of joint systems models are also valuable as they provide a representation that is easier to visualise, analyse, interpret and compare with reality (Dershowitz, 1995; Kulatilake and Wathugala, 1990).

Joint trace methods to examine expected joint patterns have been developed (Priest and Samaniego, 1983; Haines, 1984). Of note are the joint traces generated by Haines (1984) where joint property data was collected by scanline mapping and grouped according to structural regions. The method involved using Monte Carlo Sampling to generate joint traces in 2D for each individual rock type or structural region. A comparison between simulated joint traces and known field distributions illustrated that the theoretical and actual data were in reasonable agreement. However, this conclusion was based on a small database of sites surveyed, and improvements to the system can be made with an improved database.

Joint traces simplify the identification of various joint set combinations which have potential to form unstable blocks with respect to the free faces. This approach has been applied in the overall assessment of potential instability of keyblocks within a tunnel by examining structural patterns in three orthogonal directions (Haines, 1984; Goodman and Shi, 1989; Gumede, 2006; Thompson and Windsor, 1997; Stacey et al, 2005). In these cases, tunnels were viewed in plan, cross-section and longitudinal sections. By examining the intersection of the tunnel geometry in each of the views, potentially unstable rock blocks which are kinematically feasible to move are identified. The blocks identified in each of the views are totally unrelated. Dimensions of block apex height, length and area are then measured from scaled joint trace plots. This procedure is repeated a sufficient number of times to produce a statistical distribution of potentially unstable blocks. This approach has application to all types of excavations.

2.5.2 Step Path Failure

Slope instability of open pit mines cut in discontinuous rock masses is primarily controlled by geological structures such as joints, because displacements often occur along surfaces of these structures. However, it is comparatively rare to have a single sliding surface along a joint as in planar failure because joints usually lack the continuous length for failure. It is much more likely that a complex failure path (Stacey, 2007; Miller, 1983; Call and Nicholas 1978; Miller 1982; Baczynski 2000, and Baczynski, 2008) will result from combinations of several joints. This path is often referred to as a step path and it provides the continuous path needed for sliding. The step path normally traverses though both the joints and intact rock between the joints, often referred to as ‘rock bridges’ Figure 2-8. Rock bridges have been shown to provide sufficient resistance when they cover less than 10% of the rock area in hard rock slopes greater than 300m in height (Martin, 1978). Fairly recently, Diederichs (2003) proposed that even on a small very small percentage of the joint co-planar area, intact rock bridges may provide internal self-supporting load carrying capacity equivalent to artificial slope reinforcement systems (i.e. bolts or cables). However, time dependent reduction of cohesion can weaken the rock bridge and facilitate slope failure. The probability of failure of a slope modelled by Kemeny (2003) was found to increase from an initial value of 5% to 40% after one hundred years, due to the contribution of time dependent reduction of rock bridge sliding cohesion on the slope.

It has been observed (Miller, 1983) that there are two typical scales of potential sliding surfaces, i.e. those associated with major structures (such as faults or other features with lengths comparable to the size of study area) and those associated with more numerous, smaller structures (such as joints, foliations and bedding planes). Major structures normally have lengths great enough to affect overall pit slope stability. In contrast, the smaller and more numerous structures usually have lengths less than 10m and consequently influence the stability of benches because bench heights are usually 12 to 20m.

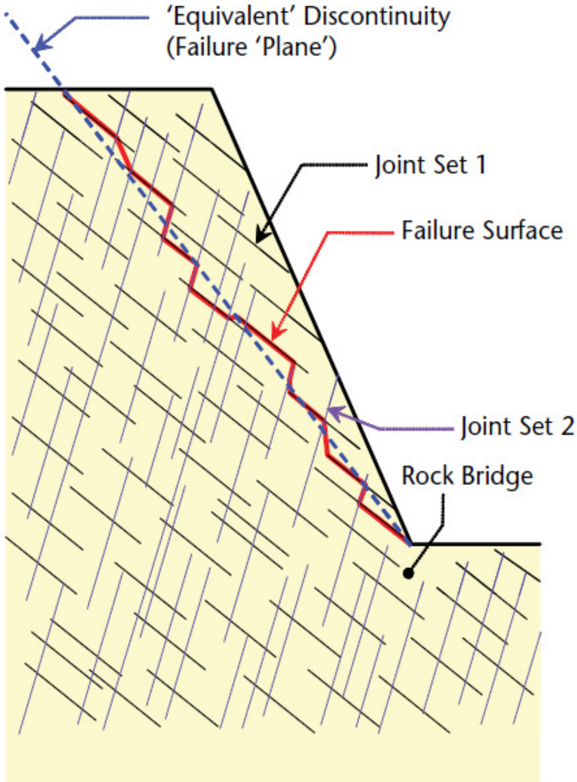

Figure 2-8: Example of step-path geometry on a rock slope (from Read and Stacey, 2009).

The slope step path failure mechanism according to Piteau and Marftin (1982) can be analyzed much more simply if it is represented in 2-dimensions as joint traces. The failure surface in this case is assumed to be sub-parallel to the strike of the slope. Jointing systems on rock slopes always pose potential danger to slope stability. Any planar or non planar surface (or 'path') through intact rock and joints in a rock mass constitutes a potential failure surface. A 'critical path' for a slope is a path of minimal safety given a jointing system and a set of strength parameters (Einstein el. al., 1983). This path is a particular configuration that has a combination of joints and intact rock portions having the minimum safety margin (SM) where:

$$SM = R - L$$

Where : R = total sliding resistance due to the frictional properties of the joints and

L = total driving force

In this case persistence or the fraction of area covered by joints play a crucial role by reducing R if persistence is high or increasing it if the persistence is low. If SM is negative i.e. L>R, then the rock mass fails. Therefore a critical path may or may not be a failure path.

In analysing step-path failures, Call and Nicholas (1978) and Miller (1982) made the following simplifying assumptions;

a) At least two joint sets characterise a step path, i.e. the master joint which daylights into the slope and gently dipping at 20º to 50º and the crossing joint steeply dipping at 50º to 90º

b) The joints strike parallel or nearly parallel to that of the slope to within ±20º. This makes it critical to map these joints on an exposure perpendicular to the slope face as these joints are highly likely to be omitted when mapping the slope face.

c) A rock bridge is more likely to fail in tension than in shear

d) Cross joints that do not intersect, but come approximately 5cm close to the end of a master joint, will allow the path to continue to the next master joint

e) The flattest path is followed, i.e. the step path will follow a master joint to the furthest cross joint further up the master joint. The path will then follow the cross joint until it intersects and continues along another master joint.

There are a number of step-path failure analysis programs that have been developed. Among them is STEPSIM4 (Baczynski 2000, and Baczynski, 2008), and the NIOSH programs, Bplane, Bstepp and Bwedge (Miller et al, 2007).

2.6 Summary

This chapter has described the formation of joints in rocks and their importance when creating excavations. Joint properties and their importance have been described. The various methods used when collecting joint data have been presented. A review of joint network modelling and how these models can be used to evaluate rock block stability and slope stability have also been discussed in this chapter. The following chapter will describe the joint and rockfall mapping that was carried out at two underground platinum mines.

3 Underground Joint and Rockfall Mapping

The previous chapter provided an in-depth description of joint properties, their importance and methods used in collecting them. Presented in this chapter is a detailed description of a joint and rockfall mapping programme. The success of this field exercise hinges on conducting the underground mapping programme at a suitable site.

3.1 Mapping site selection

The purpose of obtaining joint and rockfall data underground was to enable correlation between actual rockfalls and statistically simulated rockfalls based on the measured joint data. Once confidence has been established in the statistically simulated rockfalls using the joint data, forward analyses of expected rockfalls for future mining areas can then be carried out. In order to have confidence in the usefulness of the joint data to be acquired for the correlation process, a thorough process of selection of suitable mapping sites was undertaken.

There are two main mineral deposits that are being exploited in South Africa, i.e., the gold bearing Witwatersrand deposit and the platinum group metals and chromium bearing Bushveld Complex. The Bushveld Igneous Complex is a huge layered igneous intrusion, in which platinum group metals, comprising almost 70 % of the world's known resources, are concentrated into two exploitable horizons, that is the UG2 and Merensky reefs. The Bushveld Complex was selected as the candidate mapping environment because it is often characterised by blocky hangingwall conditions as evidenced by mine accident statistics from the DME. Mining in this area is currently taking place at shallow to medium depth. The stresses associated with these mining depths vary from low to medium stress which is favourable for gravity driven rockfalls in the stope hangingwall due to the low clamping stresses. Therefore, most rock mechanics related challenges in this area are often driven by the blocky nature of the hangingwall. However, the ground conditions in this environment vary from mine to mine, with some mines having competent and non-blocky hangingwalls. A search was made for a mine with a considerably blocky hangingwall and where rockfalls are experienced after each blast. Additionally, the selected mine had to have a well maintained rockfall database for comparison purposes. This search was done through communication with mine rock mechanics personnel, by studying mine plans, by analysing rockmass ratings and by visiting the candidate mine sites. The selection process for a site appropriate for correlation of rockfalls eventually led to two suitable stopes for each reef (UG2 and Merensky) at a platinum mine in the Bushveld Complex. An additional site (site B) was selected at a different platinum mine with very blocky Merensky reef hangingwall conditions for testing the rockfall prediction model.

3.1.1 Mine A site description

Joint and rockfall mapping was carried out in the UG2 and Merensky reef stopes at Mine A. On each of these reefs, the mapping took place on two stopes in which active mining was taking place, and these will be described in this sub-section. The summary information on the mapping area covered for both the Merensky and UG2 reefs during the mapping exercise is presented in Table 3-1. For each stope, reference positions were marked on the excavation walls from the start position of the mapping programme and the face advance measured up to the end of the mapping exercise. This information is important for the purpose of normalising the mapped rockfalls to the area mined.

Table 3-1: Mapping area covered

Stope	Face Advance(m)	Face Length(m)	Area (m^2)
Merensky 1 South	18	29	513
Merensky 2 South	15	23	338
UG2 4 North	20	28	552
UG2 3 North	10	28	280

UG2 Reef

The two panels selected for the mapping exercise in this reef were on the same raise line and are shown on the plan in Figure 3-1. They are at a depth of approximately 674 m below surface. The dip and dip direction of these stopes is 10º and 045º respectively. For the UG2 reef, mapping was mostly done on the 15C53 4N stope. The 15C53 3N stope was stopped two weeks into the mapping programme because of the bad hangingwall conditions brought about by the pothole shown on plan. The mining face of the 15C 53 4N stope was 28 m long and 52.4 m from the main raise line, close to the end of the mapping programme. There was no other significant mining that could have influenced the stress regime in the stope hangingwall, nor significant geological structures in the immediate vicinity of these stopes. These two factors can influence potential for rockfall occurrence.

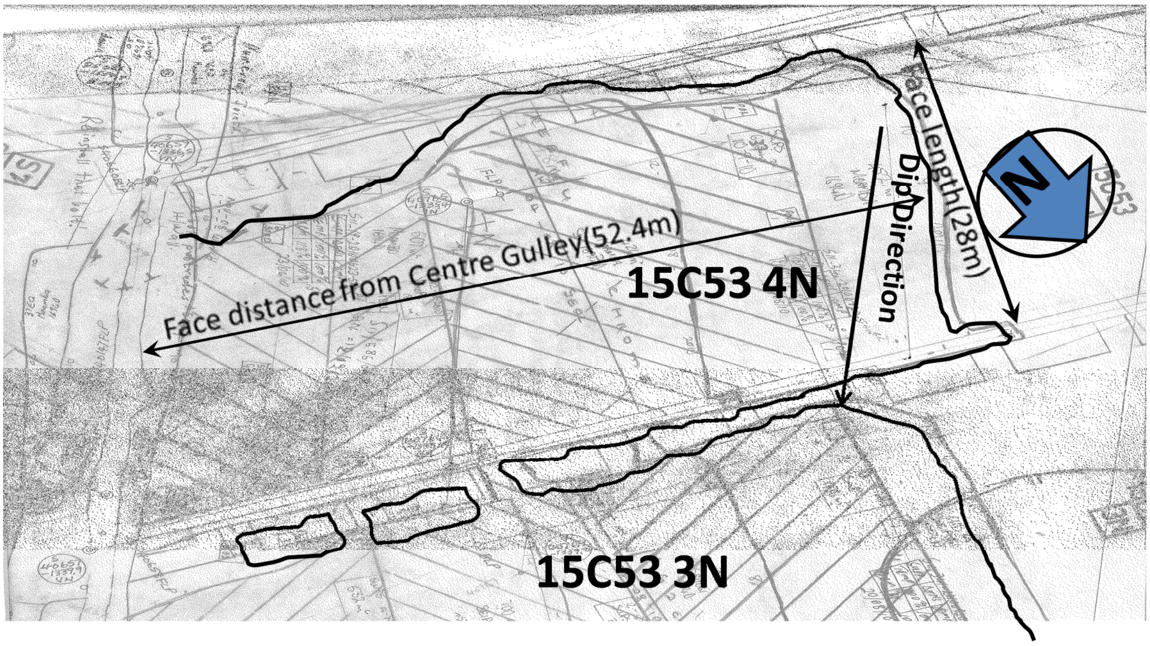

Figure 3-1: Mapped stopes on the UG2 reef

Merensky Reef

The two stopes selected for the mapping exercise in the Merensky reef are shown on plan in Figure 3-2 and are at a depth of approximately 1093 m below surface. The dip and dip direction of these stopes are 10º and 045º respectively. Most of the mapping for the Merensky reef was done in the 23 42 1S stope. When the mapping programme began, the 23 42 2S stope was still being ledged. Production mining of this stope commenced two weeks into the mapping programme. The mining face for the 23 42 1S stope was approximately 29 m long and 75 m from the main raise line at the end of the mapping programme. There was no other significant mining that could have influenced the stress regime in the stope hangingwall, nor significant geological structures in the immediate vicinity of these stopes. These two factors can influence potential for rockfall occurrence.

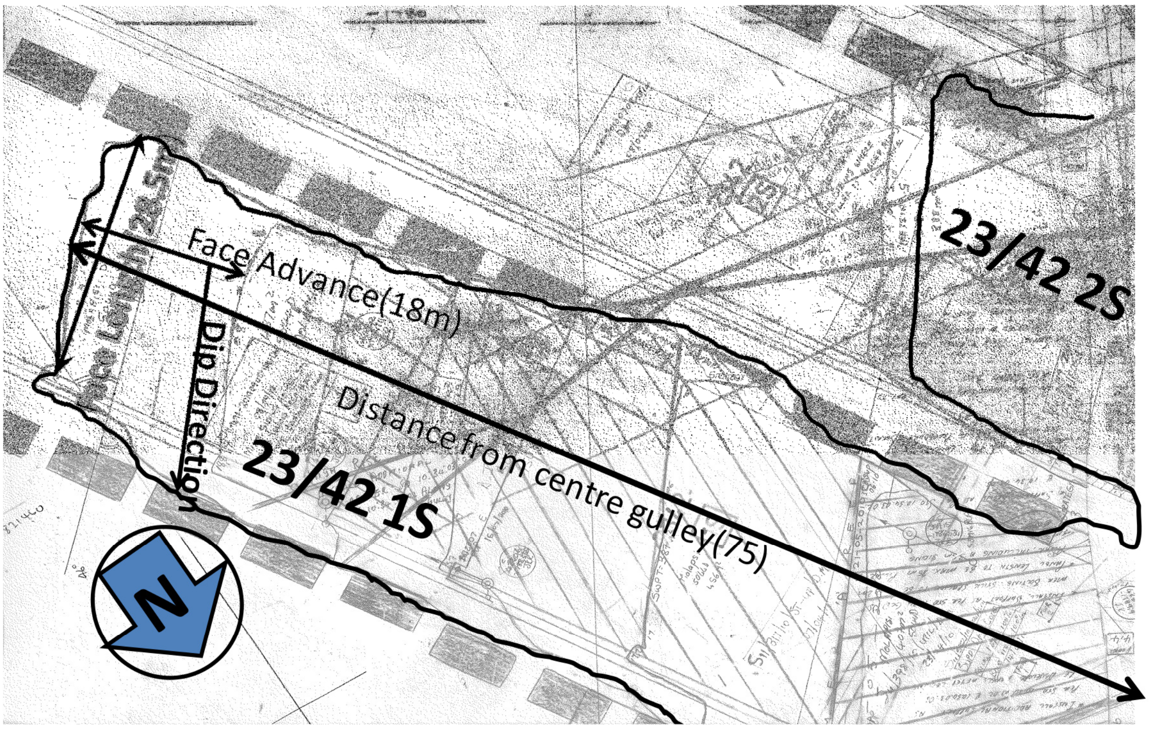

Figure 3-2: Mapped stopes on the Merensky reef

3.1.2 Mine B site description

Joint mapping was carried out in a total of five stopes and a gully development in the Merensky reef hangingwall at mine B. Joint mapping was not done on the UG2 at this mine reef because it was considered not to be significantly jointed to pose rockfall related hazards to the same magnitude as the Merensky reef. The mapped areas covered a vertical distance of approximately 500 m and slightly over 3 km of strike length of the main working areas of this reef. Mining was taking place at an average depth of 650m below surface. A list of the areas mapped and the number of joints intersected per scanline is presented in Table 3-2. An extra hangingwall development was mapped in a strike gulley in order to obtain a three dimensional view of joints in the hangingwall of the stope. At this site, a normal fault displaced the reef downwards whilst exposing the reef hangingwall at the same time.

Table 3-2: Summary of locations mapped and scanlines

Location	Scanline start position position	No of joints	Scanline Length (m)
Stope 1	Peg D1431 +6.4 m from gulley into stope on dip	25	6.41
Stope 1	D1212 in gulley	42	15.45
Stope 2	Peg D1745+2.6m on dip+3.1m on strike	100	20.85
Stope 3	Peg R8285 +2.5m on dip	10	3.52
Stope 3	Peg R8284 on strike	25	5.59
Stope 4	Peg D1752 + 1.78 from gulley into stope	33	14.77
Stope 4	Peg D1752 on strike in gulley	27	5.90
Stope 5	Peg D1239 + 4.2m into stope	73	20.26
Stope 5	Peg D1282 + 6.3m from ASG	62	20.02
Gully	5m from centre gulley into strike gulley	21	5.00
Total		**418**	**117.77**

3.2 Underground Joint Mapping Procedure

Joint information is required in order to provide data for the generation of potential keyblocks for use in a statistical stability analysis simulation. This section describes the method used to obtain the joint data. The scanline joint mapping technique (section 2.4.2) was employed. Its relative ease of use, cost and comprehensiveness in collecting joint information favoured its selection over the other methods. This method is also ideal for obtaining joint properties for use in a statistical keyblock stability analysis as it can provide statistical distributions for each joint property.

In carrying out scanline mapping underground, a measuring tape was laid on the stope hangingwall by tying it at short intervals to the support elements in order to make it taut. To reduce joint orientation bias, two tapes were laid on the hangingwall orthogonal to each other such that joints sub-parallel to one tape would be intersected by the other tape. At Mine A, one tape was laid parallel to the face, from the bottom of the panel (approximately 28 m long) to the top, whilst the other tape was laid parallel to the gulley (scanline at least 30 m long). Thorough washing down of the hangingwall surface, carried out before the mapping exercise, assisted in joint identification and collection of joint properties. Blasting and stress induced fractures were excluded from the mapping exercise. All joints greater than 0.5 m in length that intersected the scanline were considered to be of significance and were mapped for orientation, location, length and shear strength properties (joint roughness and alteration numbers). This 0.5m (lower limit) cut off joint length has also been used by Dight and Baczynski (2009).

The joint orientations were measured using a Breithaupt compass. This instrument has the advantage of simultaneously recording both the dip and dip direction of the joint. Care was taken in taking the orientations as far away as possible from the magnetic influence imposed by metallic objects, in particular roof bolts. An investigation of the magnetic influence of the orebodies on the compass was carried out, and this was found to be negligible.

The location of the joint is the distance along the tape to the point where the joint crosses the tape. The length of the joint was measured as the strike extent of the joint where it intersects the hangingwall. The joint shear strength properties were recorded using the method described by Barton (2002). The joint walls and infill material were examined by visual analysis, by rubbing hands on surfaces and by gouging out the infill to determine its properties. The orientation of each scanline was also recorded as this is important for spacing error correction as illustrated in section 2.4.1. This exercise was repeated a number of times both on dip and strike as the mining face advanced. All the information collected was recorded on log sheets, which are presented in Appendix A.

3.3 Joint Data Analysis

After completion of the joint mapping exercise, the initial step in the analysis of the joint data is to group the orientations into sets of sub-parallel joints. For this purpose, the recorded joint orientations were processed into distinct joints using DIPS, a Rocscience (2001) program designed for the clustering and analysis of joint orientation data. Since a magnetic compass was been used in collecting the orientation data at mine A, a magnetic declination of 17 degrees west (source) at this mine was used to effect a correction on the recorded orientation of the joint data to obtain the true orientation in DIPS. Similarly for mine B, a magnetic declination adjustment of 15 degrees west was effected on recorded joint orientations to cater for magnetic declination in the area in which the mine is located. The mean and standard deviation of the joint sets are then obtained as outputs from DIPS. The clustering of joint orientations is a very important step in processing joint properties as it reduces the size of the problem to be analysed. This ideology is supported by observations of keyblock failures in a pilot tunnel by Hatzor and Goodman (1992) which showed that 33 out of 35 failures were bounded by a maximum three joint sets.

Since joint lengths were challenging to measure accurately underground due to limited exposures, average joint lengths have been calculated from the recorded approximations. The most prominent joint sets (with the highest number of poles) and longest joints from mapping were given the longest lengths in the joint parameters. This is consistent with observations in the Bushveld Complex open pit platinum mines by Bye and Bell (2001) which suggest that some of the prominent joints are continuous laterally and vertically over hundreds of metres. The approach adopted in allocating joint length is also supported by extensive joint mapping experience from other sites (Call et al, 1976), which pointed out that minimum joint length is more accurately defined than maximum length because of limited joint exposures.

Joint spacing has been determined as the distance between successive joints of the same set. The location of joints in a set is used for calculating joint spacing for that particular set. This procedure is repeated for all joint sets defined in DIPS. In order to obtain the true spacing, an orientation bias is applied using the relative angle between the joint set and the scanline as described in section 2.4.

Joint friction angles have been calculated per each joint set based on the Barton (2002) model as described in section 2.4.1. In general there are three clusters of joint friction angle data. The first cluster is composed of the joints with sepentinite infill of varying thicknesses, the second is made of calcite infill joints, and the last, joints without any infill (Table 3-3). Within these clusters, the thickness of the infill material affects the friction angles. This information was used when calculating the friction angles.

Table 3-3: Joint infill descriptions and friction angles

Joint infill Description	Thickness (mm)	Jr	Ja	Friction Angle (°)
Serpentinite	1	2	4	27
	4	2	8	14
Calcite	1	3	2	56
	2	3	4	37
No infill	1	3	1	72

A normal distribution curve has been fitted to the friction angle data in order to obtain the mean and standard deviation for each joint set. An example of curve fitting is presented in Figure 3-3 for the Merensky J1 joint set. The friction angle values have been grouped per each joint set and have been plotted on the graphs (red curve). A normal distribution curve (blue curve) has been fitted ton these graphs to obtain the best fit curve and mean and standard deviation to best represent the friction values per joint set. A full set of curve fitting of friction angles per each reef and joint set are presented in Appendix C.

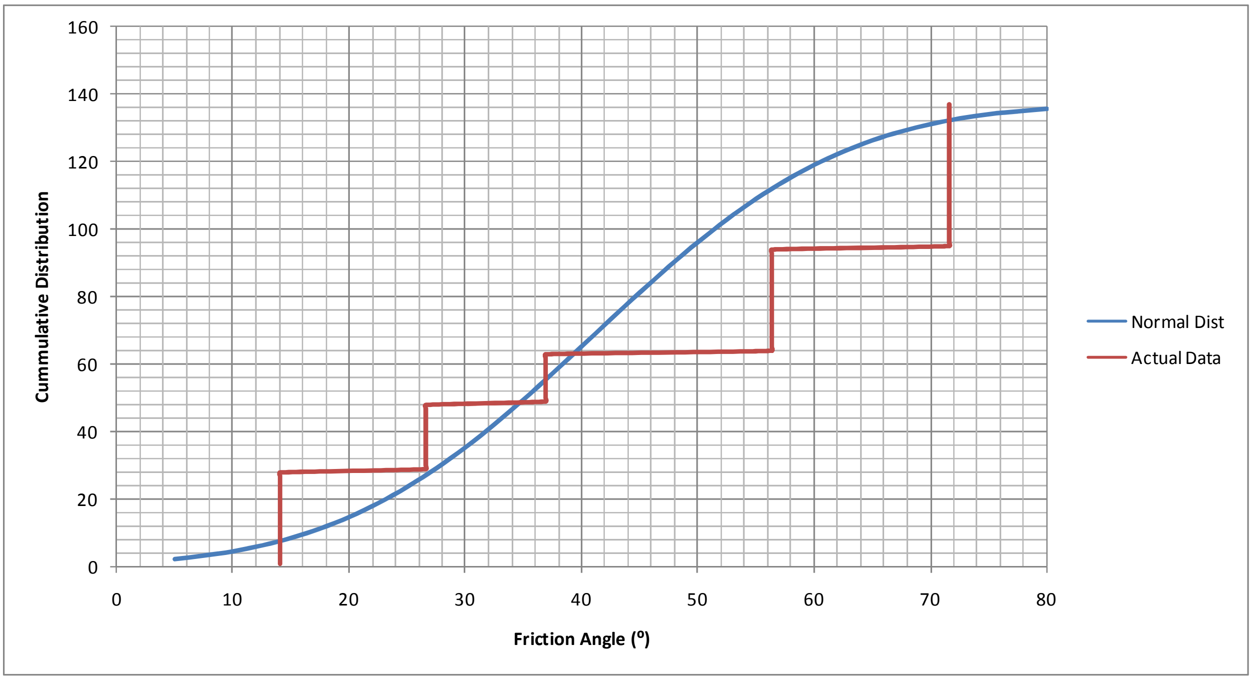

Figure 3-3: Friction angle distribution curve for Merensky J1 set

3.4 Joint Mapping Results

The joint mapping results described here provide inputs for use in the statistical keyblock generation and support system testing software package JBlock. Since JBlock is statistical keyblock stability software, the variation of the joint properties from their mean values has been calculated and is presented in this section as well.

3.4.1 UG2 reef at Mine A

For the UG2 reef, a total of 273 joint occurrences were mapped over a total scanline distance of approximately 205 m. The joint orientations from mapping have been plotted as poles in DIPS for the purpose of further processing of the joint data. Clustering of the joint orientation poles has resulted in the delineation of two main joint sets and two random sets as shown in Figure 3-4. The poles of the joints in each set can be differentiated by a distinct colour. The most prominent joints, J1 and J2 are the most frequent as signified by them having the greatest numbers of poles in the DIPS pole plot. Correspondingly, the joint spacings for these two joint sets are small compared with the other less frequent, random joints, which are sparsely spaced. Summarised joint properties from this analysis are listed in Table 3-4.

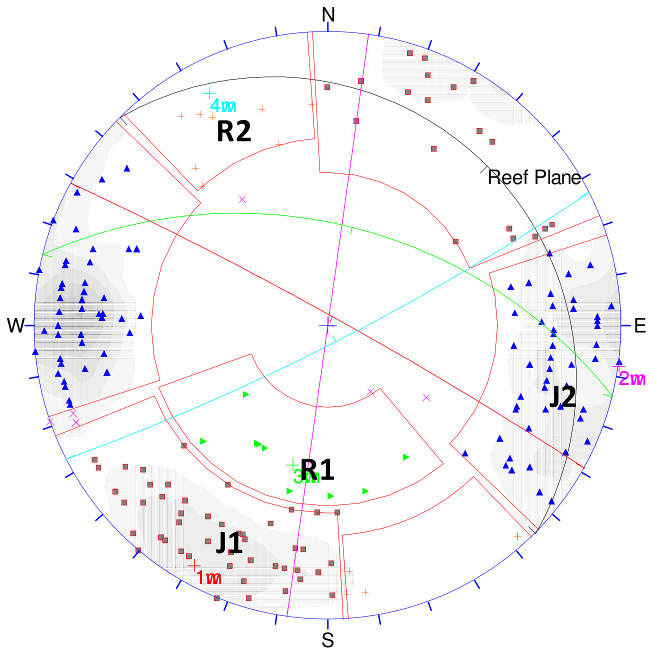

Figure 3-4: DIPS pole plot of mapped joints on UG2 reef.

Table 3-4: Summarised joint properties for UG2 reef

Set	Orientation (^{0})				Friction Angle (^{0})		Spacing (m)			Length (m)		
	Dip		Dip Direction		Mean	St dev	Min	Avg	Max	Min	Avg	Max
	Mean	St dev	Mean	St dev								
J1	82	7	029	20	35	15	0.11	1.27	12.4	20	40	50
J2	90	6	078	21	35	20	0.10	1.03	9.5	15	30	40
R1	39	13	014	8	35	20	10	20	30	2	4	6
R2	71	9	153	38	35	20	5	15	25	1	3	5

*Note: Parting plane recoded at 2.5m ± 0.5m into hangingwall, tensile strength 15kN ± 2kN

Three of the four joint sets defined for the UG2 reef are steep dipping with dips ranging between 71° and 90°. The other joint set is comprised of low angled joints. The low angled joints are critical in defining keyblocks that will eventually fall out from the hangingwall. A parting plane representing chrome stringers or triplets in the UG2 hangingwall was established from the geology department at the mine. The parting plane is often involved in creating loose keyblocks in the hangingwall. All the joint properties used in JBlock for the UG2 reef are listed in Table 3-4.

3.4.2 Merensky reef at Mine A

A total of 304 joint occurrences were mapped over a total scanline distance of approximately 187 m on the Merensky reef hangingwall. Clusters of joint orientations have been identified, delineating three main joint sets and one random set as shown by the DIPS pole plot in Figure 3-5. Each colour on the pole plot represents the joints in a distinct set. The most prominent joints, J1, J2 and J3 are the most frequent as signified by them having the greatest numbers of poles in the DIPS pole plot. Summarised joint properties from this analysis have been presented in Table 3-5. It is apparent from this that the degree of jointing in the Merensky reef stope hangingwall is greater than that in the UG2 reef stope hangingwall at Mine A.

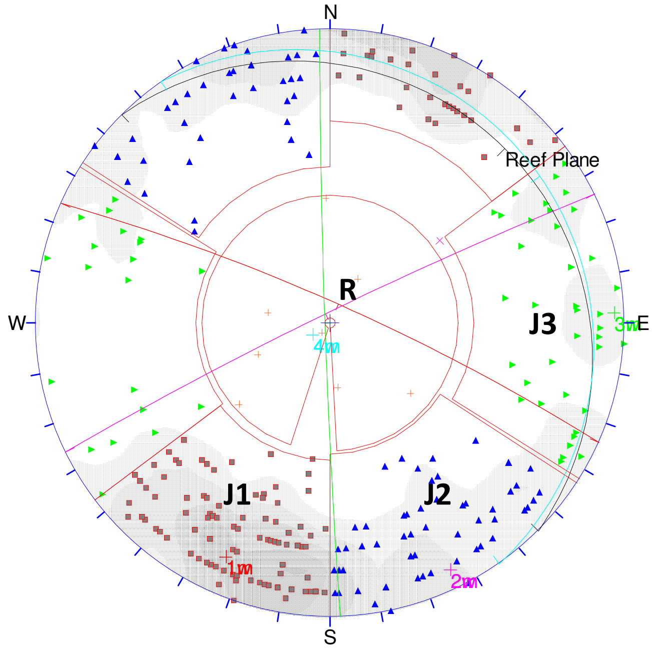

Figure 3-5: DIPS pole plot of mapped joints in Merensky reef

Table 3-5: JBlock joint input properties for Merensky reef

Set	Orientation (^{0})				Friction Angle (^{0})		Spacing (m)			Length (m)		
	Dip		Dip Direction		Mean	Stdev	Min	Avg	Max	Min	Avg	Max
	Mean	Stdev	Mean	Stdev								
J1	82	8	024	19	41	17	0.11	0.66	8.40	20	40	50
J2	86	9	334	23	42	20	0.16	1.63	9.1	15	30	40
J3	88	9	268	29	38	18	0.13	0.87	4.10	2	8	15
R	32	15	148	50	45	15	5.00	7.60	9.00	8	10	13

The majority of the joints for the Merensky reef are steep dipping with three of the four having a steep dip ranging between 82° and 88°. The other joint set consists of low angled joints, which, as indicated above, are important in that they provide keyblock release surfaces. All the joint properties used in JBlock for the Merensky reef are listed inTable 3-5.

3.4.3 Merensky reef at Mine B

Work on the stope hangingwall of this reef resulted in 418 joints being mapped on a combined scanline length of 117.8 m. There is a large scatter of poles, with the majority of the joints being sub-vertical, as illustrated by the pole plot in Figure 3-6. Although the joints could be clustered into six different joint sets, the four most common joints observed have been used in the analysis, because not more than four joint sets were identified at a single location during mapping of the individual areas. The processed average orientation and properties for the joints on this reef are listed in Table 3-6.

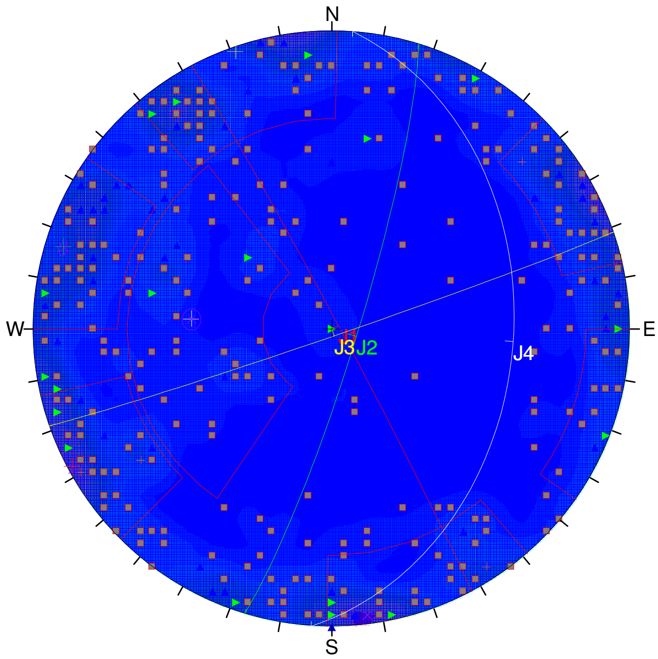

Figure 3-6: DIPS pole plot for Mine B joints

Table 3-6: JBlock joint input parameters for Mine B

Set	Orientation (^{0})				Friction Angle (^{0})		Spacing (m)			Length (m)		
	Dip		Dip Direction		Mean	Stdev	Min	Avg	Max	Min	Avg	Max
	Mean	Stdev	Mean	Stdev								
J1	88	8	062	22	33	15	0.10	0.82	5.50	30	50	60
J2	83	7	107	21	33	15	0.14	1.32	6.70	25	40	50
J3	88	8	161	23	35	18	0.11	0.65	2.30	15	20	25
J4	39	10	094	21	35	15	0.12	1.94	6.30	15	25	30

3.5 Underground Rockfall Data

The thorough selection process for ideal underground mapping panels described in section 3.1 was focused on collecting a sizeable set of rockfalls for use in a statistical analysis. The mapping of rockfalls underground was carried out in the same stopes in which joint mapping had been done at mine A. The main objective of this activity was to record a set of actual rockfalls and their respective properties, and use this information for comparison with statistically simulated rockfalls using the mapped joint data in the same area.

3.5.1 Data Collection

The mapping programme involved the mapping of joints and recording of all the rockfalls that occurred in both the UG2 and Merensky reefs in the selected stopes. To carry out the mapping, the morning shift re-entry team was accompanied as the team members entered the stopes. During re-entry, rockfalls in the stope hangingwall would be identified. A rockfall is generally identified by the mould it leaves in the hangingwall after it has fallen out. In some instances rockfalls can be identified as they occur, i.e. when barring out loose blocks to make a working area safe. All the rockfalls were noted, whether they occurred with the blast or whether they were a result of barring. For identification purposes, paint was used to mark the boundaries of the mapped rockfall mould. When inspecting the same stope after a subsequent blast, a check was made for new rockfalls and any further increase in the size of a previously mapped rockfall mould, by inspecting the paint marks on its boundary. In order to facilitate identification of new rockfalls or extension of existing rockfalls, thorough watering down of the hangingwall had to be done to make the rockfall mould paint marking visible.

In collecting rockfall data, a measuring tape was tied to the stope hangingwall, parallel to the mining face, in order to record the rockfall location distance from the gulley. Properties describing each rockfall were recorded and are listed below:

- When and how the rockfall occurred, i.e. with the blast or by barring;
- Distance of the rockfall from the gulley;
- Distance of rockfall from the face;
- Whether the rockfall failed any support units or not;
- Rockfall shape, to assist in a more accurate volume approximation;
- Average dimensions of the rockfall. The following convention was adopted in recording this data:
    1. Rockfall length was assumed to be the distance on the rockfall that is almost parallel to the mining face;
    2. Rockfall width was assumed to be the distance on the rockfall that is perpendicular to the mining face;
    3. Rockfall height was taken as an average height on each rockfall;

- The condition of the release surfaces on the rockfall, i.e. whether it is a joint or blast fracture. Signs for poor drilling in the hangingwall where the rockfall took place were recorded;
- The properties of all the rockfall release surfaces, i.e. orientation, joint roughness condition and joint alteration;
- Record any subsequent increase in the size of the rockfall.

All this information was recorded on log sheets, as shown in Appendix B. The identification and mapping of rockfalls on the stope hangingwall was a repetitive process.

3.5.2 Results

The data acquired from the rockfall mapping program has been processed in order to gain a better understanding of the rockfalls. The statistics of rockfalls mapped underground and their respective time of failure are listed in Table 3-7. The rockfalls have been categorised as failure during blast, by barring, or the cause of the rockfall being unknown. The rockfalls that occurred during the time when the team took the one week break could not be ascertained with confidence when and how they fell. The effectiveness of barring was then determined as a percentage of the total rockfalls mapped. From this analysis it can be observed that most of the recorded rockfalls occurred during the blast.

Table 3-7: Rockfall mapping data

Reef	Blasting	Barring	Unknown	Total	% Falls due to blast
Merensky	53	40	34	93	57
UG2	37	8	7	45	82
Total	90	48	41	138	65

An analysis of the joints forming rockfall release surfaces has been performed. The first part involves processing orientations of the joints that formed the release surfaces of rockfalls using DIPS. In grouping the rockfall release surface orientation poles into sets, a similar approach has been adopted to that used for the joints in section 3.3. The orientation pole concentrations of the joints that were part of the release surfaces of the rockfalls for UG2 and Merensky reefs are shown below in Figure 3-7 and Figure 3-8 respectively. It is worth noting that the pole concentrations identified from joint mapping in section 3.3 (Figure 3-4 and Figure 3-5) are related to those found in rockfall mapping. This is to be expected as the geotechnical domain for joints and rockfalls is similar.

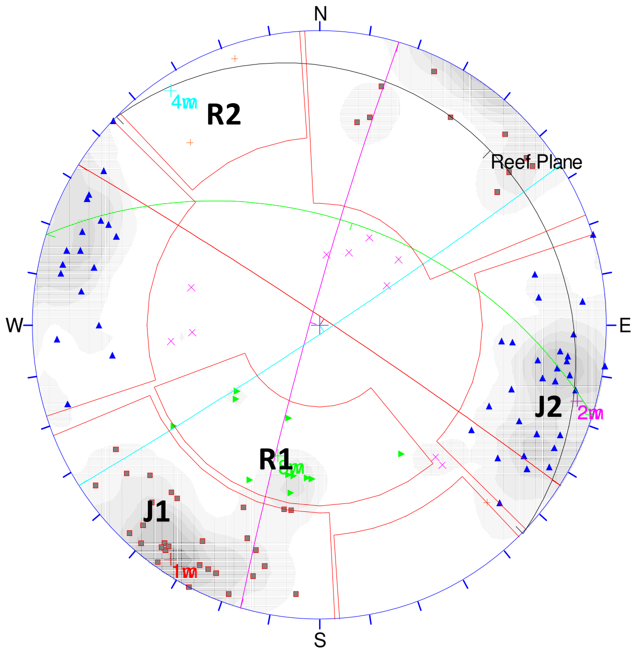

Figure 3-7: DIPS pole plot of mapped rockfalls on UG2 reef

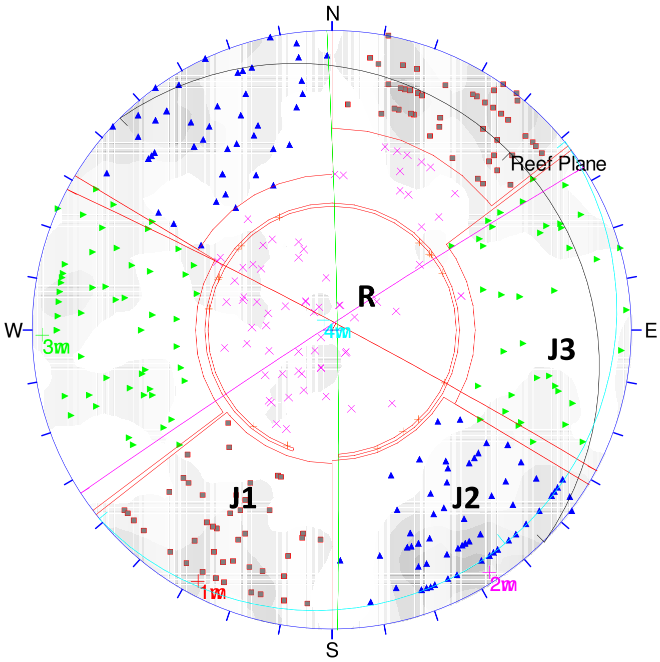

Figure 3-8: DIPS pole plot of mapped rockfalls on Merensky reef

The predominant joints defining the rockfall release surfaces are listed in Table 3-8 below. Two steep joints J1 and J3 combined with the shallow dipping random joint (R) are the predominant block-making joints for the Merensky reef rockfalls. A similar trend can also be observed for the UG2 rockfalls - the rockfall release surfaces here are the steep J1 and J2 joints, which, in combination with the shallow random joint R, delineate the rockfalls. In both reefs the shallow joints are critical for delineating and providing a release surface for keyblocks.

Some rockfalls as shown in the table, however, had fractures (F) forming some of the release surfaces of the rockfall wedges. It could not be established with confidence whether these fractures were formed as a result of blast or stress effects on the rock. Fractures also contributed to keyblock release surfaces, particularly for the Merensky reef, where there was a significant number of low angle blast fractures recorded.

Table 3-8: Joint sets resulting in rockfalls

Reef	**Number of Rockfalls**					**Joints per Block**		**Significant sets**
	J1	**J2**	**J3**	**R**	**F**	**Max**	**Min**	
Merensky	103	57	74	86	47	4	2	J1,J3 &R
UG2	45	39	-	39	17	3	2	J1,J2 &R

It is interesting to note that there are some rockfalls that are bounded by only two joints. This type of wedge forms when two sub-vertical joints opposing each other intersect on an undulating hangingwall. In the Merensky and UG2 reefs, a maximum of four and three joints respectively formed the surfaces of loose keyblocks. These observations can be related to observations made by Hatzor (1992) when analysing rockfalls in a tunnel, where 97% of the 69 rockfalls recorded were bounded by three joints only. Tharp (1985) and Goodman (1995) also concur that averages of three joint sets in general define a keyblock. Also, from this mapping exercise, the average number of joints per block is reflective of the degree of jointing for the each reef hangingwall, with the Merensky reef hangingwall being more jointed than the UG2 reef.

The shapes of the rockfall moulds have been used in determining the base areas and volumes of the rockfalls. The typical shapes of the recorded rockfalls are wedges, pyramids and tetrahedrons. These shapes could be truncated in some instances. Consideration of the rockfall shape is important for an accurate approximation of the keyblock base area and volume. The rockfall volumes, areas and heights from underground mapping are shown in Figure 3-9, Figure 3-10 and Figure 3-11 respectively. In these figures, each case is represented by two graphs, one for all the rockfalls and the other for rockfalls that had no fractures. It can be observed from the graphs that almost two thirds of rockfalls recorded in the Merensky reef had no fractures on them whilst on the other had approximately three quaters of the UG2 rockfalls did not have fractures as part of the block release surfaces. This is important for a comparative analysis with JBlock, since JBlock is reporting rockfalls created by joints only. The rockfalls have been normalised per one thousand square metres mined.

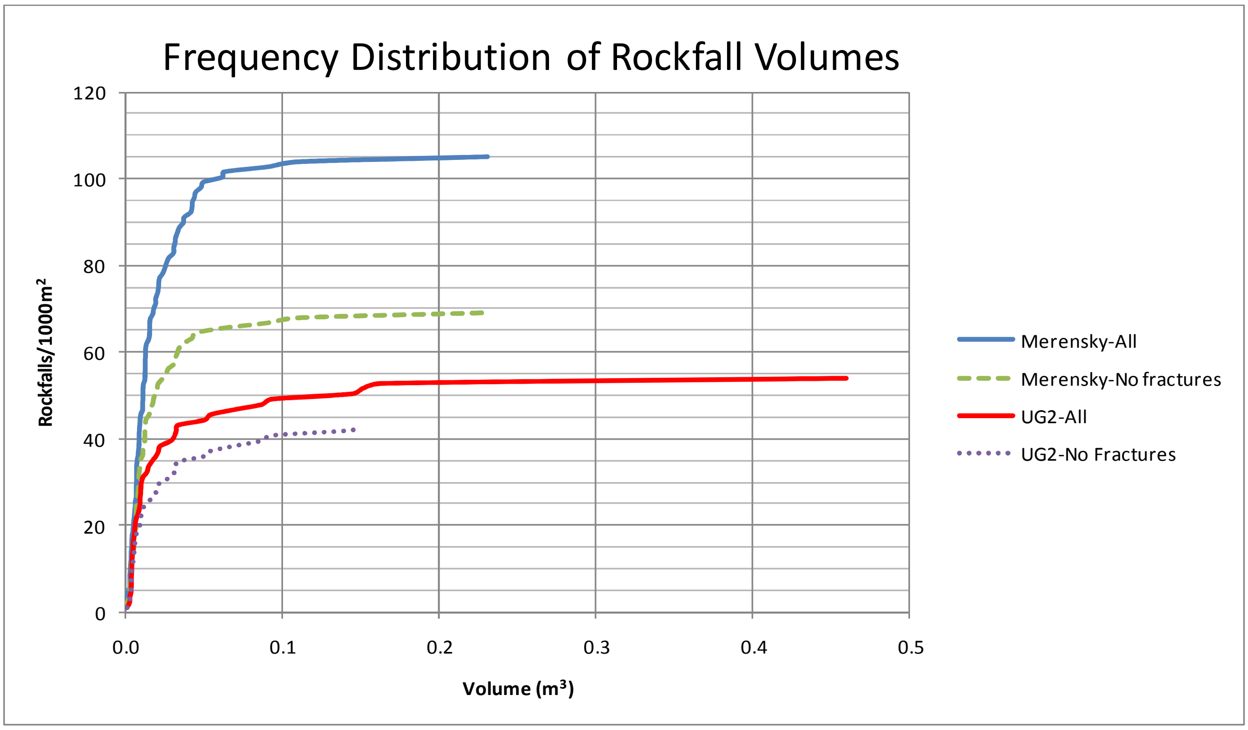

Figure 3-9: Frequency distribution of rockfall volumes

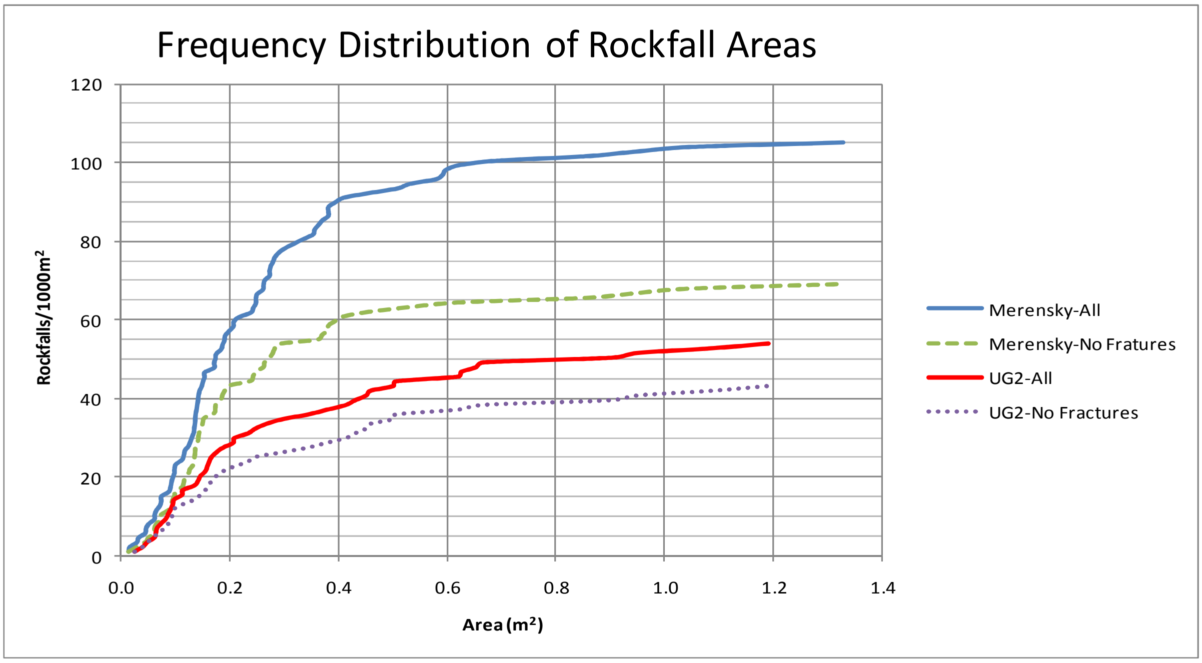

Figure 3-10: Frequency distribution of rockfall areas

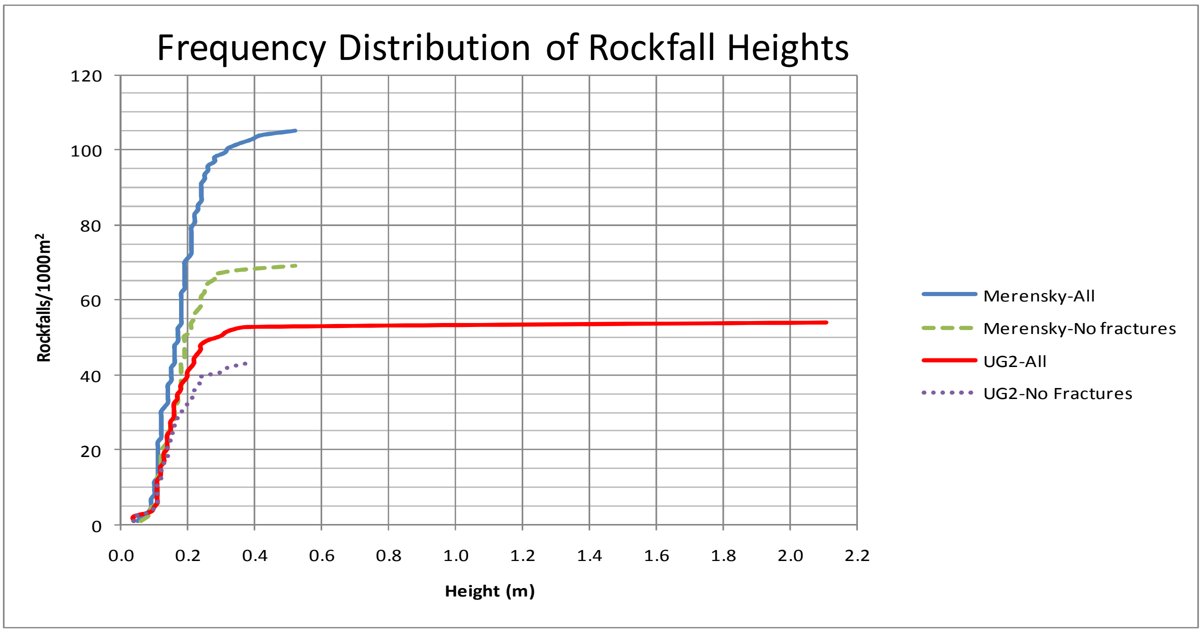

Figure 3-11: Frequency distribution of rockfall heights

The rockfalls identified during the mapping exercise for both reefs represent the small size rockfalls category. No rockfalls, which might have occurred subsequently, were mapped in the back areas during this period. It is suspected that the majority of the large rockfalls would occur in the back areas after the mining face has progressed a considerable distance from the gulley. The Merensky reef registered more rockfalls per thousand square metres mined than the UG2 reef. This corresponds with the observed relatively higher degree of jointing for the Merensky reef than the UG2 reef. The mapped rockfalls mapped here were within 4 m of the working face.

The locations of recorded rockfalls are shown in the density contour plots in Figure 3-12 and Figure 3-13 for the UG2 and Merensky reefs respectively. The rockfalls occurred at an average distance of 1.30 m and 1.69 m behind the face for the UG2 and Merensky reefs respectively, indicating that the UG2 rockfalls occurred closer to the face than the Merensky rockfalls. For comparative purposes, the 4 m boundary for the recorded rockfalls corresponds with the face area defined in JBlock.

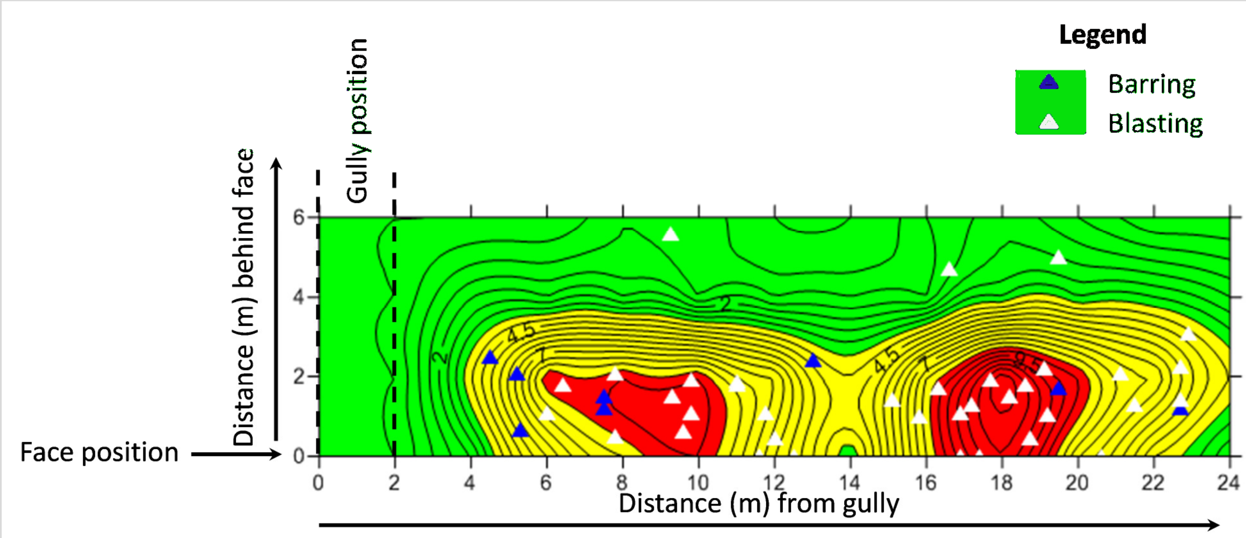

Figure 3-12: Rockfall location contour plot for UG2 reef

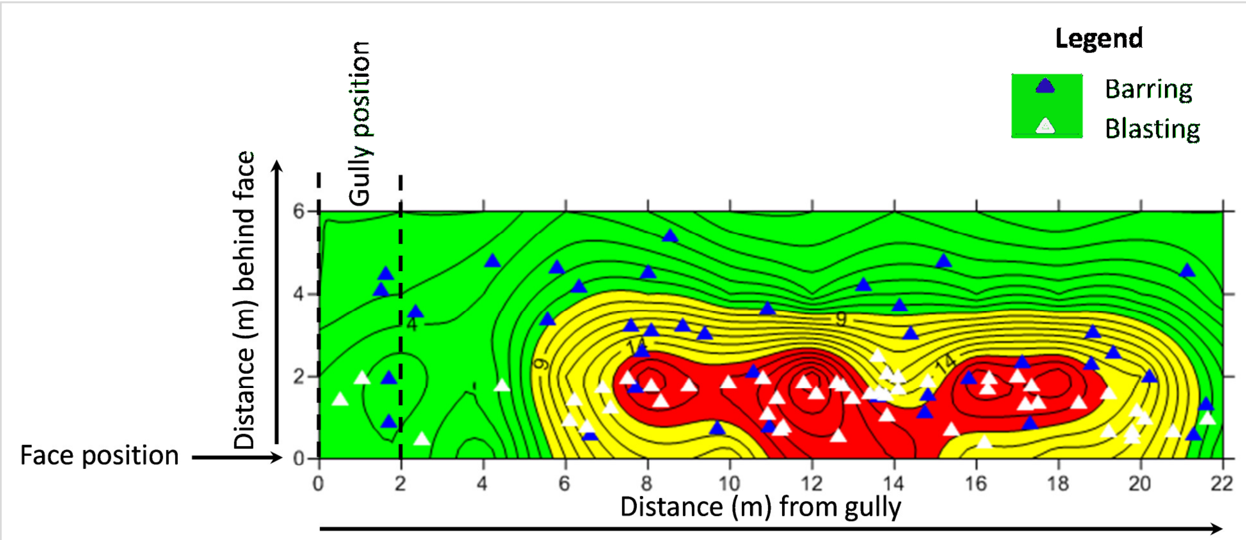

Figure 3-13: Rockfall location contour plot for Merensky reef

3.6 Summary

The mapping of rockfalls and joints at two mines has been described. Also presented in this chapter are the methods used in mapping joints and rockfalls and the analysis of these data. The results show varying degrees of jointing and frequency of rockfalls between the different reefs and mine locations. The Merensky reef at mine A is more jointed compared with the UG2 reef, resulting in a greater number of rockfalls recorded, and corresponding with the closely spaced joints. In the following chapter, the mapped joint data will be used to simulate rockfalls, which will be correlated with actual rockfalls mapped underground.

4 Statistical Keyblock Stability Analysis, Calibration and Validation

The occurrence of rockfalls in the South African platinum mines is often associated with a combination of geological structures. Chief amongst these geological structures are joints because they are generally more densely populated than any other geological structure in undisturbed rockmasses. The previous chapter focused on collecting joint and rockfall data from underground mines. This chapter provides a review of keyblock simulation and stability analysis techniques. Also to be described here is how a simulated set of rockfalls has been correlated with actual rockfalls that occurred underground so as to build confidence in the use of statistical keyblock stability methods in predicting rockfalls. This tool is useful for planning future mining support alternatives ahead of mining, in addition to the use of engineering judgement on the part of the rock engineering practitioner in the selection of stope support systems.

4.1 Review of keyblock stability analysis methods

Excavation design to ensure stability of potentially unstable keyblocks in jointed rockmasses can be carried out empirically, analytically or numerically. Empirical design methods have been applied in the support design to stabilise anticipated loose rock blocks using rockmass classification (Barton, 1976; Barton et. al, 1974; Grimstad and Barton, 1993; Bieniawski, 1973; Bieniawski, 1976; Bieniawski, 1989). These methods are normally applied when there is limited geotechnical data obtained from boreholes during the initial stages of design and mining. Success in the use of empirical methods in similar ground conditions for rock engineering design varies from site to site. The underlying weaknesses of this design approach are that site specific conditions such as geometry of the excavation and the geometrical properties of the joints are not taken into account explicitly in the design process. The importance of joint properties with regard to the stability of an excavation has been described earlier in section 2.4.1. During the construction stage of an excavation, rock surfaces are exposed and additional geotechnical data on the joints can be obtained. Armed with this additional information, analytical and numerical methods can be applied in design.

Analytical methods in analysing blocky rockmasses have been used widely in analysing single rock blocks, determining the stability of potential keybocks with or without support. One of the main analytical methods is Block Theory which has been used widely in analysing the stability of keyblock where joints have been encountered.

4.1.1 Block Theory

This theory to evaluate the stability of keyblocks, was developed over a number of years by Shi and established by Shi and Goodman (1981; 1985) and Goodman (1995). Block theory was initially developed to analyze sliding and translational failure modes only because these are the most prominent block failure modes in the field. However, Mauldon and Goodman (1990) extended this theory to also take into account rotational failure modes. This extension of block theory is however limited to tetrahedral blocks with three joint sets only. Application of block theory is limited to stability analysis in a hard and blocky rockmass where the strength of the intact rock material exceeds the strength of the joints in the rock mass.

The underlying idea behind block theory is in the identification of 'keyblocks'. A block is defined as any mass of rock bounded either by discontinuity planes entirely or by discontinuity planes and the excavation surface. A keyblock, also referred to as a keystone (Shi and Goodman, 1981; Warburton, 1983), is a kinematically unstable block on an excavation surface. Keyblocks are important in rock excavations in that, if they are not supported, they will be the first to slide or fall into the excavation. It has been shown by various authors, including an experiment by Lang (1962) that once a keyblock has been adequately supported to inhibit movement, the other blocks surrounding it will not be free to slide into the excavation. If there are no measures put in place to stabilise the excavation and stop the movement of the keyblocks, the failure of these surface blocks will allow failure of subsequent blocks. This failure process may then continue until natural arching in the rock mass prevents further unravelling, or until the opening is full of fallen material and this material then acts as a restraint. Shi and Goodman (1981) recorded a case in the Kenamo Headrace tunnel where a void of about 20 000 m^3 in volume extended 42 m above a 7.5 m diameter unlined tunnel in a granite rock mass. In a similar case in China, a railroad tunnel in limestone collapsed progressively to a height of 60 m above the original roof. In both incidents, failure of the tunnel initiated with a keyblock and progressed to subsequent blocks.

Given this background it is crucial to evaluate keyblock stability to avoid exposing personnel to unsafe conditions, and also to avoid production losses as a result of rockfalls. Rock blocks created by the intersection of joints and an excavation surface are generally classified into six types as shown in Figure 4-1 below (Goodman and Shi, 1985) and described in Table 4-1.

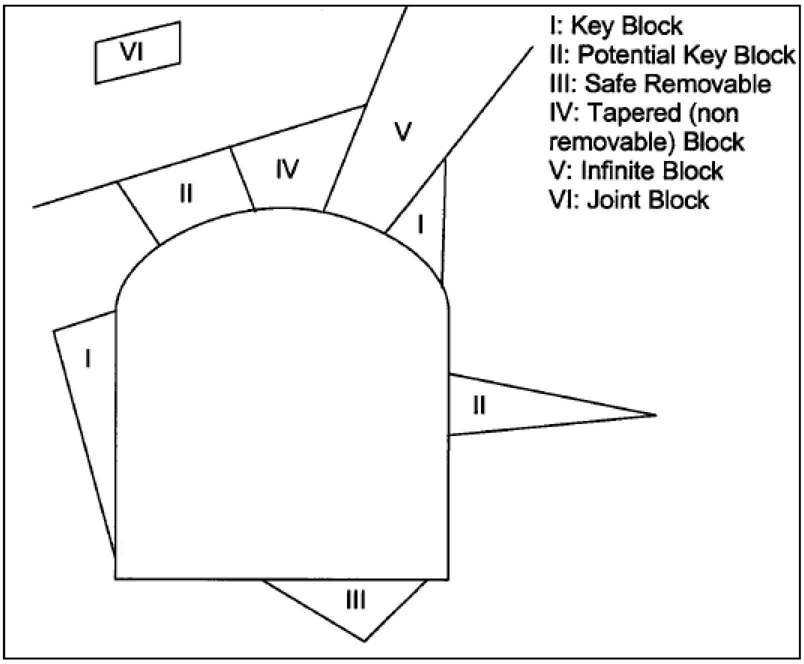

Figure 4-1: Potential block types (after Goodman and Shi, 1985)

Table 4-1: Block Types (after Goodman and Shi, 1985)

Block Type	Description
I: Key Block	Block has a safety factor < 1 or moves in the direction of resultant driving force
II: Potential Key Block	Block has a factor of safety > 1 with friction only preventing the block from moving
III: Safe Removable	The block is delineated by joints and the excavation face but not free to move because of its geometry
IV: Tapered(Non-Removable) Block	Block does not pose danger to an excavation as the delineated block is not free to move into the excavation. This block is formed when a finite block formed by joint half spaces alone is intersected by an excavation.
V: Infinite Block	This block is of no hazard to the excavation
VI: Joint Block	Block made of joint half spaces alone and has no face on the excavation perimeter

Since it is difficult to take into account the true nature of joint properties in reality, Goodman and Shi made a number of simplifying assumptions "approximate" joints in rock masses in order to use block theory:

- All joints are assumed to be perfectly planar
- Joints are assumed to be continuous through the volume of interest i.e. no joint terminates within the region of a key block (this assumption is an over-simplification of reality as joints are not continuous at all times).
- Blocks are only formed by pre-existing joints and no new joints are formed.
- Blocks defined by the joint system are assumed to be rigid, i.e. no block deformation will take place.
- Excavation and discontinuity surfaces are predetermined and the nominal surface is normally used.

Excavation surfaces mainly considered in key block analysis are single planar excavations. Adaptation of block theory to circular excavations has been done by the use of traces (Goodman and Shi, 1989). Traditionally, vector methods or graphical methods using a full sphere stereonet were used to solve the keyblock stability problem using Block Theory (Croney et. al., 1978; Warburton, 1983; Goodman and Shi, 1985, Goodman 1989).

The result of block theory assuming that the joints forming keyblocks are continuous and long, and other joint properties are at their mean values, is that calculated volumes of the keyblocks are overestimated. This concept of the maximum keyblock is dependent on the joint orientations only and is independent of joint spacings and lengths. The analysis by Goodman and Shi (1989) does not cater for the statistical variability of the joints sets. A comparison of the deterministic and statistical block theory methods was done by Windsor and Thompson (1997). They observed that very large or maximum keyblocks are created using deterministic methods. The dimensions of these large or maximum keyblocks are important for establishing the minimum safe depth of embedment of a bolt. In contrast, statistical approaches provide the full range of keyblock sizes, inclusive of the small blocks likely to fall in between support units (Chan and Goodman, 1987; Windsor and Thompson, 1997). The small blocks are of concern in that they add to ore dilution and may cause injury to workers. In a study towards the elimination of rockfall hazards, Potvin et.al (2001) investigated more than 750 rockfalls. Their data showed that the majority of rockfall injuries (91%) are from rockfalls of less than 2 tons and occurred within 10 m of active working faces. A further example is the Hex River Tunnel (SRK Internal Report, 1986), in which 81% of the rockfalls recorded (61events) occurred during the excavation cycle at the face, whilst only 19% occurred behind the face. This indicates the importance of adequate areal support coverage in the form of safety nets or other means to prevent injuries caused by these small rockfalls (Fernandes and Gardner, 2011; Skarbøvig et. al, 2011; Daehnke et al. 2001). The conclusion of the comparison of methods by Windsor and Thompson (1997) was that both methods should be used in the design of appropriate support for a blocky rock mass.

Vector methods in block theory are now built into software packages, facilitating keyblock analyses. Among these is Siromodel (Read and Ogden, 2006), Rock3D (Geo&Soft, 1999), SWEDGE (Rocscience, 2006), UNWEDGE (Rocscience, 2007), and SATIRN (Priest and Samaniego, 1998).

A simple form of keyblock analysis was described by Haines (1984) and Stacey and Haines (1984). In this method joint traces are created in two dimensions from joint data mapped in the field. An excavation outline is then superimposed on the joint traces and the closed shapes involving the joints and the excavation identify the potential keyblocks for that particular excavation. The joint traces can be created in three orthogonal planes and excavation surfaces superimposed in each of these planes. In this way the three dimensionality of the problem is conserved which is critical for any block stability analysis (Gumede, 2006; Gumede and Stacey, 2006; Stacey and Gumede, 2007; Stacey et al, 2005). These approaches allowed the probability of keyblock failure to be determined based on geometrical considerations only, not considering joint shear strengths.

Although rock engineering design has commonly used deterministic approaches, and continues to do so, probabilistic design methods are being introduced (McCullagh and Lang, 1984; Stacey, 1989; Terbrugge et al, 2006; Beauchamp et al, 1998; Dunn et.al 2008; Pierpaolo, 2005; Langston et.al, 2007; Leung and Quek, 1995; Einstein, 2003). A probabilistic design approach is largely motivated by the high degree of variability in the rock mass properties. A rock mass is usually made up of different rock materials and geological weakness planes. The rock mass information obtained from the field normally corresponds with the sampling location and may be different at other sampling locations. The variability in these properties motivate for a probabilistic approach when evaluating rockfall occurrence potential using joint data.

Using the power of block theory, Esterhuizen (2003) developed a probabilistic keyblock stability program, JBlock in which statistical distributions of orientation, length, spacing and friction angle of joints are taken into account. In the package, these parameters and their variabilities are sampled randomly to generate theoretically possible keyblocks, and to evaluate the stability of these keyblocks, taking into account joint shear strengths and installed types of supports, their locations and spacings. The outputs of the analyses are the distributions of the possible keyblocks of different volumes, and the distribution of the probability of failure of keyblocks. JBlock will be used in this research and its application is dealt with in more detail in the next section.

4.2 Jblock

In line with the trend towards probabilistic design referred to in the previous section, analyses have been carried out to determine, theoretically, the probability of occurrence of rockfalls in stopes of platinum mines in the Bushveld Complex. The measurements of actual rockfalls described in Section 3.5 provide a basis for evaluating the effectiveness of this probabilistic approach. Specifically, using the measured joint data dealt with in Sections 3.1 to 3.4, the statistical keyblock stability software JBlock (Esterhuizen, 2011) has been used to predict the occurrence of rockfalls in the UG2 and Merensky reef stopes at mine A described earlier (section 3.1.1). The approach adopted and the results obtained are described in this section.

4.2.1 JBlock Setup

The setup for a JBlock analysis involves the following:

- Stope geometries (both UG2 and Merensky stopes) are drawn and saved as JBlock file formats, called an excavation file.
- The orientations of the stope hangingwalls, the advance per blast, the advancing mining face and mining direction for excavation, are specified at this stage as well.
- Support elements are added in the excavation to create a support file. The spacings of the support elements are shown in Figure 4-2 and Figure 4-3 for the UG2 and Merensky stopes respectively. The input properties of these supports for JBlock are as follows:
  - Hydrabolts: installed as grouted tendons with a peak strength of 100kN and grout bond strength of 320kN/m
  - Mine Poles: peak strength of 270kN
- Hazard zones have been applied in JBlock as well for the UG2 and Merensky reef analyses. These are listed below:
  - Face area: this is the zone from the face to 4 m behind the face. This is the area in which most of the work in the stope, i.e, drilling, blasting, supporting and lashing, is done, and most of the workforce is confined to this area. A four year study of rock related accidents in the Bushveld Complex by Bakker (1993) revealed that this is the area in which the majority of accidents occur.
  - Sweepings area: this is the zone from the face area boundary going back to 10 m. In this region, cleaning of ore left behind during lashing is done and there are few man hours dedicated in this area.
  - Gulley area: this is the zone used for man access to the stope and for movement of ore from the stope.
  - Back area: this is zone behind the sweepings area. There is no work done in this area and no access by man to this zone.

JBlock images of the excavation and support defined are presented in Figure 4-4 and Figure 4-5 for the UG2 and Merensky reefs respectively. The hazard zones have been labelled in the JBlock excavation support support images.

- Jointing information from the underground mapping records is input. This information includes the following for each joint set:
  - Mean dip angle, and range, minimum and maximum
  - Mean dip direction angle, and range, minimum and maximum
  - Mean joint friction angle
  - The properties for large structures such as parting planes and domes can be defined as well

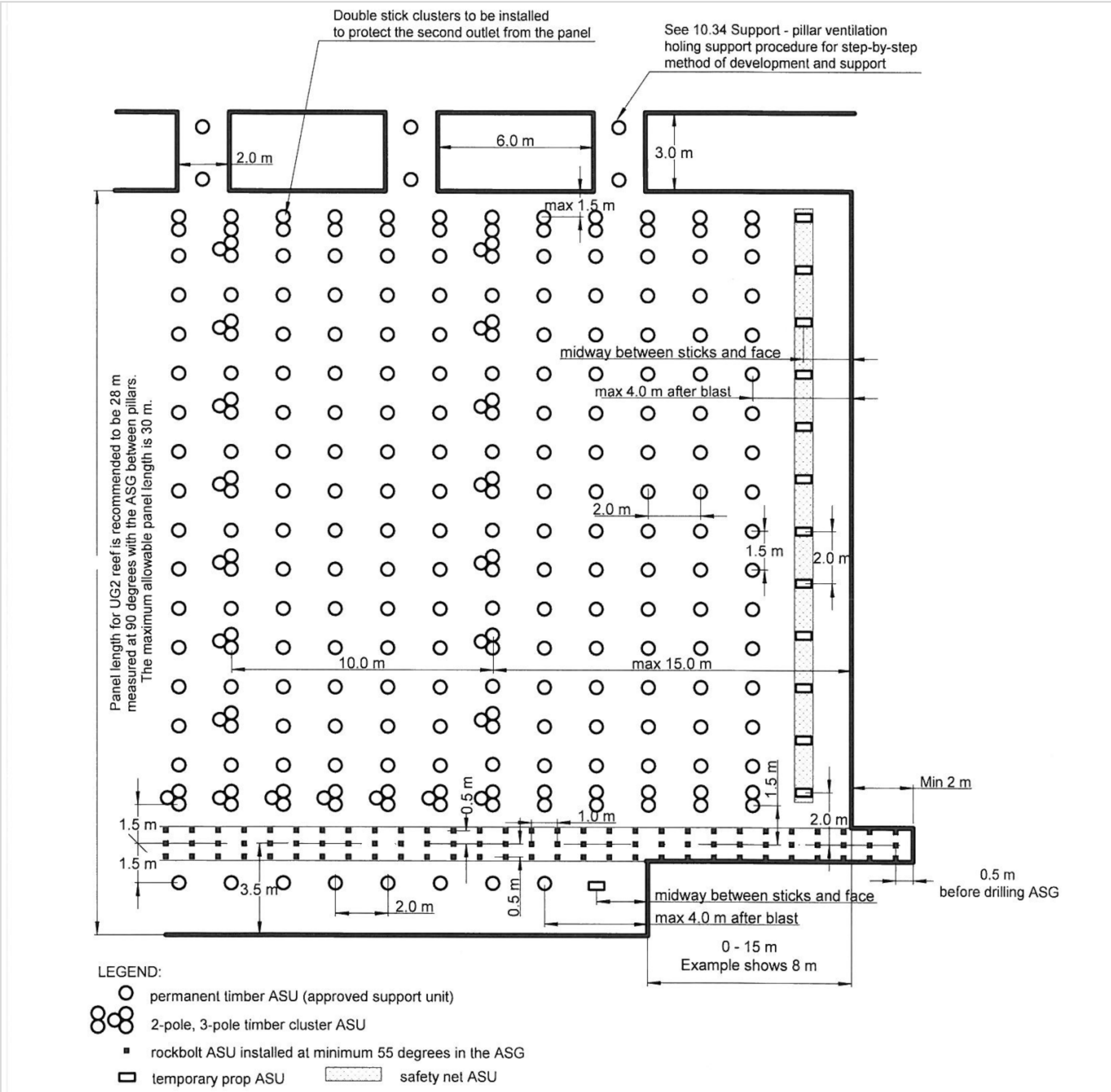

Figure 4-2: UG2 stope support standard

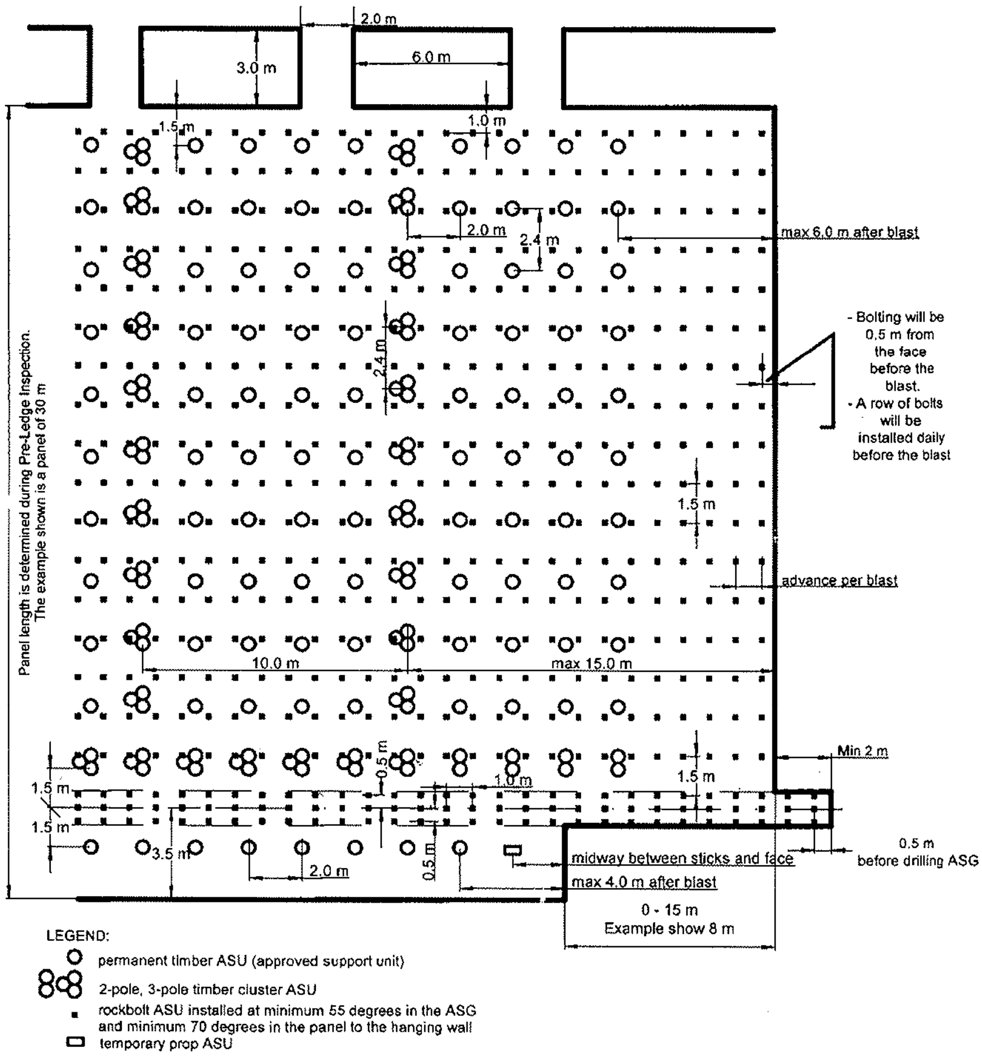

Figure 4-3: Merensky stope support standard

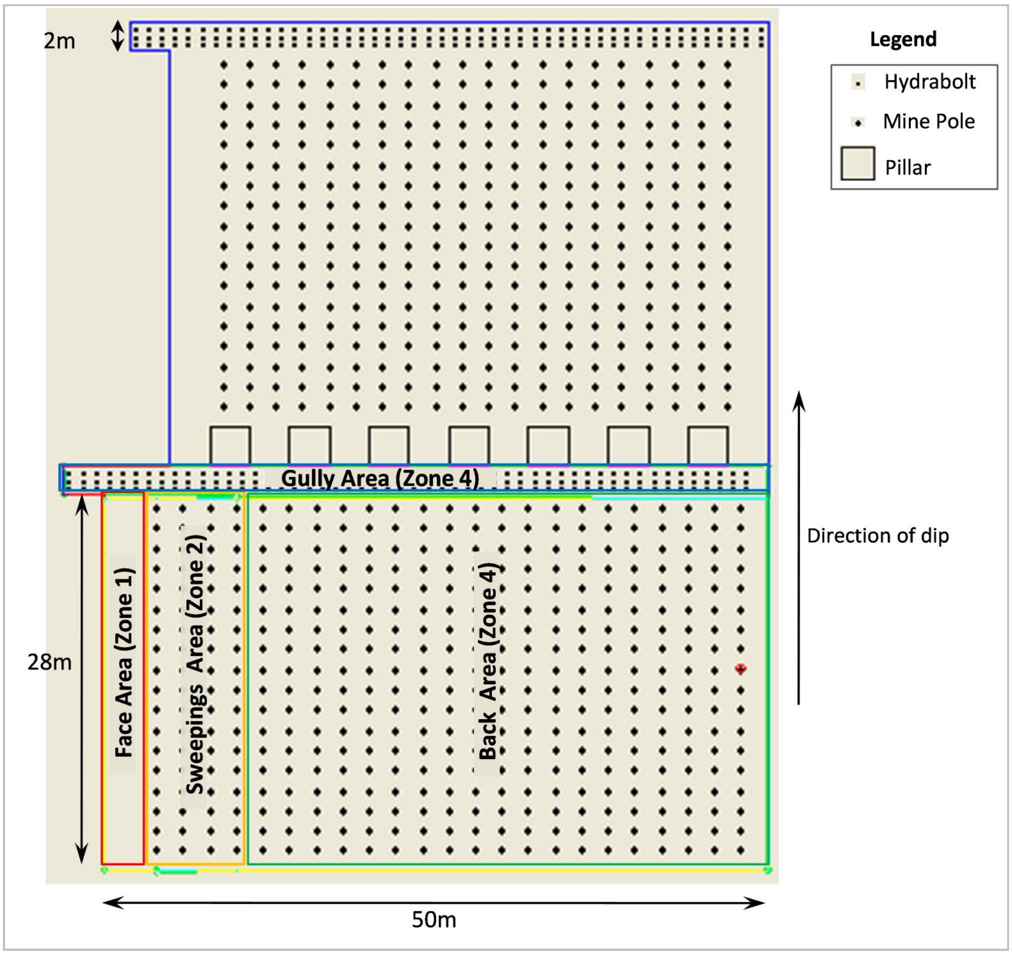

Figure 4-4: JBlock image of the excavation and support layout for UG2 reef

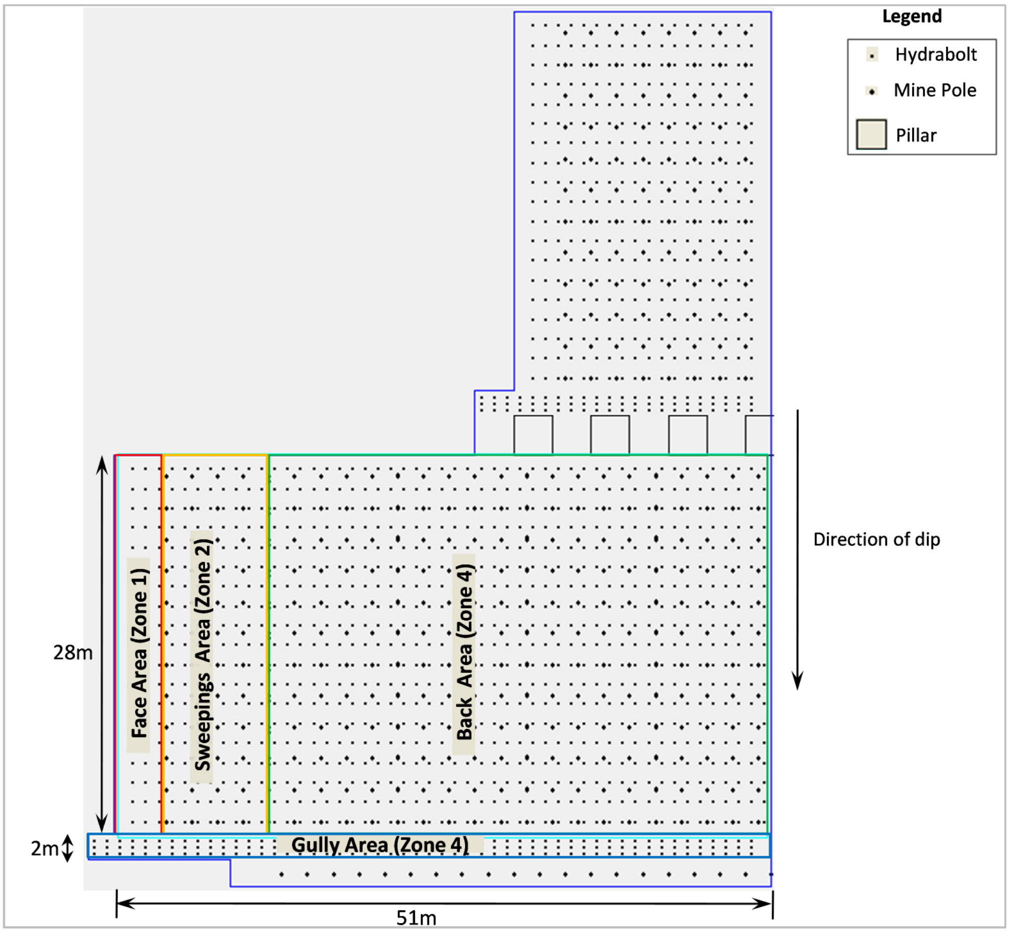

Figure 4-5: JBlock image of the excavation and support layout for Merensky reef

4.2.2 JBlock Analysis

The input data for the jointing is sampled randomly for the purpose of generating potential keyblocks. The number of keyblocks to be generated in this process is specified (commonly 1000) and thus a distribution of keyblocks can be created. All the stochastically generated keyblocks are "tested" randomly in the supported stopes (i.e., placed randomly in the stope) to evaluate the effectiveness of the support systems in holding the keyblocks. Keyblock failure can occur as a result of failure between supports, by gravity (tensile failure of bolts and compressive load of props or poles) or rotational failure of the supports. A user defined block release profile is used in placing the keyblocks in different zones. This profile is important as it is an imitation of what happens in reality where most rockfalls occur in and around the face area immediately after the joints bounding them are fully exposed. Rockfalls gradually decrease as the distance from the face incease in the back area of the stope. The weakness of this approach in JBlock at the moment is that it assumes that all keyblock sizes are released uniformly. The keyblock release profile used in the analyses is partially based on the results of the rockfall mapping data and the historical rockfall data obtained from mine A. The profile used throughout this research is shown in Figure 4-6, 65% of the rockfalls have been set to fall with the blast (zone 1), 50% of the remaining rockfalls fall at the face area (zone 2) and 99% of the keyblocks fall within 25 m from the face.

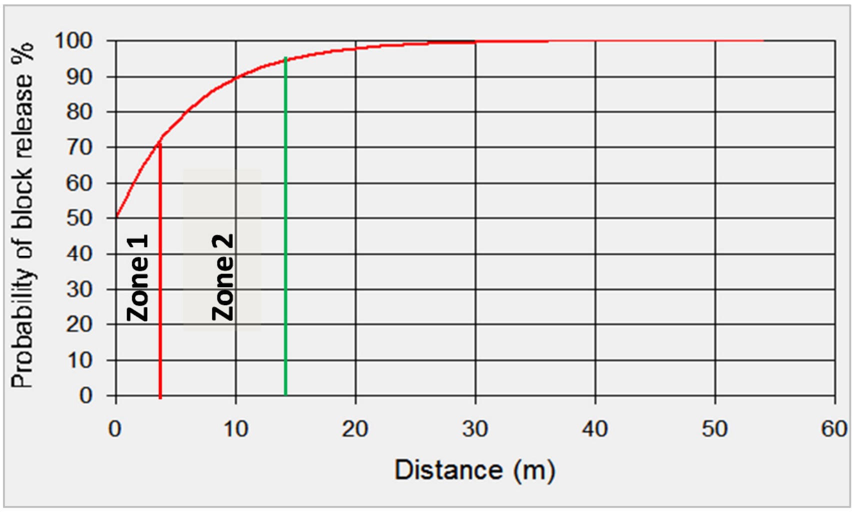

Figure 4-6: JBlock keyblock release profile

The output from JBlock is in a spreadsheet format, providing all the information on failed and stable keyblocks, together with their respective properties and the zones in which they failed. Further processing of the rockfall information can be performed on these outputs to enhance the understanding of the results. Graphical output in the form of distributions of rockfalls is also produced. These outputs will be illustrated and dealt with in more detail in the next section.

4.3 Correlation of Rockfall Data with Simulated Data

In this section, the correlation of actual rockfall data with the theoretical, simulated rockfall data, is described. The correlation exercise has been split into two parts, firstly for the small rockfalls and then secondly for the large rockfalls. The rockfalls recorded during the underground rockfall mapping exercise fall into the small rockfalls category, and will be considered separately. The injuries predicted to occur, based on the simulated rockfalls, will be compared with historical records of injuries experienced at the mine. The rockfalls causing production losses due to the requirement to re-establish the stope panel will be analysed as large rockfalls.

4.3.1 Small Rockfalls Correlation

In order to carry out the correlations, JBlock has been used to simulate rockfalls in both the UG2 and Merensky reef stopes. The output results from JBlock are presented in a spreadsheet, and include all the information on both failed and stable keyblocks, together with their respective properties. Further processing of the rockfall information was carried out on these outputs to enhance understanding the theoretical rockfall results.

The joint set data from underground mapping presented in section 3.4 has been used as the input data for the statistical simulation of keyblocks in JBlock. The excavation geometry used in JBlock is an “imitation” of the stopes in which the mapping was done, and was shown in section 4.2. Using the excavation hangingwall and the joint properties, JBlock generated both keyblocks and non-keyblocks. The former have the potential to fall from the hangingwall if they are not supported, whilst the non-keyblocks make up the remaining area and are always stable, even without being supported.

In creating blocks for both the UG2 and the Merensky reefs a minimum volume of $0.001m^3$ was specified in JBlock so as to generate blocks of similar size to those mapped underground. 74 497 blocks were created in JBlock for the UG2 reef, 31 824 of them being keyblocks and the remainder non-keyblocks. The combined simulation area representing the UG2 blocks is 59 686 m^2. The distribution of block sizes obtained from this simulation is shown in Figure 4-9. The keyblocks can be cartegorised as being either primary or seconday. The primary keyblocks are the smallest unit of keyblocks that can be created whilst secondary keyblocks are bigger composite keyblocks with a number of smaller primary keyblocks inside them.

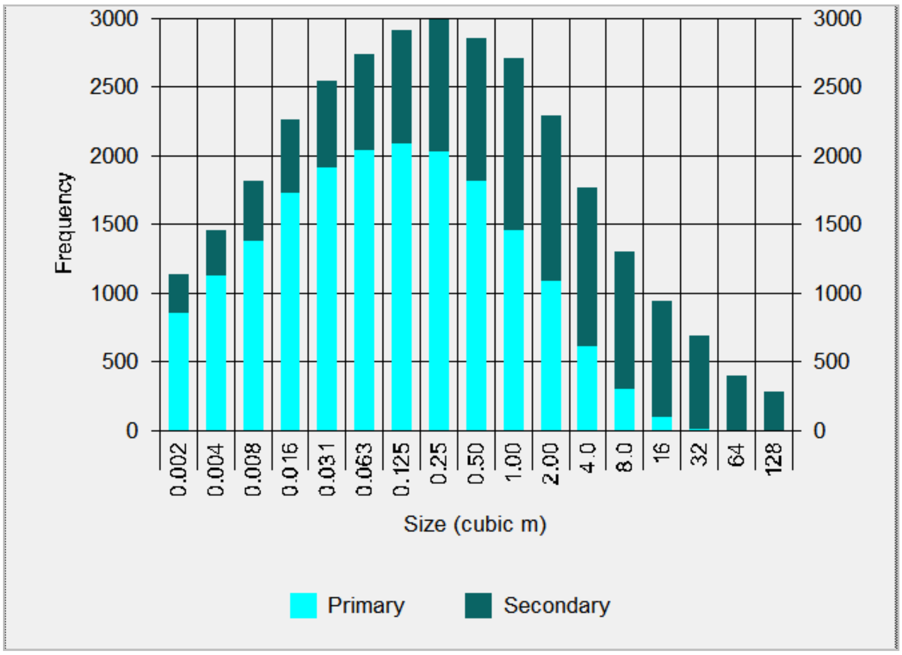

Figure 4-7: UG2 reef small rockfall keyblock distribution

In the Merensky reef stope, 64 084 blocks have been generated, 21 775 of which are keyblocks. The combined simulation area represented by the Merensky blocks is 13 012 m². The distribution of block sizes obtained in the Merensky simulation is shown in Figure 4-10.

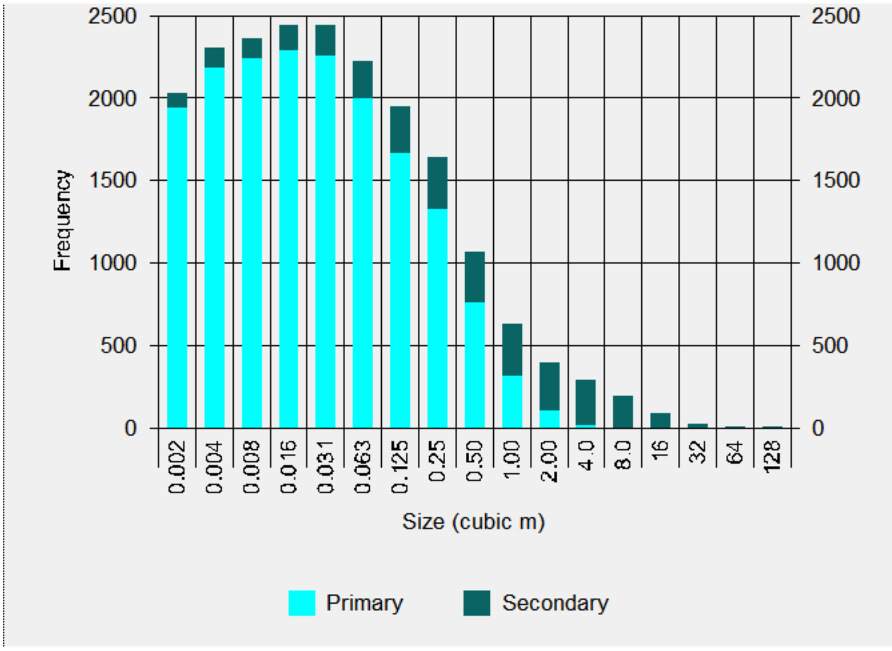

Figure 4-8: Merensky reef small rockfall distribution

The keyblocks generated have been "tested" in the supported excavation to evaluate the effectiveness of the support system in holding the keyblocks and therefore preventing rockfalls. The support properties and spacings used corresponded with the support standards at the mine, presented in section 4.2. In reality there is a horizontal clamping stress in the stope hangingwall which acts to stabilize keyblocks. JBlock assumes a constant stress in the hangingwall. Clamping stresses in the stope hangingwall depend on the ratio of the horizontal to the vertical stress at a particular location and depth below surface. In "calibrating" the JBlock simulated rockfalls with the rockmass from underground mapping, clamping stresses were varied in the analyses - initially, no clamping stress was applied when testing the keyblocks for stability; then increased clamping stress levels were applied to the JBlock keyblocks until a trend comparable to the mapped rockfalls was produced.

It has been illustrated in section 3.5.2 that most of the rockfalls recorded underground were within 4 m from the working face. Therefore, for comparison purposes, the JBlock results presented here have been screened to consider at rockfalls that occurred in the face area only, ie within 4 m of the working face.

Results of the analyses are presented in the form of graphs of numbers of rockfalls per 1000m² against rockfall volumes and rockfall areas. For the UG2 reef stopes, rockfall volume and area are presented in Figure 4-9 and Figure 4-10 respectively. Corresponding graphs for the Merensky reef stopes are presented in **Error! Reference source not found.** and Figure 4-12 respectively. For comparative purposes, the rockfalls mapped underground have been plotted on the same graphs as the JBlock rockfall results. In each of these graphs the underground mapping results are represented by the solid green and red curves. The red curves represent all mapped rockfalls, inclusive of fracture bound rockfalls, whilst the green curves represent the mapped rockfalls that were bounded by joints only. This distinction is important when comparing with the JBlock results since the JBlock rockfalls are bounded by joints only, not fractures.

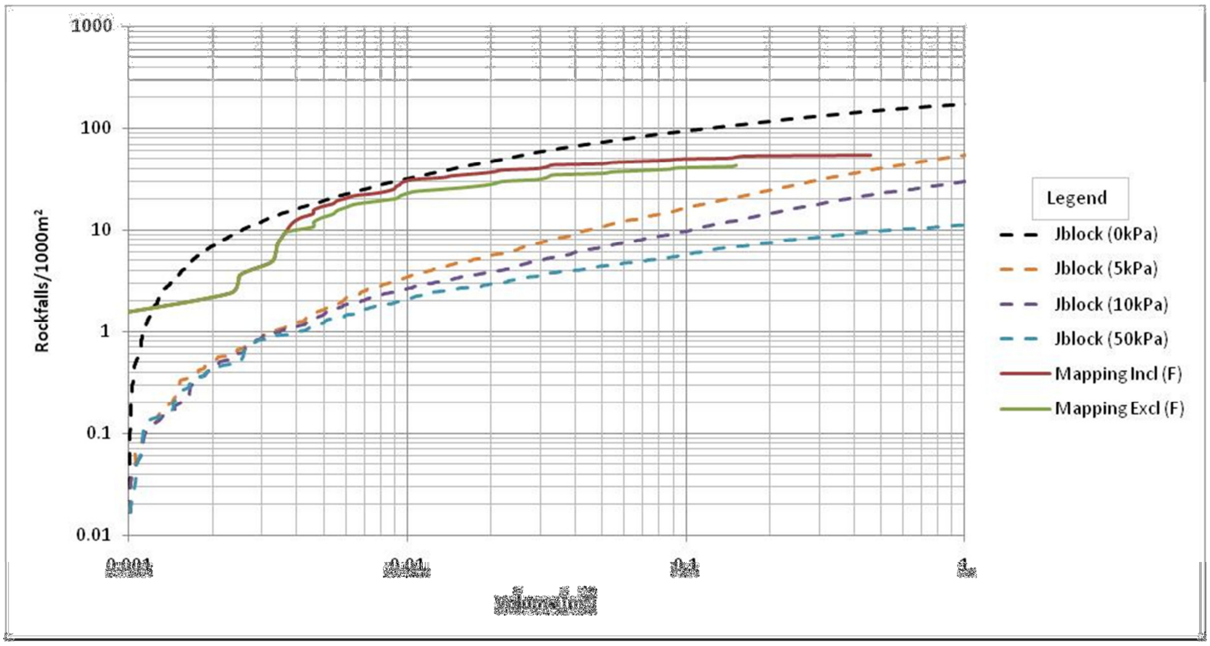

Figure 4-9: UG2 reef JBlock and mapping rockfall volume distribution

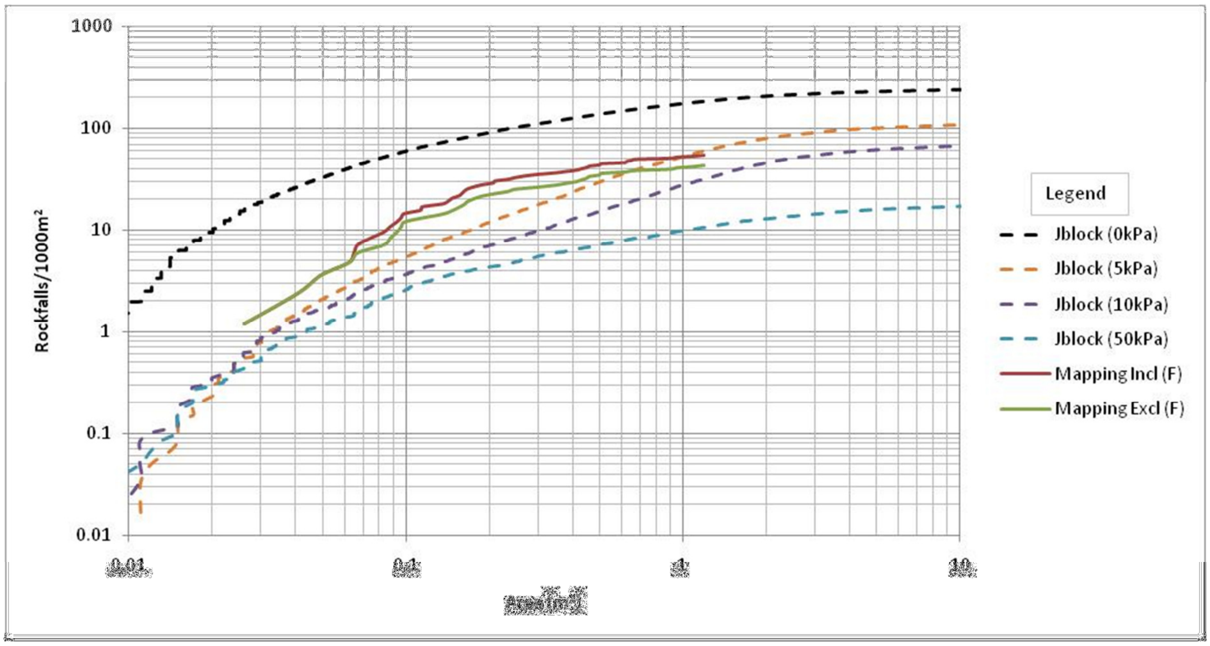

Figure 4-10: UG2 reef JBlock and mapping rockfall area distribution

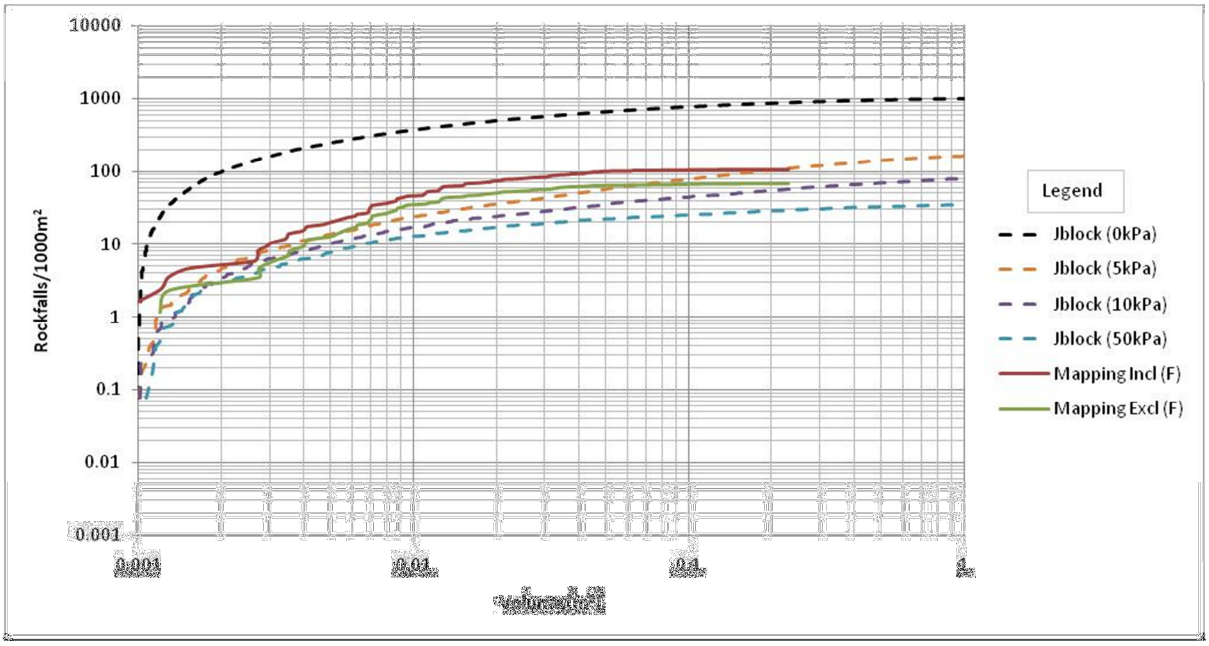

Figure 4-11: Merensky JBlock and mapping rockfall volume distribution

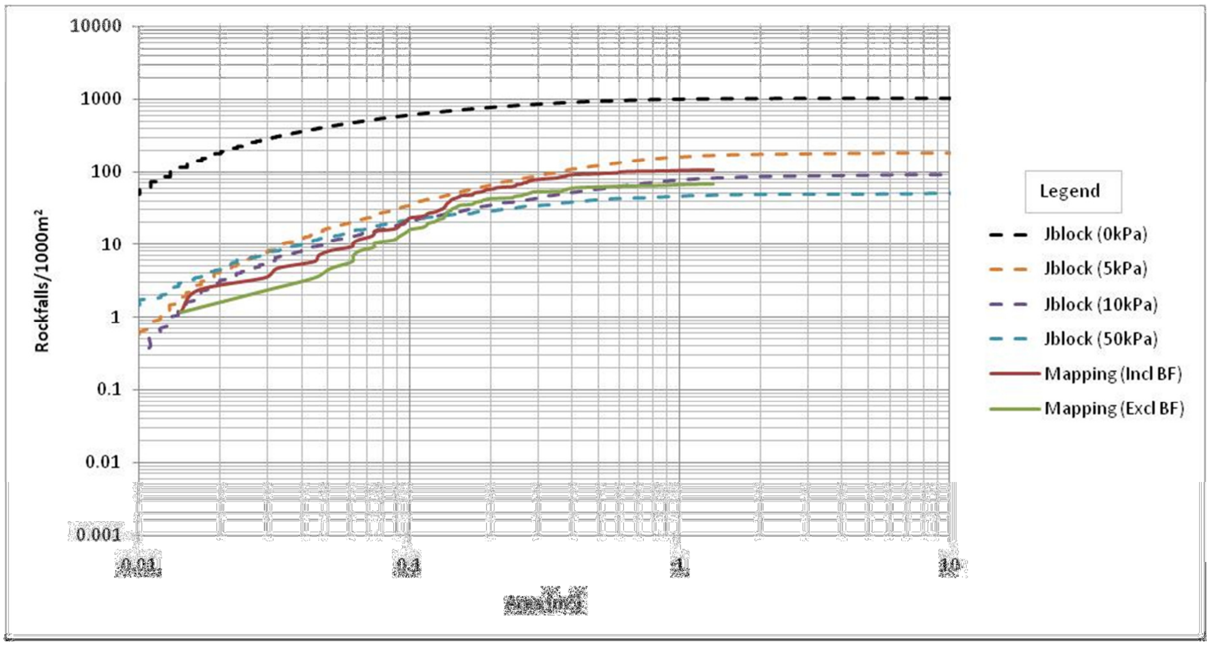

Figure 4-12: Merensky JBlock and mapping rockfall area distribution

Relationship between mapped rockfalls and JBlock simulated rockfalls

The above graphs show that excellent correlations can be obtained between the mapped rockfall data and the theoretically generated data. Visually, there appears to be a better correlation for the Merensky stopes under low clamping stresses, for small rockfalls. To quantify the agreement between one set of results and another, a measurement of error can be determined. There are several methods that can be used to define how well a simulation model is able to reproduce the data that are already known. Absolute error is the magnitude of the differences between the exact values and the simulation values. The relative error is the absolute error divided by the magnitude of the exact values. The percent error is the relative error expressed as a percentage. The L^2 relative error norm is the square root of the sum of the difference between the exact value and the approximation squared, divided by the sum of the exact values squared. The formulae for each of the error measures are as follows:

- Absolute Error: $\varepsilon = |u_e(i) - u_c(i)|$,
- Relative Error: $\eta = \dfrac{|u_e(i) - u_c(i)|}{|u_e(i)|} = \left|\dfrac{u_e(i) - u_c(i)}{u_e(i)}\right|$, $u_e(i) \neq 0$,
- Percentage Error: $\dfrac{|u_e(i) - u_c(i)|}{|u_e(i)|} * 100 = \left|\dfrac{u_e(i) - u_c(i)}{u_e(i)}\right| * 100$,

- L^2 Relative Error Norm: $L^2 = \sqrt{\frac{\sum_{i=1}^{i=NOE}(u_e(i) - u_c(i))^2}{\sum_{i=1}^{i=NOE}(u_e(i))^2}}$.

The above measures of fit are all calculated in a very similar way, where $u_e(i)$ denotes the exact values and $u_c(i)$ denotes the calculated values. When comparing the difference between the mapped and JBlock simulated rockfalls, the method of preference, and the one which is used in this study, is the L^2 relative error norm, because it calculates a sum total error that considers all the data points on the graphs to be compared.

The relationship between the simulated rockfalls and the mapped rockfalls has been evaluated for both volume and area properties. The cumulative frequency of both the actual recorded mapping data, excluding blast fractures, and the JBlock simulated data, are shown in Figure 4-13 for the Merensky reef volume at 5kPa clamping stress. The closer these two lines are to one another, the smaller the error, and the smaller the error, the better the rockfall simulation exercise. In order to compare the data, the following need to be noted:

- The mapped data is orders of magnitude less than that of the simulated JBlock data (34 actual rockfalls vs. 2348 simulated rockfalls)
- The error measure should be applied to the range of values which corresponds with the minimum and maximum values of the mapped data (the mapped data provide these parameters as JBlock has a much wider range)

In order to compare the results, the JBlock data was transformed or interpolated into a similar number of data points as the mapped data. The 2348 JBlock values are interpolated into a vector containing 34 values (the sam number as the mapped data) which still represents the total number of JBlock values. The interpolated values are shown in Figure 4-13 and they are within the same range as the mapped rockfall data. The interpolation only works to produce corresponding y-values for the interpolated curve. In this way the new 34 values for the JBlock interpolated values still represent the 2348 original values.

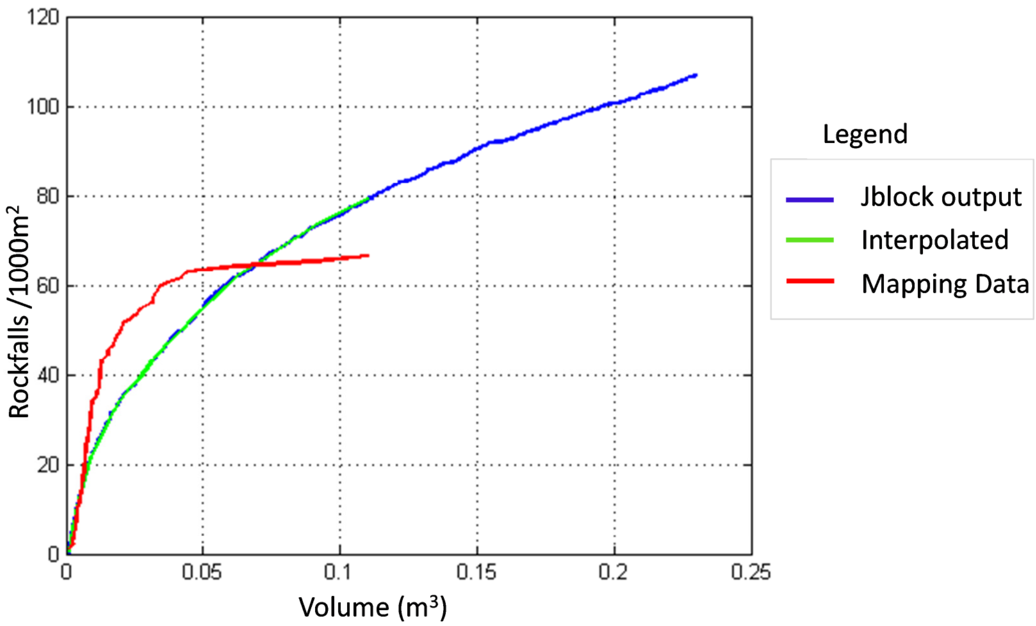

Figure 4-13: Merensky JBlock, interpolated JBlock, and mapped data representations for rockfall volumes at 5kPa clamping stress

With the interpolated values, the relative error norm was calculated for area and volume graphs. The results of the error calculations are presented in Table 4-2 and Table 4-3 for volume and area respectively.

Table 4-2: Area Correlation

Clamping Stress	% Goodness of fit	
	UG2	Merensky
0kPa	24	6
5kPa	44	54
10kPa	77	82
50kPa	27	49

Table 4-3: Volume Correlation

Clamping Stress	% Goodness of fit	
	UG2	Merensky
0kPa	48	9
5kPa	27	66
10kPa	18	52
50kPa	12	36

From these correlations, it can be observed that the JBlock rockfalls with no clamping stress have the worst representation of the mapped data for both reefs for both rockfall area and volume. The 10kPa clamping stress has a good correlation for area of rockfalls but it has a lower correlation for volume. However, the JBlock results for a 5kPa clamping stress are closest in representing the mapped rockfall data when comparing both the area and volume of rockfalls. Area generally has a better fit to the JBlock simulated rockfalls than volume for both the UG2 and Merensky reefs. It is expected that the clamping stress to give the "best fit" for simulated rockfalls will vary with depth below surface, location of mine on the Bushveld Complex, and also as a result of other local structures that may affect the stress regime on a mine.

4.3.2 Large Rockfalls and Injuries Correlation

The time available for recording rockfalls underground and the small dataset of large rockfalls has been deemed to be inadequate to carry out a conclusive rockfall correlation exercise. A larger data set, collected over many years with hundreds or thousands of rockfalls, and their consequences, is needed to better understand large rockfall behaviour.

Rockfall Data

Presented here is a set of rockfall information obtained from a number of shafts owned by the operators of mine A where a well-updated database of rockfalls is maintained. In these records there are over 17 000 recorded rockfalls since 1969. Most of these rockfalls are associated with the occurrence of a rockfall related accident. However, on a monthly cycle, strata control observers at the mine record rockfalls that occur in their respective working areas. In comparison with the mapped rockfalls, the rockfalls presented here represent mostly the large rockfalls category. It is difficult to normalise these rockfalls to an equivalent area because the mining area representing these rockfalls is not known accurately. Only the rockfalls that occurred in the stopes have been considered in this analysis as this was the focus area of this research.

Figure 4-14 presents the profile of rockfall frequency versus the distance behind the working face at which the rockfall occurred. The blue curve represents the historical mine rockfalls whilst the red curve represents the small rockfalls recorded during the course of this research. It should be noted that this graph represents the combined data for the UG2 and Merensky reef stopes mined on this property. The graph shows that 32% of the historical rockfalls fell on the face and up to 70% occurred within the face working area. Since the historical rockfalls are recorded on a monthly cycle or when there is an incident associated with a rockfall, there is a chance that the distance at which the rockfall occurs may not be have been recorded accurately. Therefore it is anticipated that the actual rockfall release profile is lies midway between the historical data and the carefully recorded rockfalls presented in Figure 4-14.

An analysis of the rockfall sizes and the distances they are released behind the face is shown in Figure 4-15. It can be observed that most of the rockfalls, irrespective of size, fall in the face area. The rockfalls gradually decrease in frequency with increasing distance from the face.

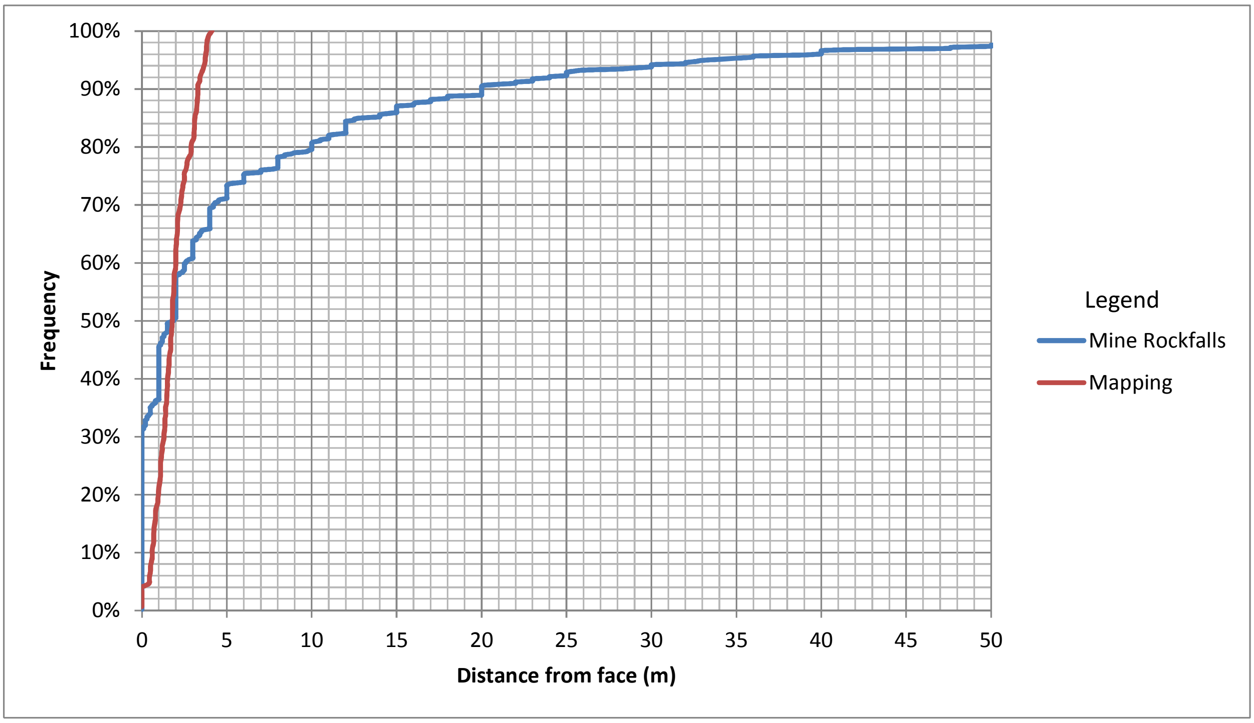

Figure 4-14: Rockfall frequency vs distance from face for mine rockfall data

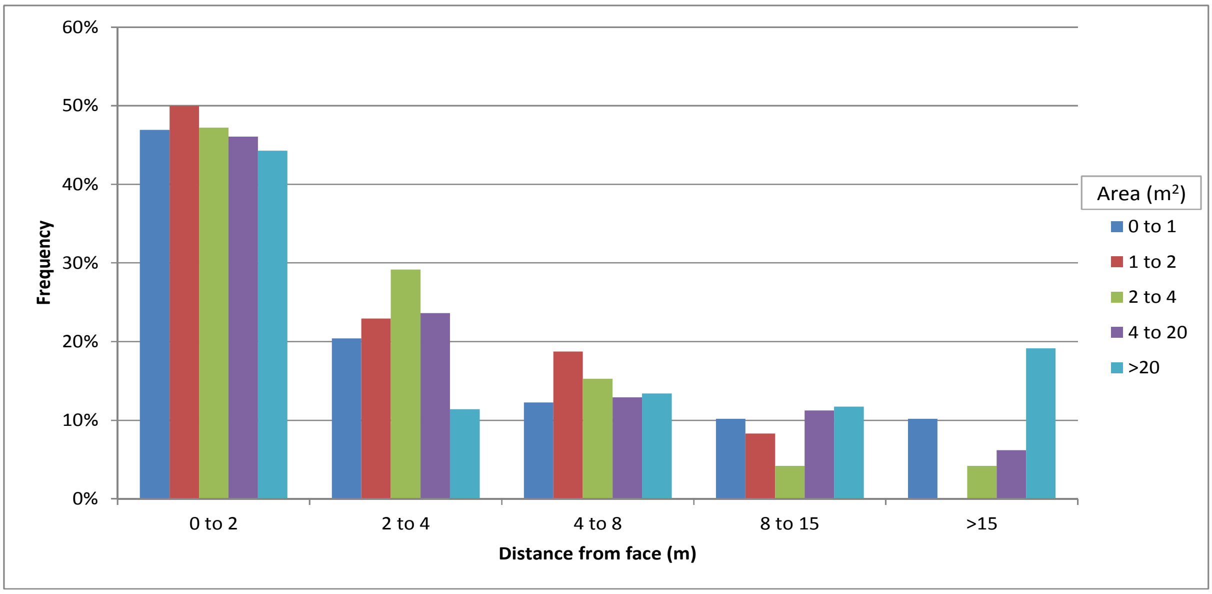

Figure 4-15: Frequency of rockfall area vs distance from face for mine rockfall data

Injuries Data

An analysis of rockfall related injuries at a number of shafts over an 8 year period on this mine is presented in Table 4-4. The proportions of the different injury categories have been calculated whilst including and excluding the non-lost time injuries. For the purpose of calculating the cost of injuries, the non-lost time injuries have been excluded, as these have no significant financial impact.

Table 4-4: Rockfall related injury and fatality ratios

Year	NLTI	LT	Reportable	Fatality	Stope production per annum (m^2)	Total Injuries /100 000m^2
2003	174	125	71	6	3 305 756	9.04
2004	204	113	67	5	3 329 560	9.52
2005	185	111	60	3	3 394 455	8.72
2006	239	107	89	3	3 446 243	10.3
2007	189	102	94	8	3 539 631	8.53
2008	185	93	71	3	3 538 085	7.66
2009	134	84	102	2	3 319 607	6.57
2010	132	125	93	11	2 873 029	8.95
Total	**1442**	**860**	**647**	**41**	**26 746 365**	
Average						**8.7**

Considering only the lost time injuries, reportable injuries and fatalities it was established that an average of 8.7 injuries/fatalities occurred per 100 000 m^2 mined. This average is important when correlating injuries predicted from the JBlock simulated rockfalls, which will be described in the next chapter dealing with case studies.

4.4 Discussion

This chapter has provided a review of keyblock simulation and stability analysis techniques. Based on the joint mapping data of Chapter 3, the statistical keyblock simulation pacakage JBlock was used to simulate potential rockfalls. From the presented simulation results, it can be concluded that there is good agreement between rockfalls predicted by JBlock and the actual rockfall data from underground mapping in the study areas covered, for the small rockfall size ranges. The maximum rockfall sizes recorded underground were 0.23m^3 and 0.46m^3 for the UG2 and Merensky stopes respectively, and these results represent the small rockfall size range. There are no reliable large rockfall data for comparison purposes. However, injuries that have been recorded on a mine over an 8 year period provide some basis for comparison with predicted injury data using JBlock rockfalls. The following chapter presents analyses of three case studies, comparing the effects of different support strategies on predicted rockfall occurrence and predicted injuries.

5 Case Studies

In the previous chapter, the methodology of keyblock stability analysis was reviewed. JBlock has been used to create rock blocks and test the keyblocks generated for different support systems. The predicted rockfalls have been correlated and compared with actual rockfalls that occurred underground. In this chapter, three Risk Evaluation case studies will be described. They have been carefully selected to demonstrate the benefit of using the risk evaluation approach to compare the cost and safety impacts of the different support strategies. The case studies are based on data collected from two mines, described in Chapter 3. It is important first to consider aspects of risk in order to understand clearly the risk evaluation case studies.

5.1 Review of Risk

The concept of risk in mining has been used widely in the design of open pits (Steffen, 2007; Narendranathan, 2009, Terbrugge et al, 2006; Stacey, 2006; Morriss and Stoter, 1983; Einstein, 1996; Horsley and Medhurst 2000). Its adoption and continued use is testimony of its success. In the past, very little has been done to introduce the risk concept to design for underground operations. However, more recently, the concept of quantifying risk has been applied to underground mining in the analysis of rockfalls (Stacey and Gumede, 2007; Joughin, 2010; and Rwodzi, 2011).

Risk is defined as the product of the probability of occurrence of an event and the consequences associated with that event (Whitman, 1983; Steffen, 2007, Cockram et al, 2004). The events of concern to rock engineers at underground mines are seismic events, panel collapses, rockbursts, support failure, pillar failure, and rockfalls among others. The consequences could be injury to personnel, financial losses and/or damage to the company image. There are many uncertainties associated with geological knowledge of the rock which necessitate that the risks associated with different excavation design approaches be quantified. The risk of injury as a result of a rockfall follows a chain of events as shown in Figure 5-1. These events are triggered by the occurrence of a rockfall (prediction using JBlock in this research) and the possibility of that rockfall occupying (occurring in) the same space and time as a person. Effective barring, identification of potential rockfalls and evacuation of people in such a place will considerably reduce the injury risk associated with a rockfall. However, the occurrence of injuries is not limited to the prediction of rockfalls alone. There are other contributing factors such as geological complexity, human behaviour, poor support installation and corrosion among others. These factors are however difficult to quantify and build into the event tree and have been omitted.

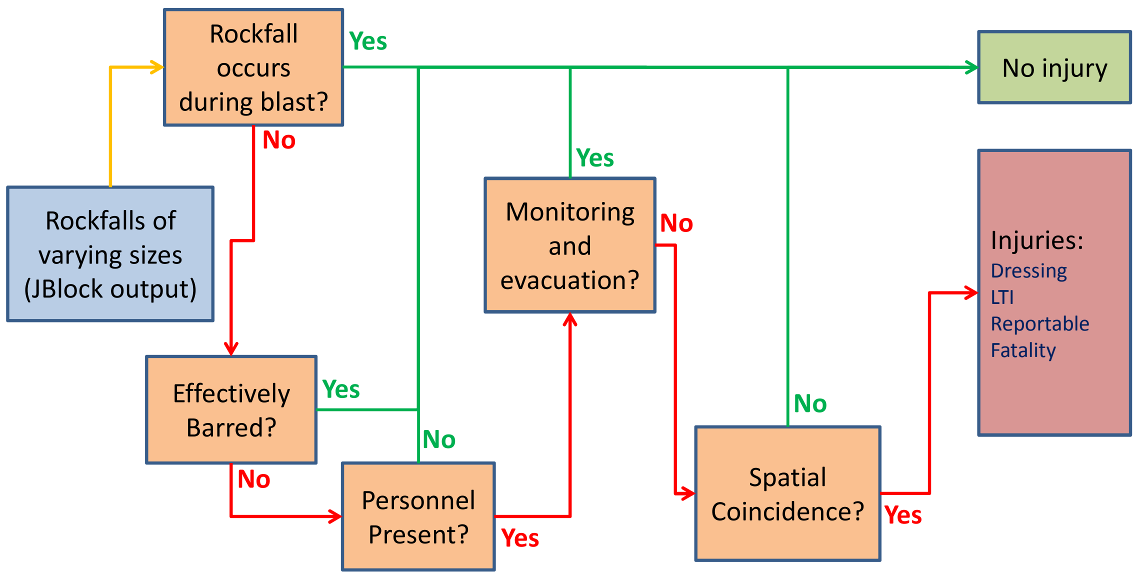

Figure 5-1: Injury Risk event tree

Apart from the injury or loss of life consequence itself, there are financial implications associated with a rockfall related injury (Rwodzi, 2011):

- Medical costs
- Production loss as a result of a mandatory (Section 54 of the Act) mine closure by the Department of Mineral Resources Inspector after a fatality
- SIMRAC (Safety in Mines Research Advisory Committee) levies related to the mine's accident record
- Legal and consulting fees associated with the event

These costs can be in the millions of rands for each fatality experienced at a mine.

When adopting the financial approach to analyse risk, it is prudent to look simultaneously at the cost of risk control and expected cost of the consequences. This has been described by Brummer and Kaiser (1995) as the risk-cost-benefit approach when evaluating the risks and costs associated with various support options. The cost of risk control and expected cost of the consequences are interrelated in that low spending to control risk results in high costs for the risk consequences and vice versa. The total cost for a risk control approach can guide the decision making process. However, the old approach when adopting a rockfall risk mitigation strategy in South African mines appears to have been guided by the cost of the risk controls alone (Ortlepp and Stacey, 1995). Design decisions were often dictated by cost cutting measures rather than from an understanding of the consequences associated with such decisions. The weakness of this approach has been exposed by quantifying the expected consequences of rockfall risk control measures in addition to the cost of rockfall control measures Rwodzi (2011). He showed that cost cutting decisions often end up being costly as a result of dealing with the consequences. In rock engineering, the rockfall risk consequences of concern are the safety and economic impacts as a result of a rockfall occurring. There are differing financial implications for the rockfalls that occur and these depend on the size and location of the rockfall (Figure 5-2). Small rockfalls in the face, sweeping and gully areas have associated dilution and production loss costs as a result of cleaning up the rockfall. If the rockfall fails support elements (JBlock provides this output) where there is people access, there is a resupport cost for that rockfall. For the large rockfalls in the face area, depending on the rockfall size, there is the potential to leave an in-stope pillar and re-establish the face, or to have a full face re-establishment.

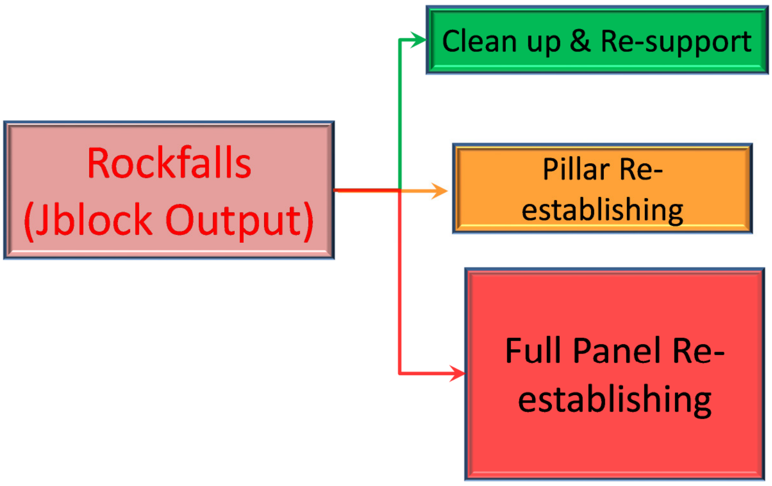

Figure 5-2: Rockfall remediation strategies

5.2 Financial and Injury Data

The parameters used to quantify financial and injury risk associated with different support strategies in the following case studies have been formulated in an almost similar manner and are presented in Appendices D.2, E.2, F.2 for the UG2 reef at mine A, and Merensky reef at mine A and B respectively. The production losses are based on long term price forecasts of platinum group metals (PGM) by five major banks presented by BMO Capital Markets (BMO, 2011). The PGM grade and metal ratios of the constituent elements are based on production figures provided in annual results of the owners of mine A and are consistent with observations made by Cawthorn (1999) and Cawthorn et al (2002) in the surrounding areas of the mine. Total mining costs have been obtained from annual results of the owners of mine A. The costs associated with injuries have been adapted from the research carried out by Rwodzi (2011). The mineral processing parameters have been adapted from SRK project experience when mining similar reefs in the Bushveld Complex. When calculating production losses, provision for an improved blasting efficiency of 70% during re-establishing has been made. This has been done so as to offset the production losses during pillar or full panel re-establishing with a faster rate of mining. The costs of different lengths of cable anchors and Hydrabolts were obtained through personal communication with the suppliers (Mathews, 2011 and New Concept Mining, 2011). Costs for mine poles have been obtained from data at the mine. The time and costs associated with drilling longer holes for longer support units has not been factored into the analysis. It is expected, however, that longer holes will increase costs associated with the support scenario.

The proportions for sub-dividing accidents into different injury categories presented in Table 4-4 in the previous chapter have been derived from a study of rockfall related accidents over an 8 year period from a number of mine shafts operated by the owners of mine A. The worker categories and the time spent in each zone are based on the mining strategy at mine A and have been established through communication with production personnel at this mine. A detailed list of the parameters and strategies for the three case studies to be presented in the following sections has been provided in the Appendices.

5.3 Case Study1 (UG2 reef at Mine A)

This case study is based on data collected on the UG2 reef from mine A. The site selection and data collection process for this case study have been described in sections 3.1.1 and 3.2 respectively.

5.3.1 Scenario Descriptions

The base case for the scenarios considered here is the support system that is currently being used for the UG2 at this mine. The support system used in the UG2 reef at mine A consists of mine poles only in the stope and 1.2m Hydrabolts in the gully. A number of support scenarios, which are mainly modifications to this support system, have been considered to compare the risk associated with rockfalls in each of the scenarios. The support scenarios considered are listed in detail below:

1. Mine poles only, this is the base case for comparative purposes. The support system layout for this scenario used at the mine is presented in Figure 4-2 and an image of this support layout reproduced in JBlock and the associated support properties has been presented in Figure 4-4.

2. Mine poles with a safety net in the working area. This support system will investigate the contribution of introducing a safety net (Skarbøvig et. al, 2011; Fernandes and Gardner, 2011) on the base case support system towards improving both safety and productivity. The safety net is a form of areal support, which has been the missing link in reducing the number of rockfalls occurring in stopes (Daehnke et al. 2001).
3. 1.2 m Hydrabolts and mine poles. This support system is an enhancement of the base case support by introducing 10T, 1.2 m Hydrabolts into the stope support. Any potential safety and profitability associated advantages as a result of this enhancement will be quantified.
4. 1.5 m Hydrabolts and mine poles. In this support system, the effect of increasing the Hydrabolt length from the initial proposed 1.2 m to 1.5 m is investigated and quantified.
5. 1.8 m Hydrabolts with mine poles. The purpose of testing this support system is to establish the cost and safety benefit that can be derived from having longer Hydrabolts than the two lengths previously considered.
6. 1.5 m cable bolts with mine poles. This support system is an enhancement of the base case support by introducing 25T, 1.5 m cable bolts in the stope support. The cable bolt support is superior in strength compared with the Hydrabolt support. Any potential safety and profit associated advantages as a result of introducing the high strength support system will be investigated and quantified.
7. 2 m cable bolts with mine poles. Potential safety and profit benefits associated with increasing the cable bolt length will be quantified in this support system.

The support scenarios described and their properties are presented in detail in Appendix D.1. In choosing these support scenarios, consideration has been given to the feasibility of installing the various support systems without a significant change in mining cycles and productivity in the stopes from the original support scenario. The support elements chosen are those readily available in the market in the Bushveld Igneous Complex underground mines. The hazard zones used in this case study are as described in section 4.2.

5.3.2 JBlock Results

Rock blocks for this case study have been generated in JBlock using the UG2 reef geometry and joint properties described in sections 3.1.1 and 3.4.1 respectively. In creating the rock blocks, JBlock has been set to create minimum and maximum block volumes of $0.01m^3$ and $10\ 000m^3$ respectively. These sizes have been selected in order to create a balanced set of blocks with both the large and small block sizes included. The rock blocks generated are made up of non-keyblocks and keyblocks. A total number of 100 574 rock blocks have been created representing a simulation area of 85 676 m^2. 38 369 of the rock blocks are keyblocks and these make up 71% of the total simulation area. The keyblocks have the potential to fall into an excavation and cause injuries and production losses when exposed in the hangingwall. These keyblocks will be tested on each support scenario considered.

The distribution of keyblock sizes generated in JBlock for the UG2 reef is shown in Figure 5-4. From this distribution it can be observed that there is a gradual reduction in the frequency of rockfalls of size greater than $0.5m^3$.

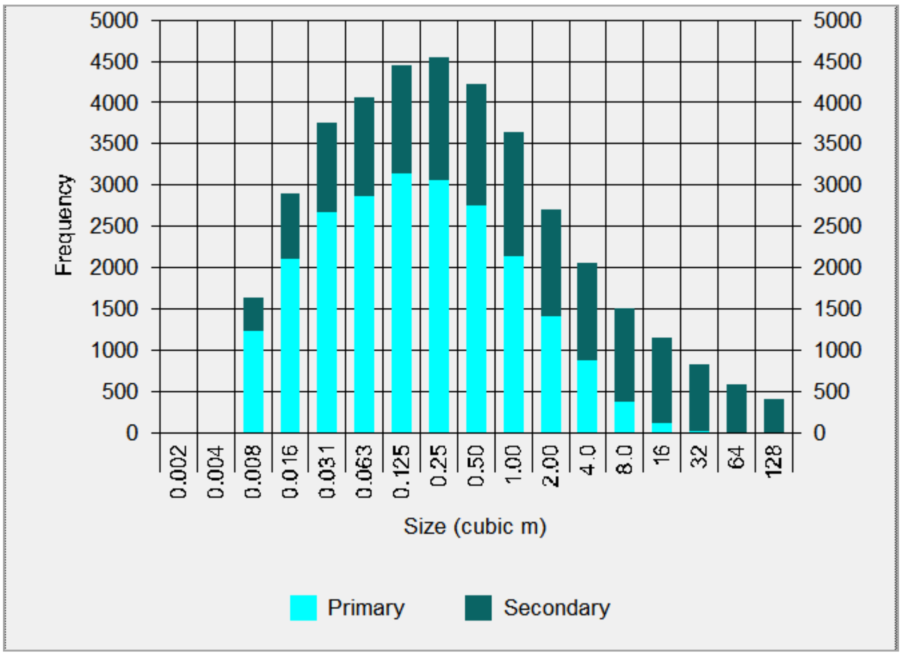

Figure 5-3: Keyblock size distribution for UG2 reef at mine A

From the correlation exercise in section 4.3, a clamping stress of 5kPa has been adopted in testing this set of keyblocks in all the described support scenarios in this case study. The JBlock rockfall results for case study 1 are presented in Table 5-1. The rockfalls affecting production have been referred to as large rockfalls in the table. These results are important because they have an effect on the cost and safety impact on the respective support scenario. In terms of rockfalls, the current support scenario used at the mine is the worst of all the systems in preventing rockfalls from occurring. Introducing a safety net to the mine poles reduces the number of rockfalls occurring by up to 50% as observed when safety nets were added to the mine poles scenario in Table 5-1. In reality once the safety net is removed, the rocks can fall to the ground. The introduction of Hydrabolts in the stope also improves the effectiveness of support in arresting rockfalls. The use of a superior strength cable anchor reduces the number of rockfalls. In both types of tendon support, the increase in length of support elements results in a decrease in the frequency of rockfalls. Dilution in this case study and the others to follow is obtained by dividing the rockfall volume by the surface area of the rockfall. This gives an average thickness of the rockfalls.

Table 5-1: Summary of rockfalls for case study 1

Support System	Large Rockfalls/1000m^2	% Area Rockfall	% Area Large Rockfall	Dilution (m)
Mine Poles	0.86	9.7	3.3	0.063
Mine Poles + Safety Net	0.34	2.8	1.6	0.020
1.2m Hydrabolt + Mine Pole	0.40	4.7	2.2	0.040
1.5m Hydrabolt + Mine Pole	0.34	4.0	1.9	0.033
1.8m Hydrabolt + Mine Pole	0.29	3.2	1.4	0.023
1.5m Cable Anchor + Mine Pole	0.05	1.8	0.2	0.011
2.0m Cable Anchor + Mine Pole	0.01	1.6	0.1	0.007

5.3.3 Risk Evaluation and Comparison of Results

Each rockfall, with each support scenario, is evaluated to determine the risk it is likely to cause. This risk for each support scenario, as described in section 5.1, depends on rockfall size and location, i.e. the zone in which it falls. The summary of risk evaluation results for this case study is presented in Table 5-2.

Table 5-2: Summary of risk evaluation results for case study 1

Support System	Cost/m^2								Injuries per 100000m^2
	Support Cost	Losses due to rockfalls						Total Cost	
		Dilution	Sweepings	Re-support	Production	Injury	Total		
Mine Poles	R 22.00	R 27.28	R 4.72	R 0.27	R 119.33	R 17.92	R 169.51	R 191.51	5.4
Mine Poles + Safety Net	R 22.00	R 8.67	R 2.62	R 0.08	R 48.72	R 4.28	R 64.36	R 86.36	1.3
1.2m Hydrabolt + Mine Pole	R 67.00	R 17.02	R 2.75	R 0.84	R 73.39	R 9.69	R 103.70	R 170.70	2.9
1.5m Hydrabolt + Mine Pole	R 73.00	R 14.09	R 2.65	R 0.65	R 57.34	R 8.52	R 83.26	R 156.26	2.6
1.8m Hydrabolt + Mine Pole	R 80.00	R 9.86	R 2.57	R 0.47	R 48.01	R 7.59	R 68.50	R 148.50	2.3
1.5m CableAncho r+ Mine Pole	R 102.00	R 4.65	R 0.22	R 0.19	R 4.10	R 3.91	R 13.06	R 115.06	1.2
2.0m Cable Anchor + Mine Pole	R 107.00	R 2.90	R 0.19	R 0.09	R 1.58	R 3.44	R 8.20	R 115.20	1.0

For all except two of the support scenarios, the highest loss contributor is the production loss. The trend in production losses is a reflection of the effectiveness of the support used to arrest rockfalls in each scenario. All the other losses listed in the table follow a similar trend to the production losses. Mine poles have the highest production losses whilst at the same time they have the least cost of support. However, when looking at the combined cost for the losses and cost of support strategy, the low support cost does not compensate for the large production losses. Therefore, the overall costs associated with a support strategy are controlled by the production losses, and every effort should be directed towards containing this cost by having a support strategy that reduces the frequency of rockfalls.

The support costs for mine poles and mine poles with safety nets are similar because a safety net is re-used for a while at the mine and the cost eventually becomes insignificant. However, the dilution, sweepings, re-support and production costs associated with the addition of a safety net are being underestimated. The safety net only protects people underneath rockfalls by holding them but these rocks will eventually fall in a controlled manner when the safety net has been removed.

The number of injuries per 100 000 m^2 mined is also highest with the mine pole support system. The injuries are again directly proportional to the frequency of rockfalls. When a safety net is added to the mine pole support there is a 76% reduction in the number of injuries. Please note that the rockfalls reported in Table 5-1 are rockfalls that occurred in all the zones whilst the injuries are only calculated for rockfalls that took place in the face area, gulley and sweepings area. Therefore, increasing areal support, in the form of safety nets, mesh or straps, in the face area alone has the ability to significantly reduce injuries, since that is where the majority of the rockfalls occur soon after being exposed. Most of the underground workforce is also confined to the face area, thereby increasing exposure and injury risk.

5.4 Case Study 2 (Merensky reef at Mine A)

This case study has been based on the mapping exercise carried out on the Merensky reef at mine A described in Chapter 3.

5.4.1 Scenario Descriptions

The base case for the scenarios considered here is the support system that is currently used at this mine. The support system used at mine A consisted of a combination of mine poles and 1.2 m Hydrabolts in the stope, and 1.2 m Hydrabolts in the gully. A number of support scenarios derived mainly from this support system have been considered to compare the risk associated with rockfalls in each of the scenarios. The support scenarios considered are listed below:

1. 1.2 m Hydrabolts and mine poles. A combination of the 10T, 1.2 m Hydrabolt and mine pole support system in the stope is currently being used for supporting the Merensky reef hangingwall at mine A. From the rockfalls experienced with this support scenario, associated potential safety and profit benefits will be quantified.
2. 1.5 m Hydrabolts and mine poles. In this support system, the effect of increasing the Hydrabolt length in the stope and gully from the initial 1.2 m is investigated and quantified.
3. 1.8 m Hydrabolts with mine poles. The purpose of testing this support system is to establish the cost and safety benefit that can be derived from having a longer Hydrabolts than the two lengths previously considered.
4. 1.5 m cable bolts with mine poles. This support system is an enhancement of the base case support by introducing 25T, 1.5 m cable bolts in the stope support. The cable bolt support is superior in strength compared with the hydrabolt support. Any potential safety and profitability associated advantages as a result of introducing the high strength support system will be investigated and quantified.
5. 2 m cable bolts with mine poles. Potential safety and cost benefits associated with increasing the cable bolt length will be quantified in this support system.
6. 1.2 m Hydrabolts, mine poles and safety net. This support scenario is an enhancement of the base case support system by adding a temporary safety net support (Skarbøvig et. al, 2011) to the existing 10T, 1.2 m Hydrabolt and mine pole system. The safety and cost benefits of introducing a safety net in the face area will be evaluated in this support scenario.

The support scenarios described and their properties are presented in detail in Appendix E. Consideration of the feasibility of installing the various support systems without a significant change in mining cycles and productivity in the stopes from the original support scenario has been made in choosing these support scenarios. The hazard zones used in this case study are as described in section 4.2.

5.4.2 JBlock Results

The Merensky reef geometry and joint properties described in sections in section 3.1.1 and 3.4.2 respectively. JBlock has been used in creating the blocks and as in the previous case study, the minimum and maximum simulated block volumes are 0.01m^3 and 10 000m^3 respectively. The blocks generated are made of non-keyblocks and keyblocks. A total number of 311 361 blocks have been created representing a simulation area of 71 907 m^2. 78 605 of the rock blocks are keyblocks and these make up 54% of the total simulation area.

The keyblocks have potential to fall into an excavation when exposed and will be tested on each support scenario considered.

The distribution of keyblock sizes generated in JBlock for the Merensky reef is shown in Figure 5-4. From this distribution it can be observed that there is a significant reduction the frequency of rockfalls of size greater than 0.25m^3.

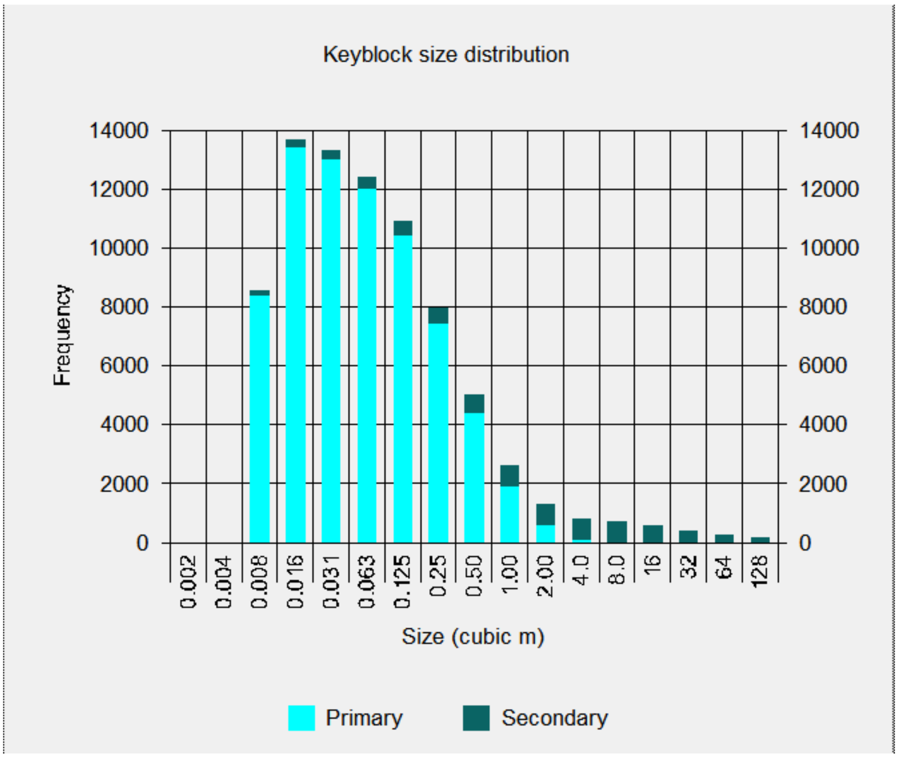

Figure 5-4: Keyblock size distribution for Merensky reef at mine A

Table 5-3: Summary of rockfalls for case study 2

Support Scenario	Large Rockfalls/1000m2	% Area Rockfall	% Area Large Rockfall	Dilution (m)
1.2m Hydrabolt + Mine Pole	3.0	12.3	6.9	0.070
1.5m Hydrabolt + Mine Pole	2.5	11.6	6.7	0.077
1.8m Hydrabolt + Mine Pole	2.4	11.3	6.3	0.067
1.5m Cable Anchor + Mine Pole	2.0	9.9	5.9	0.062
2.0m Cable Anchor + Mine Pole	1.6	8.6	5.0	0.060
1.2m Hydrabolt + Mine Pole + Net	1.1	5.5	3.5	0.022

A clamping stress of 5kPa has been used in testing this set of keyblocks in all the described support scenarios in this case study. The JBlock rockfall results for this case study are presented in Table 5-3. This case study generally has more rockfalls per area simulated compared with case study 1. The base case mine support used in this case study shows the highest number of rockfalls occurring. When a safety net is introduced to the support system being used at the mine, the number of rockfalls occurring is reduced by 63%. Similarly, increasing the Hydrabolt length and introducing a superior strength cable anchor results in an overall decrease in the frequency of rockfalls.

5.4.3 Risk Evaluation and Comparison of Results

As for the previous case study, the risk evaluation process involves each single rockfall in each support scenario. Again the risk depends on rockfall size and location of fall. The summary for risk evaluation results of this case study are presented in Table 5-4.

Table 5-4: Summary of risk evaluation results for case study 2

Support System	Cost/m^2									Injuries per 100000m^2
	Support Cost	Losses due to rockfalls							Total Cost	
		Dilution	Sweepings	Re-support	Production	Injury	Total			
1.2m Hydrabolt+Mine Pole	R 59.00	R 29.98	R 16.67	R 1.54	R 451.45	R 34.67	R 543.31		R 593.31	9.5
1.5m Hydrabolt+Mine Pole	R 65.00	R 32.99	R 16.16	R 1.43	R 409.90	R 32.01	R 492.49		R 557.49	8.7
1.8m Hydrabolt+Mine Pole	R 71.00	R 28.85	R 15.71	R 1.54	R 399.61	R 30.75	R 476.46		R 547.46	8.4
1.5m Cable Anchor+Mine Pole	R 94.00	R 26.58	R 14.15	R 1.46	R 369.00	R 27.28	R 438.46		R 532.46	7.5
2.0m Cable Anchor+Mine Pole	R 98.00	R 25.48	R 11.86	R 1.01	R 311.08	R 23.57	R 373.00		R 471.00	6.4
1.2m Hydrabolt+Mine Pole+Net	R 59.00	R 9.63	R 9.08	R 0.48	R 195.51	R 12.95	R 227.66		R 286.66	3.5

The base case support system, 1.2 m Hydrabolts and mine poles, has the highest production losses whilst at the same time the lowest cost of support. However, when looking at the combined cost for the losses and cost of support strategy, the low support cost does not compensate for the large production losses. Therefore, the costs associated with a support strategy are controlled by the production losses and every effort must be directed towards containing this cost by having a support strategy that reduces the frequency of rockfalls. The introduction of a safety net to the support results mainly in a reduction of the injuries to be experienced. The other associated costs will be identical to the support scenario with no safety net as the net does not inhibit the occurrence of a rockfall but rather controls the occurrence of a rockfall such that people will not be injured.

The number of injuries per 100 000 m^2 mined is highest with the base case 1.2 m Hydrabolt and mine pole support system. The injuries are again directly proportional to the frequency of rockfalls. The introduction of a safety net to the base case support results in 63% less injuries than when there is no net. As in case study 1, increasing areal support in the form of nets in the face area alone is very effective in reducing injuries. Increasing the tendon support length also reduces the frequency of rockfalls and at the same time the injuries associated with that particular support scenario. In this case study, the 2 m 25T cable anchor support system predicts the lowest injury risk and has the lowest overall cost because of its ability to support the greatest number of keyblocks.

5.5 Case Study 3 (Stope cable anchors at Mine B)

The Merensky reef at Mine B is extremely blocky and therefore case study 3 has been focused on the Merensky reef only. The mine changed its stope support system from its old 12T, 1.5 m cable anchors, used in combination with mine poles, to a new 25T, 3 m cable anchor support with no mine poles. The mine wanted to better understand the performance of their current 25T, 3m cable anchor support system in comparison with the old support system, and also to investigate possible improvements to the system.

5.5.1 Scenario Descriptions

Mine B had been using 1.5 m long (12T) cable anchors with in-stope mine poles (pencil sticks) (Figure 5-5) and decided to change this support, replacing it with a 3 m long (25T) cable anchor, timber-less support system (Figure 5-6). The main differences between these two support layouts is that the old system has mine poles, plus cables anchors which are spaced on a 0.9 m by 1.5 m grid. In the replacement support system, the 3m cable anchors are spaced on a grid of 1 m by 1.5 m, and there are no mine poles. The risks and costs associated with the change in support strategy were investigated and quantified in this case study.

The support layout and properties utilised in JBlock for this case study have been adapted from the mine standards. The hazard zones used in this case study are as described in section 4.2. The specified strength of the cable anchors, 200kN, has been downgraded from 250kN to cater for possible poor bolt installations at the mine.

Table 5-5: Case study 3 support scenario and strengths

Support Scenario	**Support unit strength**
1.5m Cable Anchor Support	200kN
2.0m Cable Anchor Support	200kN
2.5m Cable Anchor Support	200kN
3.0m Cable Anchor Support	200kN
3.5m Cable Anchor Support	200kN
4.0m Cable Anchor Support	200kN
1.5m Cable Anchor + Mine Poles	120kN for cables, 250kN for Mine poles

The stope layout for the support scenarios and the support properties used for this case study are detailed in Appendix F.

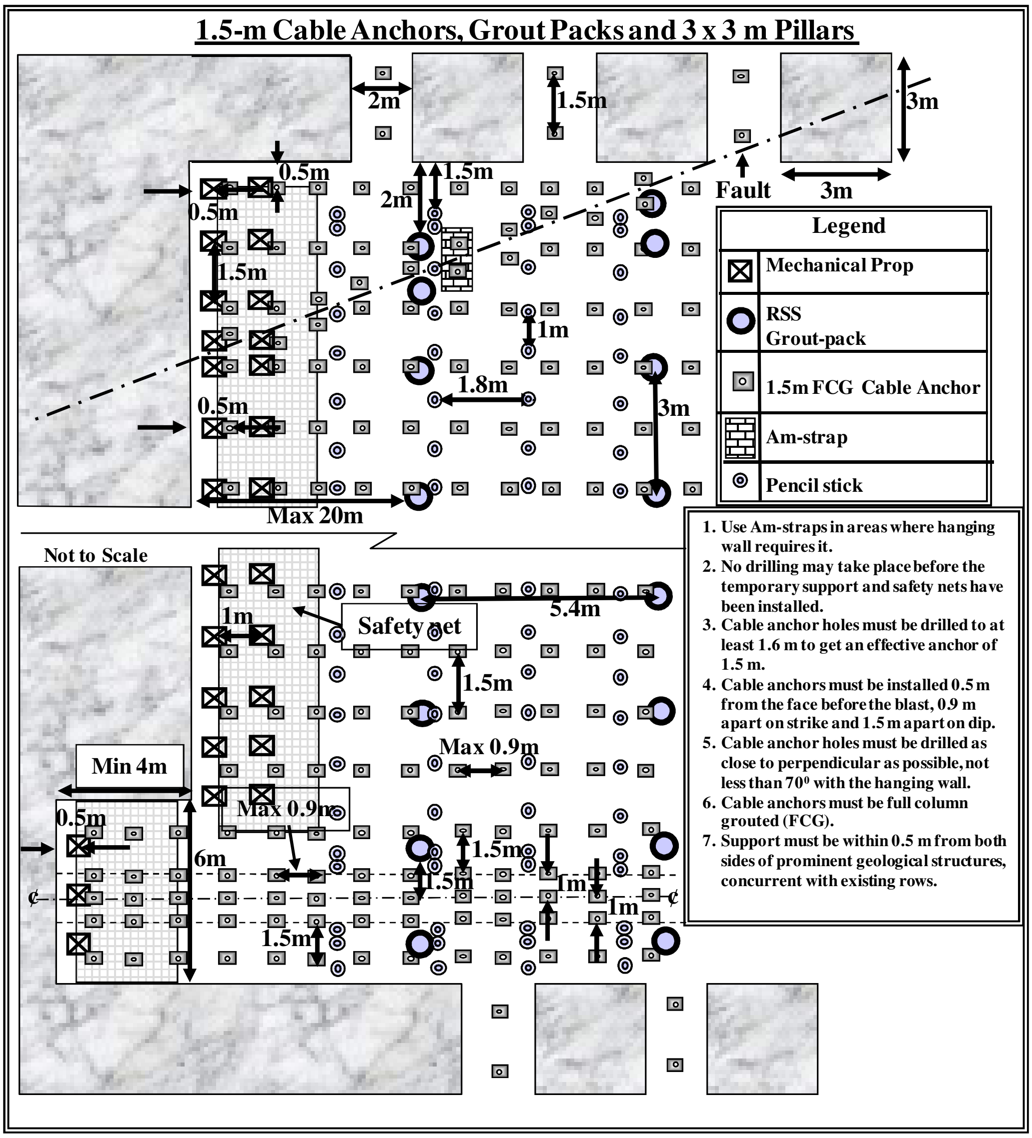

Figure 5-5: 1.5 m Cable Anchor support system

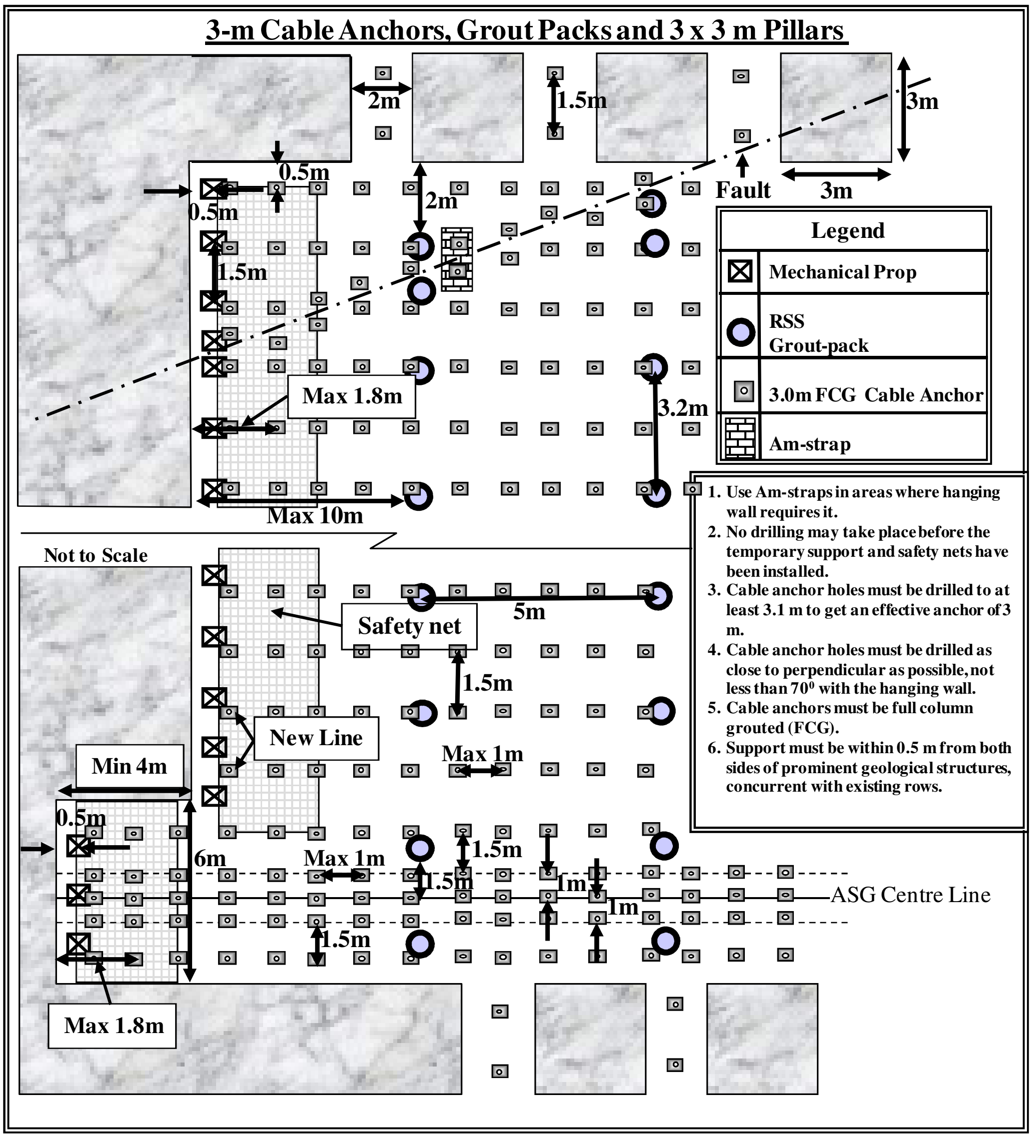

Figure 5-6: 3 m Cable Anchor support system

5.5.2 JBlock Results

The Merensky reef geometry and joint properties described in sections in sections 3.1.2 and 3.4.3 respectively. In creating the rock blocks, JBlock has again been set to create minimum and maximum block volumes of $0.01m^3$ and $10\,000m^3$ respectively. A total number of 409 084 blocks have been created representing a simulation area of 40 659 m^2. 73 611 of the rock blocks are keyblocks and these make up 49% of the total simulation area.

The distribution of keyblock sizes generated in JBlock for the Merensky reef is shown in Figure 5-7. From this distribution it can be observed that there is a significant reduction in the frequency of rockfalls of size greater than $0.125m^3$.

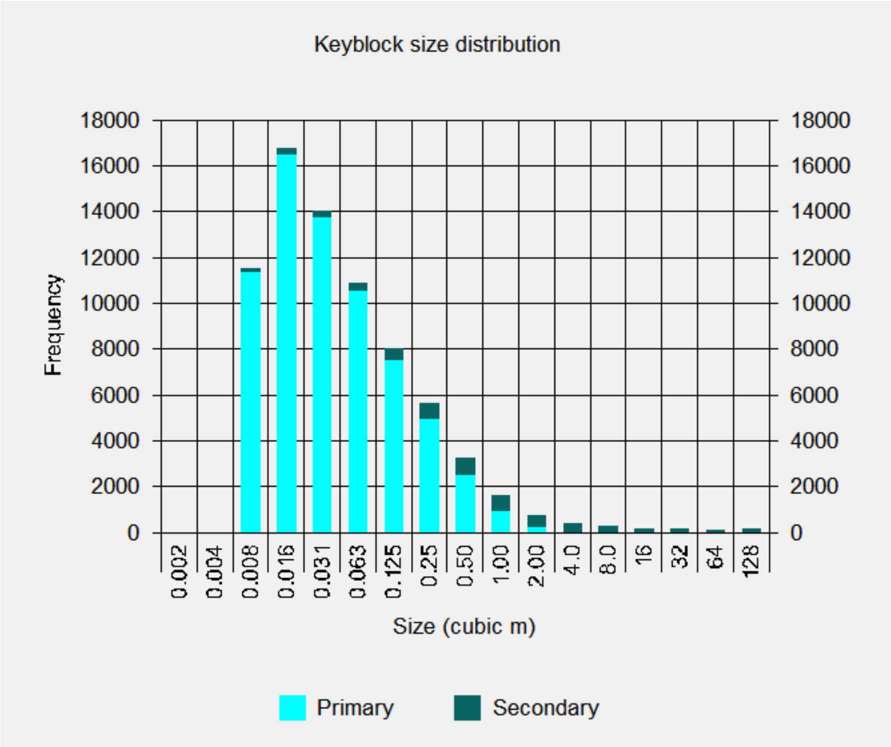

Figure 5-7: Keyblock size distribution for Merensky reef at mine B

A clamping stress of 5kPa has been adopted in testing all the described support scenarios in this case study. The keyblocks that failed in the JBlock analyses for case study 3 are presented in Table 5-6.

Table 5-6: JBlock results for case study 3

Support System	Large Rockfalls/1000m^2	% Area Rockfall	% Area Large Rockfall	Dilution (m)
1.5m Cable Anchors	1.22	8.3	4.8	0.086
2.0m Cable Anchors	0.89	7.9	3.7	0.076
2.5m Cable Anchors	0.74	7.7	3.5	0.071
3.0m Cable Anchors	0.69	7.5	3.2	0.065
3.5m Cable Anchors	0.52	7.2	2.8	0.063
4.0m Cable Anchors	0.51	7.0	2.7	0.061
1.5m (12T)+Pencil Sticks	1.08	8.0	3.9	0.079

The 1.5 m 25T cable anchor support system records the highest number of rockfalls predicted. As the cable anchor length is increased, the numbers of rockfalls predicted decreases. An analysis of the the rockfalls that occurred as a result of support failures is presented in Figure 5-8, and illustrates the effect of increased cable bolt length.

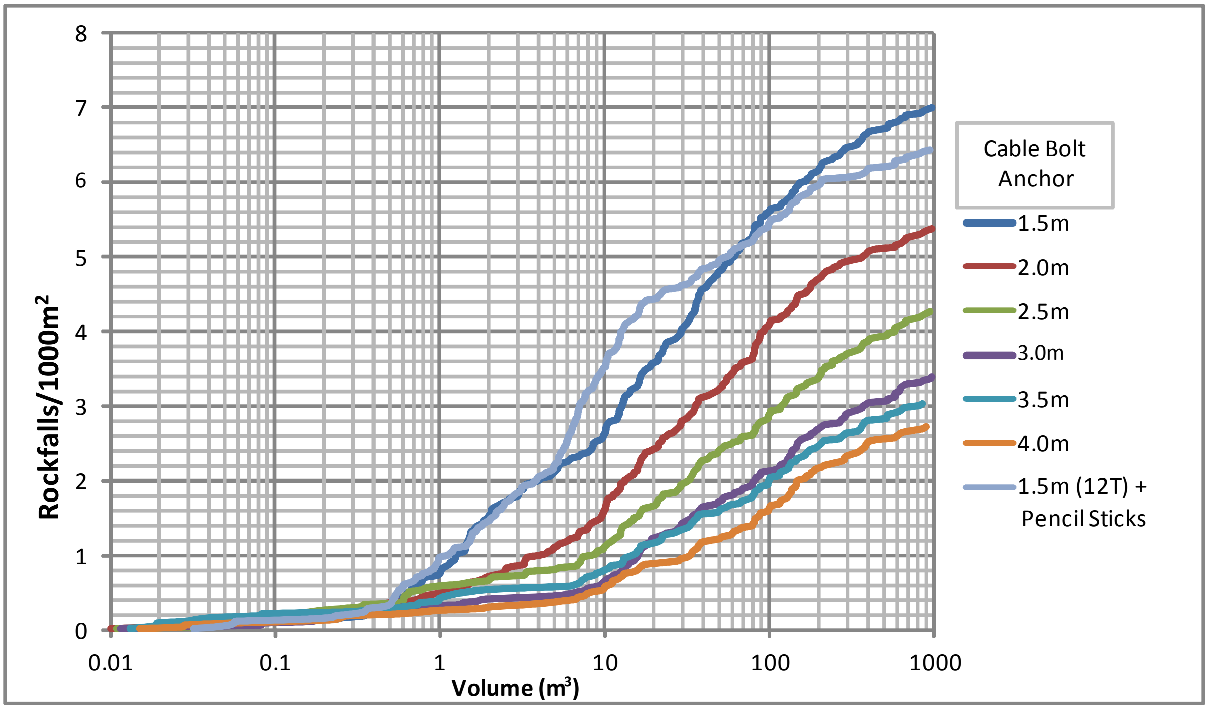

Figure 5-8: Rockfalls in which support failed for case study 3

What is evident from this study is that increasing the length of the cable anchors reduces the number of rockfalls that are expected to occur in the mining area.

5.5.3 Risk Evaluation and comparison results

The results for the risk associated with each support scenario are directly related to the frequency of rockfalls and are presented in Table 5-7. Although the lower strength cable anchors are cheaper that the higher strength cable anchors, they are on a denser spacing pattern and mine poles are also included in the support scenario, making this support scenario more expensive than the rest in this case study. The cost of drilling has not been included in the analyses because it could not be ascertained. It is expected that the overall drilling cost for a support scenario will be affected by the length of cable anchor used, with highest costs expected for the longest cables. The time spent whilst drilling is also likely to influence the economics of the support scenarios. Both of these factors will influence the cost of the support. In a similar fashion to case studies 1 and 2, the production losses constitute the highest cost. The costs are directly proportional to the number of rockfalls and the numbers decrease with increasing length of cable anchor.

Table 5-7: RiskEval case study 3 results

Support Scenario	Cost/m²								Injuries/100 000m²
	Support Cost	Losses due to rockfalls						Total Cost	
		Dilution	Sweepings	Re-support	Production	Injury	Total		
1.5m Cable Anchors	R 80.00+	R 25.93	R 11.57	R 1.11	R 564.35	R 31.64	R 634.60	R 714.60	5.9
2.0m Cable Anchors	R 84.00+	R 23.96	R 9.28	R 0.88	R480.21	R 27.34	R 541.67	R 627.57	5.1
2.5m Cable Anchors	R 89.00+	R 23.22	R 8.66	R 0.81	R 401.13	R 26.42	R 460.24	R 549.24	5.1
3.0m Cable Anchors	R 94.00+	R 22.52	R 7.16	R 0.73	R 394.72	R 25.87	R 451.00	R 545.00	4.8
3.5m Cable Anchors	R 99.00+	R 20.33	R 6.27	R 0.69	R 279.38	R 22.41	R 329.08	R 428.08	4.6
4.0m Cable Anchors	R 104.00+	R 19.60	R 6.27	R 0.65	R 254.63	R 22.86	R 304.01	R 408.01	4.5
1.5m (12T)+Pencil Sticks	R 121.00+	R 24.60	R 9.72	R 0.87	R 551.00	R 28.59	R 614.78	R 735.78	5.4

The predicted number of injuries is highest when using the 1.5 m cable anchor. There is a reduction in the number of rockfalls when comparing the old (12T) 1.5 m cable anchors plus mine pole support with the replacement (25T) 3 m cable anchors. The injuries and costs are directly proportional to the number of rockfalls experienced with each support scenario. An increase in the cable bolt length results in a reduction in the number of rockfalls and the risks associated with them.

5.6 Summary

In this chapter, three case studies have been presented. In each case study, different support scenarios have been considered and the rockfall injury and cost risk associated with each scenario has been quantified. Risk was evaluated for each rockfall that has been simulated in JBlock. It has been demonstrated that improving a support scenario by increasing the length, strength and areal coverage of support units results in reduced numbers of injuries, as well as reduced overall costs, even though direct costs may increase. It has been demonstrated in two of the case studies that over 60% of injuries can be eliminated by introducing a safety net to a support system. The approach presented can be used in the selection of the optimum support that will result in minimal injuries and losses for a particular geotechnical domain. The uncertainity of support performance using the traditional trial and error method when mining in a new area can be significantly reduced.

6 Conclusions and Recommendations

As a result of the need to improve safety and profitability, there has been a recent shift in rock engineering from the traditional deterministic methods towards the use of probabilistic methods for evaluating stability. The probabilistic keyblock stability methods allow rockfalls to be predicted based on joint data collected by mapping of rock surfaces.

In the research carried out, an underground mapping programme was executed in two platinum mines of the Bushveld Igneous Complex. The joint property data, joint dip, dip direction, spacing and length/size, has been processed to produce the statistical variability of these properties. It is believed that this has produced a database joint data for the mines that has not existed before. In addition, a programme of underground mapping was also carried out to record actual rockfalls and their statistics – volume, area, length and location with respect to the face.

The joint data has been used to simulate potential keyblocks and hence predict rockfalls using JBlock, a probabilistic keyblock stability method. A clamping stress in the stope hangingwall was applied in JBlock to allow calibration the numbers and sizes of simulated rockfalls with the actual recorded rockfall data. Reasonable correlations were obtained between the simulated rockfalls and the actual recorded rockfalls for the small rockfalls category, giving confidence in the JBlock rockfall prediction approach. The research work has provided a validated method that can be used for comparative stope support design in the tabular stopes of the Busveld Complex mines.

Using this approach, different support scenarios have been tested on three case studies to investigate their effectiveness in reducing rockfalls. An analysis of injury and cost risk has been carried out for each support scenarios considered in each case study. The following conclusions can be drawn from the case studies:

- Increasing the length of tendon support results in reduced numbers of rockfalls, and hence a reduction in predicted injuries.
- Using areal support such as safety nets considerably reduces the predicted numbers of injuries.
- In almost all support scenarios, the largest cost was that of loss of production.

- Increasing support, and hence direct support costs, in almost all cases considered reduced the overall costs owing to the reduction in consequential costs such as production losses.

Importantly, the approach allows the risk of injury to mineworkers, and the financial risk due to loss of potential revenue as a result of rockfalls to be quantified.

The research described in this dissertation has proven that, based on knowledge of joint characteristics in the rockmass, realistic predictions of potential rockfalls can be made. This provides the basis for a rational and more robust design of appropriate stope support to enhance safety, and add value for the mine, taking risk into account quantitatively. The rock engineering design process therefore becomes a strategic design process rather than the tactical process that is the common practice on most mines at present. The output of the research is a stope support design method that can be implemented immediately in the Bushveld Complex mines, and the expected result is improved safety and profitability.

The rockfalls mapped underground in this research lie in the small rockfall category. Therefore the comparisons made between mapped and simulated rockfalls has been limited to the small rockfalls category only. This limitation can be remedied by further rockfall mapping underground in order to develop a larger and more balanced database of both small and large rockfalls. There is also need to improve JBlock to ensure that it provides even better predictions of rockfalls. These two shortcomings represent areas requiring further research.

7 References

Adu-Acheampong, A., (2003). Importance of geotechnical field mapping in assessing the stability of underground excavations. SME Annual Meeting, February 24-26, Cincinnati.

Baczynski N.R.P., (2000). STEPSIM4 'step–path' method for slope risks. In Proceedings of the GeoEng2000 Conference, Melbourne. Vol. 2: 86–92.

Baczynski N.R.P., (2008). STEPSIM4 Revised: Network Analysis Methodology for Critical Paths in Rock Mass Slopes. In Proceedings of the 1st Southern Hemisphere International Rock Mechanics Symposium, Perth. Australian Centre for Geomechanics. Vol. 1: 405-418.

Baecher, G.B; Lanney, N.A, and Einstein H.H, (1977). Statistical description of rock properties and sampling. Proceedings 18th US Symposium on Rock Mechanics, June 22-24, Colorado

Baecher, G.B., and Lanney, N.A. (1978). Trace length biases in joint surveys. Proceedings 19th U.S. Symposium on Rock Mechanics, Nevada, pp. 56-65.

Baecher G.B., (1983). Statistical analysis of rock mass fracturing. Journal of Mathematical Geology, 15 (2): 329-347.

Baker, D., (1993). Some notes on the statistics on rock engineering problems and fall of ground accidents in the South African mining industry for the period 1998-1992 with special reference to the Bushveld Igneous Complex mines. Rock Engineering Problems Related to Hard Rock Mining at Shallow and Intermediate Depth. SANGORM Symposium, Rustenburg, pp.1-19.

Barton, N.R. (1973). Review of a new shear strength criterion for rock joints. Engineering Geology, 7: 287-332.

Barton, N., Lien, R., and Lunde, J., (1974). Engineering classification of rock masses for the design of tunnel support. Rock Mechanics. 6 (4): 189-236.

Barton, N., (1976). The shear strength of rock and rock joints. International Journal of Rock Mechanics and Mining Sciences and Geomechanical Abstracts. 13: pp. 1-24.

Barton, N.R., and Choubey, V., 1977. The shear strength of rock joints in theory and practice. Rock Mechanics. 10 (1):1-54.

Barton, N., Bandis, S., and Bakhtar, K., (1984). Strength, deformation and conductivity coupling of rock joints. International Journal of Rock Mechanics and Mining Sciences and Geomechanical Abstracts. 22 (3): pp. 121-140.

Barton, N.R., and Bandis, S.C., (1990). Review of predictive capabilities of JRC-JCS model in engineering practice. Proceedings International Symposium on Rock Joints, Loen, Norway.

Barton, N., (2002). Some new Q-value correlations to assist in site characterisation and tunnel design. International Journal of Rock Mechanics and Mining Sciences. 39 (2): 185–216.

Beauchamp, K.J., Carvalho, J., Castro, L., and Morrison, D.M., (1998). Probabilistic Analysis for Ground Support for Underground Mines. CIM. Montreal

Bieniawski, Z.T., (1976). Rock mass classification in rock engineering, In Proceedings of the Symposium on Exploration for Rock Engineering. Balkema. pp. 97-106

Bieniawski, Z.T., (1973). Engineering classification of jointed rock masses. Transactions South African Institution of Civil Engineers. 15:335-344.

Bieniawski, Z.T., (1989) Engineering Rock Mass Classifications, Wiley, New York.

Billaux, D.B., Luvison, C., and Darcel B.P., (2006). 3FLO: calculs d'ecoulements tridimensionnels. Bases theoretiques. User's Manual, 3FLO Version 2.31. Itasca.

Birch, J.S., (2006). Using 3DM Analyst Mine Mapping Suite for Rock Face Characterisation. Proceedings of the ARMA GoldenRocks Conference, Denver, Colorado.

BMO Capital Markets, 2011 (www.bmocm.com).

Brady, B.H.G, and Brown E.T., (2004). Rock Mechanics for Underground Mining, Third Edition, Springerlink.

Brown E.T., (2007). Block Caving Geomechanics, 2nd Edition. JKMRC, Brisbane.

Brummer, R.K, and Kaiser, P.K., (1995). Risk-cost-benefit analysis for support design in burst prone mines. Institute of Mining and Metallurgy Conference, Risk Assessment in the Extractive Industries, University of Exerter, Exerter, UK

Brzovic A., and Villaescusa E., (2007). Rock mass characterization and assessment of block-forming geological discontinuities during caving of primary copper ore at the El Teniente mine, Chile. International Journal of Rock Mechanics and Mining Sciences. 44 (4): 565–583.

Business Report, 2011, http://www.iol.co.za/business/rising-sa-mine-deaths-need-urgent-attention-1.1055349

Bye, A.R., and Bell, F.G., (2001). Stability assessment and slope design at Sandsloot open pit, South Africa. International Journal of Rock Mechanics and Mining Sciences. 38: 449–466.

Call, R.D., Savely, J., and Nicholas, D.E., (1976), Estimation of joint set characteristics from surface mapping data. Proceedings 17th US Symposium on Rock Mechanics.

Call, R.D., and Nicholas, D.E, (1978). Prediction of step-path failure geometry for slope stability analysis. Proceedings19th US Symposium on Rock Mechanics.

Cawthorn, R.G., (1999). The platinum and palladium resources of the Bushveld Complex. South African Journal of Science. 95: 481-489.

Cawthorn, R.G., Merkle, R.K.W., and Viljoen, M.J., (2002). Platinum-Group element deposits in the Bushveld Complex, South Africa. In 'The Geology, Chemistry, Mineralogy and Mineral Beneficiation of Platinum-Group elements. Canadian Institute of Mining and Metallurgy. Special Volume 54: 389-429.

Chamber of Mines (2011). www.bullion.org.za

Chan, L.Y., and Goodman, R.E. (1987). Predicting the number of dimensions of key blocks of an excavation using block theory and joint statistics. In Proceedings 28th U.S. Rock Mechanics Symposium. A.A. Balkema, Rotterdam, pp. 81-87.

Clark, I., (1979). Practical Geostatistics. Applied Science Publishers.

Cockram, M. J., Makinen, E. O., and Kirsten, H. A. D., (2004). A methodology to quantify risk and an application to remnant mining. Proceedings 2nd International Seminar on Deep and High Stress Mining. SAIMM, Johannesburg, February 2004.

Coulomb, C.A., (1776). Essai sur une application des rëgles de maximis et minimis a quelques problèmes de statique, relatifs a l'architecture, Mémoires de Marhématique de l'Académie Royale des Sciences, Paris, 7, 343 – 382.

Croney, P., Legge, T.F., and Dhalla, A., (1978). Location of block release mechanisms in tunnels from geological data and the design of associated support. Computer Methods in Tunnels Design, The Institution of Civil Engineers, London. pp. 97-119.

Cundall, P.A, (1979). A Computer Model for Simulating Progressive Large Scale Movements in Blocky Rock Systems. Proceedings Symposium of the International Society of Rock Mechanics, Nancy, France.

Cundall, P.A, and Hart, R. D, (1992). Numerical Modelling of Discontinua. Engineering Computations. 9: 101-113.

Daehnke, A., Van Zyl, M., and Roberts, M.K.C., (2001). Review and Application of Stope Support Design Criteria. Journal of the South African Institute of Mining and Metallurgy. 101 (3):135–164.

Dershowitz, W.S., and Einstein, H. H., (1988). Characterising Rock Joint Geometry with Joint System Models, Rock Mechanics and Rock Engineering. 21: 21 -51

Dershowitz, W.S., 1984, Rock Joint Systems, Ph.D. Thesis, Massachusetts Institute of Technology, Cambridge, Massachusetts.

Dershowitz, W.S., Lee, G., Geier, J., and LaPointe, P.R. (1998). FracMan: Interactive discrete feature data analysis, Geometric modeling and exploration simulation, User Documentation, Golder Associates Inc., Seattle - Washington.

Dershowitz, W.S, (1995). Interpretation and Synthesis of Discrete Fracture Orientation, Size, Shape, Spatial Structure and Hydrologic Data by Forward Modelling in Fractured and Jointed Rock Masses. Proceedings of the Conference on Fractured and Jointed Rock Masses. Lake Tahoe, California, USA. A.A. Balkema, Rotterdam. June 3-5.

Diederichs, M.S., (2003). Rock fracture and collapse under low confinement conditions. Rock Mechanics and Rock Engineering. 36 (5): 339-381.

Dight, P.M., and Baczynski, N.R.C., (2009). Rock bridges and their influence on slope stability. International Symposium on Rock Slope Stability in Open Pit and Civil Engineering, Santiago, Chile.

DME, 2010. http://dmr.gov.za/health-statistics.html

Dunn, M.J., Earl, P.J. and Watson, J., (2008). Support design using probabilistic keyblock methods. Proceedings 6th International Symposium on Ground Support in mining and civil Engineering construction. SAIMM, SANIRE and ISRM.

Einstein, H.H., (2003). Uncertainty in Rock Mechanics and Rock Engineering – Then and Now. ISRM – Technology roadmap for rock mechanics, South African Institute of Mining and Metallurgy.

Einstein, H.H., (1996). Risk and Risk Analysis in Rock Engineering. Tunelling and Underground Space Technology. 11 (2): 141-155.

Einstein, H.H., and Baecher, G.B., (1983). Probabilistic and Statistical Methods in Engineering Geology. Rock Mechanics and Rock Engineering. 16: 39-72.

Esterhuizen, G.S., (2011). Personal communication

Esterhuizen, G.S., (2003). J Block user manual, Pretoria.

Esterhuizen, G.S., and Streuders, S.B., (1998). Rockfall hazard evaluation using probabilistic keyblock analysis. Journal of the South African Institute of Mining and Metallurgy. 98 (2): 59-63.

Fernandes, N.D, and Gardner, L.J., (2011). The ongoing evolution of stope panel support at Impala Platinum Limited. Journal of the South African Institute of Mining and Metallurgy. 111(1): 55–62.

Fisher, R.A., (1953). Dispersion on a sphere. Proceedings of the Royal Society of London, Series A, 217: 295–305.

Gaich, A., Pötsch, M., and Schubert, W., (2006). Basics and application of 3D imaging systems with conventional and high-resolution cameras. Proceedings of the ARMA Golden Rocks Conference, Denver, Colorado, June 17-19.

Geo&Soft, (1999). Geo&Soft International, ROCK3D-identification, geometric reconstruction and stabilization of complex rock blocks, User's Guide and Windows Based Code.

Goodman, R. E., and Shi, G., (1985). Block theory and its application in rock engineering. Prentice Hall.

Goodman, R.E., 1989. Introduction to Rock Mechanics. Second Edition, New York: John Wiley & Sons.

Goodman, R.E., (1995). Block theory and its application. Geotechnique. 45(3): 383-423.

Grady, L.A., (1983). The Application of Geostatistical Techniques to the Analysis of Joint Data. MSc Thesis, University of Witwatersrand, Johannesburg

Grenon, M. and Hadjigeorgiou, J. (2003). Open stope stability using 3D joint networks. Rock Mechanics and Rock Engineering. 36 (3): 183-208.

Grimstad, E., and Barton, N., (1993). Updating the Q-System for NMT. Proceedings International Symposium on Sprayed Concrete - Modern use of wet mix sprayed concrete for underground support. Norwegian Concrete Association. Fagernes. Oslo.

Gumede, H., (2006). Development of data sets on joint characteristics and consideration of associated instability for a typical South African gold mine. MScEng Dissertation, University of the Witwatersrand.

Gumede, H., and Stacey, T.R., (2006). Measurement of typical joint characteristics in South African Gold mines and the use of these characteristics in the prediction of rockfalls. Journal of the South African Institute of Mining and Metallurgy. 107 (5): pp. 335-344

Haines, A., and Marker, H.F., (1992). Tunnel Design Optimisation Utilising Rigorous PC-Based Geomechanical Techniques. Design and Construction of Tunnels, South African National Council On Tunnelling, Maseru, Lesotho. pp. 141-146.

Haines, A., (1984). The application of generated rock mass discontinuity patterns, Proceedings 8^{th} Regional Conference for Africa on Soil Mechanics and Foundation Engineering, Harare, Zimbabwe, pp. 13-21

Hamdi E., and du Mouza J., (2004). A methodology for rock mass characterisation and classification to improve blast results. International Journal of Rock Mechanics and Mining Science. 42 (2), pp. 177–194.

Hatzor, Y., and Goodman, R.E., (1992). Application of block theory and the critical key block concept to tunnelling: Two case histories. Proceedings Conference on Fractured and Jointed Rock Masses. Lake Tahoe, Lawrence Berkeley Laboratory, California.

Hobbs, B.E., Means, W.D., and Williams, P.F., (1976). An outline of Structural Geology, Wiley, New York.

Horsley T. P., and Medhurst, T. P. (2000). Quantifying geotechnical risk in the mine planning process. Proc. MassMin, Brisbane, Australia. October 29 – November 2. pp. 105 – 112.

Hudson, J.A., Priest, S.D., (1979). Discontinuities and Rock Mass Geometry. International Journal of Rock Mechanics and Mining Sciences and Geomechanical Abstracts. 16: 339-362.

Hustrulid, W.A., (1982). Underground Mining Methods Handbook, SME, Port City Press, Maryland.

ISRM (1978): Suggested methods for the quantitative description of discontinuities in rock masses. International Journal of Rock Mechanics and Mining Sciences and Geomechanical Abstracts. 15(6): 319–368.

Ivanova, V.M., (1995). Three Dimensional Stochastic Modelling of Rock Fracture Systems. MSc Thesis. Massachusetts Institute of Technology.

Ivanova, V.M., (1998). Geologic and Stochastic Modelling of Fracture Systems in Rocks. PhD Thesis. Massachusetts Institute of Technology.

Jaeger, J.C., (1971). Eleventh Rankine Lecture: Friction of rocks and stability of rock slopes. Geotechnique 21 (2): 97-134.

Jing, L., and Hudson, J.A., (2002). Numerical methods in rock mechanics. International Journal of Rock Mechanics and Mining Sciences. 39(4): 409-427.

Joughin, W. C., (2008). A preliminary model for quantifying the risk of rockfalls and evaluating the benefits of safety spending. In Proceedings of the 1st Southern Hemisphere International Rock Mechanics Symposium, Perth. Australian Centre for Geomechanics. Vol. 1: 589-604.

Joughin W.C., (2010). Risk in Rock Engineering Design. Rock Engineering for Managers In Hard Rock Tabular Mines School. SAIMM. Misty Hills, June 1-2.

Kemeny, J., and Post, R., 2003. Estimating three-dimensional rock discontinuity orientation from digital images of fracture traces. Computers and Geosciences. 29: 65-77.

Kemeny, J., (2003). The time dependent reduction of sliding cohesion due to rock bridges along discontinuities:a fracture mechanics approach. Rock Mechanics and Rock Engineering. 36 (1): 27-38.

Kulatilake, P.H.S.W., and Wu, T.H., (1984 a). Sampling bias on orientation of discontinuities. Rock Mechanics and Rock Engineering. 17: 243-254.

Kulatilake, P.H.S.W., and Wu, T.H., (1984 b). Estimation of mean trace length of discontinuities, Rock Mechanics and Rock Engineering. 17: 215-232.

Kulatilake, P.H.S.W., (1988). Software manual for FRACNTWK – a computer package to model discontinuity geometry in rock masses,Technical report submitted to Metropolitan Water District of Southern Califonia.

Kulatilake, P.H.S.W., and Wathugala D.N., (1990). Stochastic three dimensional modeling including a verification to an area in Stripa Mine, Sweden. In Proceedings Mechanics of Jointed and Faulted Rock. Vienna, Austria. pp. 71-82.

Kulatilake, P.H.S.W, (1993). Application of probability and statistics in joint network modelling in three dimensions. In Proceedings of The Conference on Probabilistic Methods in Geotechnical Engineering, Balkema. pp. 63-87.

Landanyi, B., and Archambault, G., (1969). Simulation of Shear Behavior of a Jointed Rock Mass. In Proceeding of Eleventh Symposium of Rock Mechanics, Berkeley, California, pp. 105-125.

Lang, T.A., (1961). Theory and practice of rock bolting. Trans. Am. Inst. Min. Engrs., 220: 333-348.

Langston, R.B., Kirsten, H.A.D., Howell, G.C., and Marjerison, J.A., (2007). Classification based probabilistic design of ground support. Proceedings of the International Workshop on Rock Mass Classification in Underground Mining. NIOSH.

Leith C.K., (1923) Structural Geology, Holt, New York, pp. 29 – 99.

Leung, C.F., and Quek, S.T., (1995). Probabilistic stability analysis of excavations in jointed rock. Canadian Geotechnical Journal. 32 (3): 397-407.

Mahtab, M.A., and Yegulap, T.M., (1984). A similarity test for grouping orientation data in rock mechanics. In : Proceedings of 25th US Symposium on Rock Mechanics. Evanston, Illinois. pp. 495-502.

Mathews, D. (M and J Mining Supplies), 2011. Personal communication

Martin, D.C., (1978). The influence of fabric geometry and fabric history on the stability of rock slopes. MSc dissertation, Imperial College, London.

Mauldon, M., Mauldon J.G., (1997). Estimating mean fracture trace length and density from observations in convex windows. Rock Mechanics and Rock Engineering, 31(4): 201-216.

Mauldon, M., and Goodman, R.E., (1990). Rotational Kinematics and Equilibrium of Blocks in a Rock Mass. International Journal of Rock Mechanics and Mining Sciences. 27(4): 291-301.

McCullagh, P., and Lang, P., (1984). Stochastic models for rock instability. Journal of the Royal Statistical Society. 46(2): 344-352.

Merrien-Soukatchoff, V., Korini, T., and Thoraval, A., (2011). Use of an Integrated Discrete Fracture Network Code for Stochastic Stability Analyses of Fractured Rock Masses. Rock Mechanics and Rock Engineering. 44: 129-147.

Miller, S.M., (1982). Statistical and Fourier Methods for Probabilistic Design of Rock Slopes. Phd dissertation. University of Wyoming.

Miller, S.M., (1983). Probabilistic analysis of bench stability for use in designing open pit mine slopes. In Proceedings of the 24th U.S Symposium on Rock Mechanics: 621-629.

Miller, S.M., Whyatt, J.K., Dwyer, J.G., and McHugh, E., (2007). A user's guide for the Bplane, Bstepp and Bwedge computer programs. NIOSH Publication No. 2007-108

Morriss, P., and Stoter, H.J., (1983). Open-cut slope design using probabilistic methods. Proceedings 5th ISRM Congress, Melbourne, Australia. Rotterdam: Balkema.

Narendranathan S., (2009). Fundamentals of Probabilistic Slope Design and It's Use in Pit Optimization, 43rd US Rock Mechanics Symposium and 4th U.S.-Canada Rock Mechanics Symposium, Asheville, ARMA

New Concept Mining, 2011. Personal communication

Ortlepp, W.D., and Stacey, T.R., (1995). Technical note: Safety and cost implications in the spacing of support. Journal of The South African Institute of Mining and Metallurgy. 95(3): 141-146.

Pahl, P.J., (1981). Estimating the mean length of discontinuity traces. International Journal of Rock Mechanics and Mining Abstracts. 18: 221-228.

Patton, F.D., (1966). Multiple modes of shear failure in rock. In Proceedings 1st International Congress. International Society of Rock Mechanics., Colouste Gulbenkian Foundation, Lisbon, pp. 509-513.

Pierce, M., Cundall, P.A., Potyondy, D., and Mas Ivars, D., (2007). A synthetic rock mass model for jointed rock. In Rock Mechanics: Meeting Society's Challenges and Demands, Proceedings: 1st Canada-U.S. Rock Mechanics Symposium Vol. 1, pp. 341-349

Pierpaolo, P., (2005). A probabilistic design approach for tunnel supports. Computers and Geotechnics. 32(7): 520–534.

Piteau, D.R., (1970). Geologic factors significant to the stability of slopes cut in rock. In Planning Open Pit Mines Symposium, Johannesburg. SAIMM.

Piteau, D.R., and Martin, D.C., (1982). Mechanics of Slope Failure. 3rd Conference on Stability in Surface Mining, AIME, Vol.3, pp113-169.

Poropat, G.V., (2006). Remote 3D Mapping Of Rock Mass Structure. Proceedings of the ARMA GoldenRocks Conference, Denver, Colorado, June 17 - 19.

Potvin, Y., Nedin, P., Sandy, M., Rosengren, K., and Rosengren, M.D., (2001). Towards the Elimination of Rockfall Fatalities in Australian Mines. MERIWA Project No. M341.

Potyondy, D.O, and Cundall, P.A, (2004). A Bonded-Particle Model for Rock. International Journal of Rock Mechanics and Mining Sciences. 41(8): 1329-1364.

Price, N.J., (1966). Fault and joint development in brittle and semi-brittle rock. Pergamon Press, London.

Priest S.D., (1985). Hemispherical Projection Methods in Rock Mechanics. George Allen and Unwin

Priest, S.D., and Samaniego, J.A., (1983). A model for the analysis of discontinuity characteristics in two dimensions. In Proceedings. 5th International Society for Rock Mechanics Congress, Melbourne

Priest, S.D., and Hudson, J.A., (1981). Estimation of discontinuity spacing and trace length using scanline surveys. International Journal of Rock Mechanics and Mining Sciences and Geomechanics Abstracts 18(3): 183-197.

Priest, S.D., and Hudson, J.A., (1976). Discontinuity spacings in rock. International Journal of Rock Mechanics and Mining Sciences and Geomechanics Abstracts. 13(5): 135-148.

Priest S.D., (1993). Discontinuity Analysis for Rock Enfineering. Chapman and Hall, London

Rashad, M.Z.; El-Sageer H.A., (1992). Determination of the direction of tunnels in jointed rocks using key block theory. AMIE 44: 1169–1174

Read, J.R.L., and Ogden, A.N., (2006). Developing new approaches to rock slope stability analyses. In: International Symposium on Stability of Rock Slopes in Open Pit Mining and Civil Engineering. The South African Institute of Mining and Metallurgy.

Read, J.R.L, Stacey, P., (2009). Guidelines for Open Pit Slope Design. CSIRO Publishing, Victoria, Australia.

Roberds, W.J. and Einstein, H.H., (1978). Comprehensive Model for Rock Discontinuities. Journal for the Geotechnical Engineering Division, ASCE. 104 (5). pp. 553-569.

Robertson, A. MacG., (1970). The Interpretation of Geological factors for use in Slope Theory. Proceedings Symposium on the Theoretical Background to the Planning of Open Pit Mines with Special Reference to Slope Stability. South Africa, Balkema, pp. 55-71.

Rocscience, 2001. Dips User's Guide.

Rocscience, 2006. SWEDGE User's Guide.

Rocscience, 2007. UNWEDGE User's Guide.

Rowe, W.D., (1979). What is an acceptable risk and how can it be determined? In Energy Risk Management. Goodman G.T., and Rowe W.D., (eds.), Academic Press, London.

Rwodzi, L., (2011). Rockfall Risk: Quantification of the consequences of rockfalls, Msc Dissertation, University of the Witwatersrand.

Savely J.P., (1972). Orientation and engineering properties of jointing in the Sierra pit, Arizona. MSC Thesis, University of Arizona, Tucson.

Shi, G.H., (1988). Discontinuous Deformation Analysis – A New Numerical Method for the Statics and Dynamics of Block System. Ph.D. Thesis, Department of Civil Engineering, University of California, Berkley.

Shi, G.H., Goodman, R.E., 1981. A New concept for support of underground and surface excavations in discontinuos rocks based on a keystone principle. Rock Mechanics from Research to Application: Proceedings 22nd Symposium of Rock Mechanics.MIT, Massachusets

Shi., G., (2006). Producing joint polygons, cutting joint blocks and finding key blocks for general free surfaces. Chinese Journal of Rock Mechanics and Engineering, Vol. 25, No. 11.

Skarbøvig, N.M., Lamos, A.W., and Lamos, R.A., (2011). Mine safety net development and applications. Journal of The Southern African Institute of Mining and Metallurgy. 111(1): 19-28

SRK Internal Report, 1986

Stacey T.R., and Haines, A., (1984). Design of large underground openings in rock – an integrated approach. Proceedings Seminar on Design and Construction of Large Underground Openings. The Southern African Institute of Mining and Metallurgy.

Stacey, T.R, Wesseloo, J. and Bell, G., (2006). Predicting the stability of rockpasses from the geological structure. Journal of the South African Institute of Mining and Metallurgy. 105 (11): 803-808.

Stacey, T. R., (2006). Design – A Strategic Issue, Proc of 2nd Int. Seminar on Strategic vs. Tactical Approaches in Mining, Perth, Australian Centre for Geomechanics

Stacey, T.R, Terbrugge, P.J. and Wesseloo, J., (2006). Risk as a Rock Engineering Design Criterion. Deep and High Stress Mining. Proc. 3rd Int. Seminar on Deep and High Stress Mining, Quebec City, Canada, October 2006, Laval University, Section 27, pp. 14.

Stacey, T.R. (1989) Potential rockfalls in conventionally supported stopes - a simple probabilistic approach. The Journal of the South African Institute of Mining and Metallurgy. 89 (4). pp. 111-115.

Stacey, T.R., (2007). Is Rock Engineering Addressing Risk Appropriately? Redefining the boundaries Part 2, Proc. SANIRE 2007 Symposium, Free State, South Africa.

Stacey, T.R., and Gumede, H., (2007) Evaluation of risk of rock fall accidents in gold mine stopes based on measured joint data. The Journal of the South African Institute of Mining and Metallurgy. 107(5): 345-350.

Stacey, T.R., Wesseloo, J., Bell, G., (2005). Predicting the stability of rockpasses from the geological structure. The Journal of the South African Institute of Mining and Metallurgy. 105(11): 803-808

Stacey, T.R. and Bartlett, P.J., (1990). Probabilistic evaluation of ore pass stability and support. Static and Dynamic Considerations in Rock Engineering. A A Balkema, pp: 309-315

Starzec, P., and Andersson, J., (2002). Probabilistic predictions regarding key blocks using stochastic discrete fracture networks – example from a rock cavern in south-east Sweden. Bulletin of Engineering Geology and the Environment. 61(4): 363-378.

Steffen, O.K.H., (2007). Mine Planning – Its Relationship to Risk Management, Australian Centre for Geomechanics, Newsletter. 29: 1-6.

Steffen, O.K.H.; Kerrich, J.E., and Jennings, J.E., (1975). Recent developments in the interpretation of data from joint surveys in rock masses. Proceedings 6th Regional Conference for Africa on Soil Mechanics and Foundation Engineering. 2: 17-26

Sturzenegger M., and Stead, D., (2009). Quantifying discontinuity orientation and persistence on high mountain rock slopes and large landslides using terrestrial remote sensing techniques. Journal of Natural Hazards and Earth System Sciences. 9: 267–287.

Suppe, J., (1985). Principles of structural geology. Prentice-Hall, USA.

Terbrugge, P.J., Wesseloo, J., Venter, J., and Steffen, O.K.H., (2006). A risk consequence approach to open pit slope design, Journal of the South African Institute of Mining and Metallurgy. 106(7): 503–511.

Terzaghi, R., (1965). Sources of error in joint surveys. Geotechnique, 5(3): 287-304.

Thompson, A.G., (2002). Stability assessment and reinforcement of block assemblies near underground excavations. In: Hammah R, Bawden W, Curran J, Telesnicki M, eds. Proceedings of the NARMS–TAC Conference (July 7–10, 2002). Vol. 2. Toronto, Ontario, Canada: University of Toronto Press, pp. 1439–1446.

Tonon, F., Kottenstette, J.T., (2006). Laser and Photogrammetric Methods for Rock Face Characterisation: A Workshop. Proceedings of the ARMA Golden Rocks Conference, Denver, Colorado, June 17 - 19.

Tyler, D.B., Trueman, R., and Pine, R.J., (1991). Rockbolt support design using a probabilistic method of keyblock analysis. In Rock Mechanics as a Multidisciplinary Science, (ed. J.C. Roegiers). Rotterdam: Balkema. pp. 1037-1047.

Ulusay, R., and Hudson, J.A., (2007). The Coplete ISRM Suggested Methods for Characterization, Testing and Monitoring: 1974-2006. ISRM.

Veneziano, D., (1978). Probabilistic model of joints in rock. Unpublished manuscript, Massachusetts Institute of Technology.

Villaescusa, E., 1993. Statistical modelling of rock jointing. Proceedings Conference on Probabilistic Methods in Geotechnical Engineering, Canberra, Australia, pp 221-231.

Viner, H.C., (2002). Risk management lecture notes. School of Mining Engineering. Witwatersrand University.

Warburton, P.M., (1980). Stereological interpretation of joint trace data: Influence of joint shape and implications for geological surveys. International Journal of Rock Mechanics and Mining Sciences and Geomechanical Abstracts. 17: 305-316

Warburton, P.M., (1983). Applications of a new computer model for reconstructing blocky rock geometry – Analysing single block stability and identifying keystones. 5th ISRM International Congress on Rock Mechanics. F225-F230.

Whitman, R.V. (1983), The 7th Terzaghi lecture, Evaluating and calculated risk in geotechnical engineering. Journal of Geotechnical Engineering. 110(2): 145-188

Windsor, C.R., and Thompson, A.G., (1997). A Course on Structural Mapping and Structural Analysis. Rock Technology Pty Ltd, Perth

Young, D.S, and Hoerger, S.F., (1989). Probabilistic and deterministic key block analyses. Rock Mechanics as a Guide for Efficient Utilization of Natural Resources: Proceedings 30th U.S. Symposium on Rock Mechanics. A A Balkema Morgantown, 19–22 June. Pp: 227–234.

Zhang L., (2004). Drilled Shafts in Rock: Analysis and Design. A. A. Balkema Publishers.

Zhang, L., and Einstein H.H., (1998). End bearing capacity of drilled shafts in rock. Journal of Geotechnical and Geoenvironmental Engineering. 124(7):574-584.

http://financialresults.co.za/2010/implats_ar2010/downloads/implats_ar2010.pdf

http://financialresults.co.za/2010/implats_ar2010/downloads/implats_mineral_resource_statement2010.pdf

http://www.angloplatinum.com/business/operations/overview.asp

Appendix A. Joint Mapping Data

A.1 UG2 reef

		Rock			Orientation		Infill		Joint wall		Joint wall roughness			
Joint set or structure	Location	Type	Weathe-ring	Hard-ness	Dip	Dip Direction	Thick-nes	Type	Separation	Hardness	Micro	Macro	Dip ends	Comments
joint set	1.45	Pyro	1	3	50	48	2		2	3	5	2	7.9	Serp infill
joint set	2.2	Pyro	1	3	65	49	2		2	3	5	2	9.9	Serp infill
jont set	5.72	Pyro	1	3	80	24	1		1	3	5	2	3.8	Serp infill
jont set	6.97	Pyro	1	3	75	40	1		1	3	5	2	7.5	Serp infill
jont set	7.92	Pyro	1	3	75	45	1		1	3	5	2	3.5	Serp infill
jont set	9	Pyro	1	3	80	35	1		1	3	5	2	3.5	Serp infill
jont set	9.6	Pyro	1	3	85	219	1		1	3	5	2	3.5	Serp infill
jont set	18.7	Pyro	1	3	60	30	1		1	3	5	2	4.9	Serp infill
joint set	19.2	Pyro	1	3	70	33	2		2	3	6	2	4.9	Calc infill
joint set	20.24	Pyro	1	3	78	65			2	3	6	2	6.6	No fill
joint set	20.6	Pyro	1	3	85	88	1		2	3	5	2	5.5	Serp infill
joint set	21.35	Pyro	1	3	80	27	1		1	3	5	2	6.4	Serp infill
joint set	21.69	Pyro	1	3	65	28	1		1	3	5	2	6.4	Serp infill
joint set	22.20	Pyro	1	3	80	205	1		2	3	5	2	6.8	Serp coatings
joint set	22.42	Pyro	1	3	80	205	1		1	3	5	2	3.2	Serp coatings
joint set	22.47	Pyro		3	80	205	1		1	3	5	2	3.6	Serp coatings
joint set	22.92	Pyro	1	3	50	47	1		1	3	5	2	8	Serp coatings
joint set	23.57	Pyro	1	3	82	23	3		3	3	5	2	8	Serp coatings
joint set	23.57	Pyro	1	3	75	39	2		2	3	5	2	7.8	Serp infill
joint set	24.03	Pyro	1	3	75	23	1		1	3	6	2	6.6	No fill
joint set	24.12	Pyro	1	3	75	23			2	3	6	2	5.9	No fill
joint set	24.55	Pyro	1	3	85	26	1		1	3	6	2	6.5	No fill
jont set	25.28	Pyro	1	3	78	16	2		2	3	5	2	5.9	Serp infill
joint set	25.76	Pyro	1	3	85	55	1		1	3	5	2	5.9	Serp infill
joint set	25.89	Pyro	1	3	85	55	1		1	3	5	2	5.9	Serp infill
joint set	26	Pyro	1	3	65	67	1		1	3	5	2	6.5	Serp infill
joint set	26.67	Pyro	1	3	75	49	1		1	3	5	2	4.3	Serp infill
joint set	27.25	Pyro	1	3	60	64	1		1	3	5	2	5.2	Serp infill
joint set	27.98	Pyro	1	3	75	62	1		1	3	6	2	5	Calc infill
joint set	28.17	Pyro	1	3	50	44	2		2	3	5	2	2.9	Serp infill
joint set	28.30	Pyro	1	3	75	62	1		1	3	6	2	2.9	Calc infill
joint set	28.55	Pyro	1	3	75	49	2		2	3	5	2	2.6	Serp infill

joint set	28.75	Pyro	1	3	75	49	2		2	3	5	2	3.3	Serp infill
joint set	1.5	Pyro	1	3	77	69	1	Serp	1	3	5	2	10.1	Serp coatngs
joint set	2.2	Pyro	1	3	85	9	2	Serp	2	3	5	2	3.4	Serp nfll
jont set	5.32	Pyro	1	3	65	330	1	Serp	1	3	5	2	4.7	Serp coatngs
jont set	5.79	Pyro	1	3	75	303	1	Serp	1	3	5	2	6.7	Serp coatngs
jont set	6.48	Pyro	1	3	88	283	1	Serp	1	3	5	2	7.7	Serp coatngs
jont set	7	Pyro	1	3	88	283	1	Serp	1	3	5	2	8.3	Serp coatngs
jont set	8.97	Pyro	1	3	85	315	1	Serp	1	3	5	2	7.3	Serp coatngs
jont set	9.15	Pyro	1	3	85	315	1	Serp	1	3	6	2	3.6	Serp mxed wth pryo hard
joint set	9.3	Pyro	1	3	85	315		No Fll	2	3	6	2	3.6	No fll
joint set	9.62	Pyro	1	3	85	315		No Fll	2	3	6	2	5.2	No fll
joint set	10.32	Pyro	1	3	90	88		No Fll	2	3	6	2	4.2	No fll
joint set	11.18	Pyro	1	3	70	228		No Fll	1	3	6	2	5.9	No fll
joint set	11.63	Pyro	1	3	75	114	1	Serp	1	3	5	2	7.1	Serp coatngs
joint set	12.40	Pyro	1	3	55	163	2	Calc	2	3	6	2	4.9	Calc coatngs
joint set	13.97	Pyro	1	3	77	308	1	Serp	1	3	5	2	4.1	Serp nfll
joint set	14.43	Pyro		3	80	301	1	Serp	1	3	5	2	5.3	Calc nfll
joint set	15.39	Pyro	1	3	85	140		No Fll	1	3	6	2	4.4	No fll
joint set	16.1	Pyro	1	3	75	295	3	Serp	3	3	5	2	4.4	Serp nfll
joint set	16.25	Pyro	1	3	80	322	1	Calc	1	3	6	2	3.8	Calc coatngs
joint set	16.86	Pyro	1	3	80	322	2	Serp	2	3	5	2	3.8	Serp coatngs
joint set	16.95	Pyro	1	3	80	322	1	Serp	1	3	5	2	3.8	Serp coatngs
jont set	17.39	Pyro	1	3	78	168	2	Serp	2	3	5	2	3.2	Serp nfll
joint set	17.91	Pyro	1	3	82	162	1	Serp	1	3	5	2	3.8	Serp nfll
joint set	23.3	Pyro	1	3	78	197		No Fll	1	3	6	2	3.6	No fll
joint set	23.44	Pyro	1	3	80	29	1	Calc	1	3	6	2	4.3	Calc infill
joint set	23.64	Pyro	1	3	80	29		No Fll	1	3	6	2	2.6	No fll
joint set	23.88	Pyro	1	3	75	323	1	Serp	1	3	5	2	2.3	Serp infill
joint set	25.06	Pyro	1	3	75	314	1	Calc	1	3	6	2	3.8	Calc nfll
joint set	25.15	Pyro	1	3	75	314	2	Serp	2	3	5	2	1.5	Serp nfll
joint set	25.26	Pyro	1	3	70	259	2	Serp	2	3	6	2	3.6	Serp mxed wth non softenng
joint set	26.64	Pyro	1	3	75	301	3	Serp	3	3	5	2	3.7	Serp nfll
joint set	27.40	Pyro	1	3	85	305		No Fill	1	3	6	2	3.9	No fill
joint set	27.5	Pyro	1	3	85	305	2	Serp	2	3	5	2	3.9	Serp coatngs
joint set	27.73	Pyro	1	3	77	269	2	Serp	2	3	5	2	3.4	Serp coatngs
joint set	28	Pyro	1	3	70	307	3	Serp	3	3	5	2	2.9	Serp infill
joint set	28.9	Pyro	1	3	75	289	2	Serp	2	3	5	2	4	Serp coatings
joint set	29.83	Pyro	1	3	85	315		No Fll	1	3	6	2	5.5	No fll
joint set	31.3	Pyro	1	3	65	182	1	Serp	1	3	5	2	5.5	Serp coatings
joint set	31.3	Pyro	1	3	65	283	1	Serp	1	3	6	2	5.5	Serp infill + pyroxenite

joint set	2.25	Pyro	1	3	76	38	2	Serp	2	3	5	2	7.9	Calc infill
joint set	3.81	Pyro	1	3	75	264	2	Serp	2	3	5	2	9.9	Serp infill
jont set	4.82	Pyro	1	3	90	39	1	Serp	1	3	5	2	3.8	Serp coatings
jont set	5.23	Pyro	1	3	85	91	1	Serp	1	3	5	2	7.5	Serp infill
jont set	7.00	Pyro	1	3	80	19	1	Serp	1	3	5	2	3.5	Serp infill
jont set	7.72	Pyro	1	3	80	19	1	Serp	1	3	5	2	3.5	Serp infill
jont set	7.98	Pyro	1	3	80	19	1	Serp	1	3	5	2	3.5	Serp infill
jont set	8.82	Pyro	1	3	80	35	1	Serp	1	3	6	2	4.9	Calc infill
joint set	9.13	Pyro	1	3	80	35		No Fll	2	3	6	2	4.9	Serp infill
joint set	9.40	Pyro	1	3	85	294		No Fll	2	3	6	2	6.6	Serp infill
joint set	9.65	Pyro	1	3	75	292		No Fll	2	3	6	2	5.5	Calc infill
joint set	9.68	Pyro	1	3	60	16		No Fll	1	3	6	2	6.4	Serp coatings
joint set	9.92	Pyro	1	3	60	16	1	Serp	1	3	5	2	6.4	Serp infill
joint set	11.25	Pyro	1	3	80	281	1	Calc	2	3	6	2	6.8	No fill
joint set	11.32	Pyro	1	3	60	4	1	Serp	1	3	5	2	3.2	Serp infill
joint set	12.40	Pyro		3	55	346	1	Serp	1	3	5	2	3.6	Serp infill
joint set	13.45	Pyro	1	3	75	279		No Fll	1	3	6	2	8	Serp infill
joint set	14.18	Pyro	1	3	75	279	3	Serp	3	3	5	2	8	Serp infill
joint set	14.90	Pyro	1	3	75	279	1	Calc	1	3	6	2	6.6	Serp infill
joint set	15.62	Pyro	1	3	70	157		No Fll	2	3	6	2	5.9	Calc infill
joint set	16.20	Pyro	1	3	85	325		No Fll	1	3	6	2	6.5	Serp coatings
jont set	17.17	Pyro	1	3	85	54	5	Serp	5	3	5	2	5.9	No fill
joint set	17.66	Pyro	1	3	85	54	1	Serp	1	3	5	2	5.9	No fill
joint set	17.48	Pyro	1	3	85	54		No Fll	1	3	6	2	5.9	Serp infill
joint set	17.82	Pyro	1	3	85	325	1	Calc	1	3	6	2	6.5	Serp coatings
joint set	18.21	Pyro	1	3	88	33		No Fll	1	3	6	2	4.3	Serp coatings
joint set	18.50	Pyro	1	3	88	33	1	Serp	1	3	5	2	5.2	No fill
joint set	19.04	Pyro	1	3	65	20	1	Calc	1	3	6	2	5	Calc infill
joint set	19.45	Pyro	1	3	85	35	2	Serp	2	3	5	2	2.9	Serp infill
structure /shear zone	20.1-21.50	Pyro			75	298							10.8	Shear Zone intensely jointed
														Shear Zone intensely jointed
joint set	21.90	Pyro	1	3	80	54		No Fill	1	3	6	2	2.9	No fill
joint set	22.65	Pyro	1	3	75	180	2	Serp	2	3	5	2	2.6	No fill
joint set	23.35	Pyro	1	3	88	217	2	Serp	2	3	5	2	3.3	No fill
joint set	24.45	Pyro	1	3	83	39	3	Serp	3	3	5	2	1.4	Calc infill
joint set	24.65	Pyro	1	3	83	39	2	Serp	2	3	5	2	3.6	No fill
joint set	24.98	Pyro	1	3	83	39		No Fll	1	3	6	2	3.5	Serp infill
joint set	25.42	Pyro	1	3	85	121	1	Serp	1	3	5	2	7.9	Serp infill
joint set	26.37	Pyro	1	3	85	121	1	Serp	1	3	6	2	4.5	Serp infill
joint set	26.70	Pyro	1	3	85	66		No Fll	1	3	6	2	3.6	Serp infill and pyroxenite hard

joint set	0.82	Pyro	1	3	68	105	1	Serp	2	3	5	2		Serp coatngs
joint set	0.92	Pyro	1	3	85	291	2	Serp	2	3	5	2		Serp nfll
jont set	1.04	Pyro	1	3	80	103	1	Serp	1	3	5	2		Serp coatngs
jont set	1.13	Pyro	1	3	80	103	1	Serp	1	3	5	2		Serp coatngs
jont set	1.32	Pyro	1	3	75	95	1	Serp	1	3	5	2		Serp coatngs
jont set	2.06	Pyro	1	3	75	95	1	Serp	1	3	5	2		Serp coatngs
jont set	2.27	Pyro	1	3	75	95	1	Serp	1	3	5	2		Serp coatngs
jont set	2.46	Pyro	1	3	75	95	1	Serp	1	3	6	2		Serp mxed wth pryo hard
joint set	2.47	Pyro	1	3	85	13		No Fll	2	3	6	2		No fll
joint set	2.73	Pyro	1	3	85	287		No Fll	2	3	6	2		No fll
joint set	2.75	Pyro	1	3	85	287	1	No Fll	2	3	6	2		No fll
joint set	2.91	Pyro	1	3	75	95	1	No Fll	1	3	6	2		No fll
joint set	3.08	Pyro	1	3	85	107	1	Serp	1	3	5	2		Serp coatngs
joint set	3.20	Pyro	1	3	85	107	1	Calc	2	3	6	2		Calc coatngs
joint set	3.32	Pyro	1	3	85	107	1	Serp	1	3	5	2		Serp nfll
joint set	4.53	Pyro		3	85	100	1	Serp	1	3	5	2		Calc nfll
joint set	4.75	Pyro	1	3	85	16		No Fll	1	3	6	2		No fll
joint set	4.88	Pyro	1	3	70	298	3	Serp	3	3	5	2		Serp nfll
joint set	4.9	Pyro	1	3	86	97	1	Calc	1	3	6	2		Calc coatngs
joint set	5.27	Pyro	1	3	70	298		No Fll	7	3	6	2		Serp coatngs
joint set	5.42	Pyro	1	3	70	298		No Fll	1	3	6	2		Serp coatngs
jont set/Dome	5.92	Pyro	1	3	70	262	5	Serp	5	3	5	2		Serp nfll
joint set	5.95	Pyro	1	3	70	298	1	Serp	1	3	5	2		Serp nfll
joint set	5.63	Pyro	1	3	70	298		No Fll	1	3	6	2		No fll
joint set	6.25	Pyro	1	3	85	99	1	Calc	1	3	6	2		Calc infill
joint set	6.69	Pyro	1	3	70	129		No Fll	1	3	6	2		No fll
joint set	6.90	Pyro	1	3	70	129	1	Serp	1	3	5	2		Serp infill
joint set	7.10	Pyro	1	3	85	86	1	Calc	1	3	6	2		Calc nfll
joint set	7.36	Pyro	1	3	85	90	2	Serp	2	3	5	2		Serp nfll
joint set	8.05	Pyro	1	3	80	275	2	Serp	2	3	6	2		Serp mxed wth non softenng
joint set	8.57	Pyro	1	3	80	275	3	Serp	3	3	5	2		Serp nfll
joint set	8.90	Pyro	1	3	90	102		No Fill	1	3	6	2		No fill
joint set	9.09	Pyro	1	3	88	325	2	Serp	2	3	5	2		Serp coatngs
joint set	9.23	Pyro	1	3	88	325	2	Serp	2	3	5	2		Serp coatngs
joint set /Dome	9.86	Pyro	1	3	70	320	3	Serp	3	3	5	2		Serp infill
joint set	9.93	Pyro	1	3	70	109	2	Serp	2	3	5	2		Serp coatings
joint set	10.52	Pyro	1	3	75	288		No Fll	1	3	6	2		No fll
joint set	10.55	Pyro	1	3	85	285	1	Serp	1	3	5	2		Serp coatings
joint set	10.85	Pyro	1	3	90	57	1	Serp	1	3	6	2		Serp infill + pyroxenite
joint set	10.90	Pyro	1	3	72	286		No Fll	1	3	6	2		No fll

joint set	11.09	Pyro	1	3	80	111	2	Serp	2	3	5	2		Serp nfll
joint set	11.29	Pyro	1	3	80	283	1	Serp	1	3	5	2		Serp nfll
joint set	11.86	Pyro	1	3	65	293		No fill	1	3	6	2		No fill
joint set	12.6	Pyro	1	3	80	283	1	Serp	1	3	5	2		Serp nfll
joint set	12.80	Pyro	1	3	70	311	8	Serp	8	3	6	2		Serp mxed wth non softenng
joint set	12.94	Pyro	1	3	80	103	2	Calc	2	3	6	2		Calc infill
joint set	13.27	Pyro	1	3	75	282	3	Serp	3	3	6	2		Serp mxed wth non softenng
joint set	13.94	Pyro	1	3	70	275		No Fll	1	3	6	2		No fll
joint set	14.18	Pyro	1	3	70	275	1	Serp	1	3	5	2		Serp coatngs
joint set	14.36	Pyro	1	3	90	294		No Fll	1	3	6	2		No fll
joint set	15.00	Pyro	1	3	85	274	4	Serp	4	3	6	2		Serp mxed wth non softenng
joint set	15.48	Pyro	1	3	55	254	30	Serp	30	3	6	2		Serp mxed wth non softenng
joint set	16.55	Pyro	1	3	80	263	3	Calc	3	3	6	2		Calc nfll
joint set	16.80	Pyro	1	3	88	106	1	Serp	1	3	6	2		Calc nfll
joint set	17.41	Pyro	1	3	65	14	1	Serp	1	3	5	2		Serp coatngs
joint set	17.62	Pyro	1	3	75	109	1	No Fll	1	3	6	2		No fll
joint set	17.79	Pyro	1	3	75	109	1	Calc	1	3	6	2		Non softenng nfll
joint set	18.05	Pyro	1	3	75	109	2	Calc	2	3	6	2		Calc nfll
joint set	18.30	Pyro	1	3	75	109	2	Serp	2	3	6	2		Calc nfll
joint set	1.45	Pyro	1	3	50	48	2		2	3	5	2	7.9	Serp infill
joint set	2.2	Pyro	1	3	65	49	2		2	3	5	2	9.9	Serp infill
jont set	5.72	Pyro	1	3	80	24	1		1	3	5	2	3.8	Serp infill
jont set	6.97	Pyro	1	3	75	40	1		1	3	5	2	7.5	Serp infill
jont set	7.92	Pyro	1	3	75	45	1		1	3	5	2	3.5	Serp infill
jont set	9	Pyro	1	3	80	35	1		1	3	5	2	3.5	Serp infill
jont set	9.6	Pyro	1	3	85	219	1		1	3	5	2	3.5	Serp infill
jont set	18.7	Pyro	1	3	60	30	1		1	3	5	2	4.9	Serp infill
joint set	19.2	Pyro	1	3	70	33	2		2	3	6	2	4.9	Calc infill
joint set	20.24	Pyro	1	3	78	65			2	3	6	2	6.6	No fill
joint set	20.6	Pyro	1	3	85	88	1		2	3	5	2	5.5	Serp infill
joint set	21.35	Pyro	1	3	80	27	1		1	3	5	2	6.4	Serp infill
joint set	21.69	Pyro	1	3	65	28	1		1	3	5	2	6.4	Serp infill
joint set	22.20	Pyro	1	3	80	205	1		2	3	5	2	6.8	Serp coatings
joint set	22.42	Pyro	1	3	80	205	1		1	3	5	2	3.2	Serp coatings
joint set	22.47	Pyro		3	80	205	1		1	3	5	2	3.6	Serp coatings
joint set	22.92	Pyro	1	3	50	47	1		1	3	5	2	8	Serp coatings
joint set	23.57	Pyro	1	3	82	23	3		3	3	5	2	8	Serp coatings
joint set	23.57	Pyro	1	3	75	39	2		2	3	5	2	7.8	Serp infill
joint set	24.03	Pyro	1	3	75	23	1		1	3	6	2	6.6	No fill
joint set	24.12	Pyro	1	3	75	23			2	3	6	2	5.9	No fill
joint set	24.55	Pyro	1	3	85	26	1		1	3	6	2	6.5	No fill

jont set	25.28	Pyro	1	3	78	16	2		2	3	5	2	5.9	Serp infill
joint set	25.76	Pyro	1	3	85	55	1		1	3	5	2	5.9	Serp infill
joint set	25.89	Pyro	1	3	85	55	1		1	3	5	2	5.9	Serp infill
joint set	26	Pyro	1	3	65	67	1		1	3	5	2	6.5	Serp infill
joint set	26.67	Pyro	1	3	75	49	1		1	3	5	2	4.3	Serp infill
joint set	27.25	Pyro	1	3	60	64	1		1	3	5	2	5.2	Serp infill
joint set	27.98	Pyro	1	3	75	62	1		1	3	6	2	5	Calc infill
joint set	28.17	Pyro	1	3	50	44	2		2	3	5	2	2.9	Serp infill
joint set	28.30	Pyro	1	3	75	62	1		1	3	6	2	2.9	Calc infill
joint set	28.55	Pyro	1	3	75	49	2		2	3	5	2	2.6	Serp infill
joint set	28.75	Pyro	1	3	75	49	2		2	3	5	2	3.3	Serp infill
joint set	1.5	Pyro	1	3	77	69	1	Serp	1	3	5	2	10.1	Serp coatngs
joint set	2.2	Pyro	1	3	85	9	2	Serp	2	3	5	2	3.4	Serp nfll
jont set	5.32	Pyro	1	3	65	330	1	Serp	1	3	5	2	4.7	Serp coatngs
jont set	5.79	Pyro	1	3	75	303	1	Serp	1	3	5	2	6.7	Serp coatngs
jont set	6.48	Pyro	1	3	88	283	1	Serp	1	3	5	2	7.7	Serp coatngs
jont set	7	Pyro	1	3	88	283	1	Serp	1	3	5	2	8.3	Serp coatngs
jont set	8.97	Pyro	1	3	85	315	1	Serp	1	3	5	2	7.3	Serp coatngs
jont set	9.15	Pyro	1	3	85	315	1	Serp	1	3	6	2	3.6	Serp mxed wth pryo hard
joint set	9.3	Pyro	1	3	85	315		No Fll	2	3	6	2	3.6	No fll
joint set	9.62	Pyro	1	3	85	315		No Fll	2	3	6	2	5.2	No fll
joint set	10.32	Pyro	1	3	90	88		No Fll	2	3	6	2	4.2	No fll
joint set	11.18	Pyro	1	3	70	228		No Fll	1	3	6	2	5.9	No fll
joint set	11.63	Pyro	1	3	75	114	1	Serp	1	3	5	2	7.1	Serp coatngs
joint set	12.40	Pyro	1	3	55	163	2	Calc	2	3	6	2	4.9	Calc coatngs
joint set	13.97	Pyro	1	3	77	308	1	Serp	1	3	5	2	4.1	Serp nfll
joint set	14.43	Pyro		3	80	301	1	Serp	1	3	5	2	5.3	Calc nfll
joint set	15.39	Pyro	1	3	85	140		No Fll	1	3	6	2	4.4	No fll
joint set	16.1	Pyro	1	3	75	295	3	Serp	3	3	5	2	4.4	Serp nfll
joint set	16.25	Pyro	1	3	80	322	1	Calc	1	3	6	2	3.8	Calc coatngs
joint set	16.86	Pyro	1	3	80	322	2	Serp	2	3	5	2	3.8	Serp coatngs
joint set	16.95	Pyro	1	3	80	322	1	Serp	1	3	5	2	3.8	Serp coatngs
jont set	17.39	Pyro	1	3	78	168	2	Serp	2	3	5	2	3.2	Serp nfll
joint set	17.91	Pyro	1	3	82	162	1	Serp	1	3	5	2	3.8	Serp nfll
joint set	23.3	Pyro	1	3	78	197		No Fll	1	3	6	2	3.6	No fll
joint set	23.44	Pyro	1	3	80	29	1	Calc	1	3	6	2	4.3	Calc infill
joint set	23.64	Pyro	1	3	80	29		No Fll	1	3	6	2	2.6	No fll
joint set	23.88	Pyro	1	3	75	323	1	Serp	1	3	5	2	2.3	Serp infill
joint set	25.06	Pyro	1	3	75	314	1	Calc	1	3	6	2	3.8	Calc nfll
joint set	25.15	Pyro	1	3	75	314	2	Serp	2	3	5	2	1.5	Serp nfll

joint set	25.26	Pyro	1	3	70	259	2	Serp	2	3	6	2	3.6	Serp mxed wth non softenng
joint set	26.64	Pyro	1	3	75	301	3	Serp	3	3	5	2	3.7	Serp nfll
joint set	27.40	Pyro	1	3	85	305		No Fill	1	3	6	2	3.9	No fill
joint set	27.5	Pyro	1	3	85	305	2	Serp	2	3	5	2	3.9	Serp coatngs
joint set	27.73	Pyro	1	3	77	269	2	Serp	2	3	5	2	3.4	Serp coatngs
joint set	28	Pyro	1	3	70	307	3	Serp	3	3	5	2	2.9	Serp infill
joint set	28.9	Pyro	1	3	75	289	2	Serp	2	3	5	2	4	Serp coatings
joint set	29.83	Pyro	1	3	85	315		No Fll	1	3	6	2	5.5	No fll
joint set	31.3	Pyro	1	3	65	182	1	Serp	1	3	5	2	5.5	Serp coatings
joint set	31.3	Pyro	1	3	65	283	1	Serp	1	3	6	2	5.5	Serp infill + pyroxenite

A.2 Merensky reef

LOCALITY		23_42_1S&2S
SURVEYED BY	CHRIS AND JOEL	

Joint set or structure	Location	Rock			Orientation		Infill		Joint wall		Joint wall roughness	Dip length		Comments
		Type	Weathering	Hard-ness	Dip	Dip Di-rection	Thick-nes	Type	Sepa-ration	Hard-ness	Micro	Macro		
J	0.35	Pyro	1	3	80	28	1mm		1mm	3	6	2	8.2	Calcite Infill
J	0.83	Pyro	1	3	85	30	1mm		1mm	3	6	2	8.4	Calcite Infill
J	0.96	Pyro	1	3	80	225	1mm		1mm	3	6	2	3.64	Calcite Infill
J	1.65	Pyro	1	3	80	50	2mm		2mm	3	6	2	7.65	Calcite Coating
J	2.17	Pyro	1	3	75	215	-		2mm	3	6	2	6.37	No infill
J	2.29	Pyro	1	3	85	190	1mm		1mm	3	6	2	7.45	Calcite Infill
J	3.05	Pyro	1	3	70	356	1mm		2mm	3	6	2	6.62	Calcite Coating
J	3.82	Pyro	1	3	75	356	2mm		3mm	3	6	2	5.41	Calcite Infill
J	6.42	Pyro	1	3	80	358	2mm		3mm	3	5	2	11.5	Serpentinite Infill
J	7.70	Pyro	1	3	85	175	2mm		2mm	3	6	2	7.15	Calcite Infill
J	9.15	Pyro	1	3	80	204	2mm		2mm	3	6	2	3.92	Calcite Infill
J	10.60	Pyro	1	3	70	265	1mm		1mm	3	6	2	3.76	No infill
J	11.12	Pyro	1	3	80	190	2mm		2mm	3	6	2	4.24	Calcite Infill
J	11.63	Pyro	1	3	88	180	2mm		2mm	3	6	2	16.82	Calcite Infill
J	13.10	Pyro	1	3	85	358	-		2mm	3	6	2	10.24	No infill
J	14.40	Pyro	1	3	85	205	1mm		1mm	3	6	2	5.02	Calcite Infill
J	15.50	Pyro	1	3	70	10	1mm		1mm	3	6	2	7.11	Calcite Infill
Joint	2.52	Pyro	1		90	222	2mm	Sep	2mm	3	5	2	3.30	
Joint	3.10	Pyro	1		85	210	1mm	Calc	1mm	3	6	2	3.18	
Joint	3.70	Pyro	1		85	54	2mm	Sep	2mm	3	5	2	5.16	
Joint	3.80	Pyro	1		75	56	1mm	Sep	1mm	3	5	2	6.36	

Joint	4.12	Pyro	1		65	33			1mm	3	6	2	7.66	No Infill
Joint	4.45	Pyro	1		80	46			2mm	3	6	2	7.55	No Infill
Joint	4.75	Pyro	1		75	48	3mm	Sepc	3mm	3	5	2	3.76	
Joint	5.55	Pyro	1		90	230	1mm	Calc	1mm	3	6	2	12.44	
Joint	6.03	Pyro	1		85	220	1mm	Calc	1mm	3	6	2	7.67	
Joint	7.31	Pyro	1		70	351	3mm	Sep	3mm	3	5	2	4.42	
Joint	8.85	Pyro	1		85	18	2mm	Sepc	2mm	3	5	2	6.43	
Joint	9.03	Pyro	1		85	20	2mm	Sep	2mm	3	5	2	6.04	
Joint	10.85	Pyro	1		80	225	3mm	Calcc	3mm	3	6	2	3.21	
Joint	11.60	Pyro	1		65	185			1mm	3	6	2	4.44	No Infill
Joint	12.49	Pyro	1		65	300	1mm	Calc	1mm	3	6	2	10.61	
Joint	13.25	Pyro	1		90	176	2mm	Sep	2mm	3	5	2	6.88	
Joint	13.64	Pyro	1		80	330	1mm	Calc	1mm	3	6	2	6.57	
Joint	14.02	Pyro	1		20	230	1mm	Calc	1mm	3	6	2	6.40	
Joint	14.05	Pyro	1		80	15			2mm	3	6	2	4.55	No Infill
Joint	14.11	Pyro	1		85	180	2mm	Sep	2mm	3	5	2	4.09	
Joint	15.27	Pyro	1		80	188	1mm	Calc	1mm	3	6	2	4.97	
Joint	16.80	Pyro	1		90	178	2mm	Calcc	2mm	3	6	2	6.01	
Joint	17.23	Pyro	1		24	116			1mm	3	6	2	3.7	No Infill
Joint	18.92	Pyro	1		46	195			1mm	3	6	2	3.23	No Infill
Joint	19.35	Pyro	1		60	24	2mm	Calc	2mm	3	6	2	3.80	
Joint	0.05	Pyro	1		80	357	3mm	Sep	3mm	3	5	2	5.21	
Joint	0.24	Pyro	1		85	176	1mm	Calc	1mm	3	6	2	4.74	
Joint	0.42	Pyro	1		85	145	1mm	Calc	1mm	3	6	2	6.07	
Joint	1.82	Pyro	1		85	180			2mm	3	6	2	2.16	No Infill
Joint	3.44	Pyro	1		85	220			1mm	3	6	2	4.58	No Infill
Joint	5.28	Pyro	1		85	160			1mm	3	6	2	6.38	No Infill
Joint	5.95	Pyro	1		85	162	2mm	Calc	2mm	3	6	2	5.75	
Joint	7.05	Pyro	1		85	344			2mm	3	6	2	6.78	No Infill
Joint	8.66	Pyro	1		90	349			3mm	3	6	2	3.62	No Infill
Joint	9.50	Pyro	1		85	169			1mm	3	6	2	3.83	No Infill
Joint	10.36	Pyro	1		85	340			2mm	3	6	2	3.66	No Infill
Joint	11.85	Pyro	1		85	11			1mm	3	6	2	5.58	No Infill
Joint	12.82	Pyro	1		75	33			1mm	3	6	2	4.57	No Infill
Joint	13.36	Pyro	1		65	55			2mm	3	6	2	3.23	No Infill
Joint	13.63	Pyro	1		85	20			3mm	3	6	2	6.60	No Infill
Joint	14.10	Pyro	1		80	15	2mm	Calc	2mm	3	6	2	4.89	
Joint	14.80	Pyro	1		85	214			1mm	3	6	2	4.65	No Infill
Joint	15.44	Pyro	1		80	215	1mm	Calc	1mm	3	6	2	5.94	
Joint	16.58	Pyro	1		85	38	1mm	Calc	1mm	3	6	2	3.51	

Joint	17.22	Pyro	1		75	24	2mm	Calc	2mm	3	6	2	4.27	
Joint	17.71	Pyro	1		75	32	1mm	Calc	1mm	3	6	2	4.52	
Joint	18.32	Pyro	1		88	8			2mm	3	6	2	4.51	No Infill
Joint	19.64	Pyro	1		75	15	3mm	Sep	3mm	3	5	2	3.74	
Joint	20.91	Pyro	1		85	16			1mm	3	6	2	7.78	No Infill
Joint	22.02	Pyro	1		75	31	2mm	Sep	2mm	3	5	2	4.48	
Joint	23.80	Pyro	1		70	35			1mm	3	6	2	3.65	No Infill
Joint	24.75	Pyro	1		60	52			1mm	3	6	2	3.11	No Infill
Joint	25.33	Pyro	1		90	178	2mm	Sep	2mm	3	5	2	3.36	
Joint	26.32	Pyro	1		75	25	1mm	Calc	1mm	3	6	2	3.03	
Joint	26.63	Pyro	1		75	28	2mm	Calc	2mm	3	6	2	3.69	
Joint	27.20	Pyro	1		72	41			1mm	3	6	2	3.93	No Infill
Joint	27.65	Pyro	1		75	30	2mm	Calc	2mm	3	6	2	3.21	
Joint	28.07	Pyro	1		90	192	1mm	Calc	1mm	3	6	2	4.57	
Joint	28.53	Pyro	1		85	25	1mm	Calc	1mm	3	6	2	3.15	
Joint	29.80	Pyro	1		85	5			2mm	3	6	2	3.15	No Infill
J	1.02	Pyro	1	3	70	355			2mm	3	6	2	5.40	No infill
J	1.88	Pyro	1	3	70	7			1mm	3	6	2	10.08	No infill
J	2.35	Pyro	1	3	80	14			1mm	3	6	2	6.73	No infill
J	3.27	Pyro	1	3	75	13			2mm	3	6	2	6.55	No infill
J	3.27	Pyro	1	3	80	161			2mm	3	6	2	3.30	No infill
J	5.18	Pyro	1	3	70	25			1mm	3	6	2	7.00	No infill
J	6.75	Pyro	1	3	80	16			2mm	3	6	2	7.03	No infill
J	6.86	Pyro	1	3	85	43			1mm	3	6	2	6.20	No infill
J	8.66	Pyro	1	3	52	41			1mm	3	6	2	6.64	No infill
J	9.54	Pyro	1	3	80	46			1mm	3	6	2	6.70	No infill
J	10.00	Pyro	1	3	78	54			2mm	3	6	2	5.35	No infill
J	10.90	Pyro	1	3	72	53			1mm	3	6	2	5.77	No infill
J	11.20	Pyro	1	3	75	49	2mm		2mm	3	5	2	6.40	Serpentinite Infill
J	12.05	Pyro	1	3	70	82	1mm		1mm	3	5	2	6.63	Serpentinite Infill
J	12.10	Pyro	1	3	55	25	1mm		2mm	3	5	2	8.20	Serpentinite
J	12.61	Pyro	1	3	72	22	1mm		1mm	3	5	2	6.71	Serpentinite Infill
J	12.75	Pyro	1	3	95	34	2mm		2mm	3	5	2	7.48	Serpentinite Infill
Dyke	12.75	Pyro	Lamprophyre Dyke 40mm thick											
J	13.95	Pyro	1	3	80	62	1mm		1mm	3	5	2	6.90	Serpentinite Infill
J	14.42	Pyro	1	3	75	48	1mm		2mm	3	5	2	7.43	Serpentinite Infill
J	14.90	Pyro	1	3	80	228	1mm		2mm	3	5	2	4.80	Serpentinite
J	15.50	Pyro	1	3	87	63	1mm		2mm	3	5	2	4.46	Serpentinite Infill
J	15.50	Pyro	1	3	88	40	1mm		2mm	3	5	2	4.85	Serpentinite Infill
J	16.08	Pyro	1	3	64	38	1mm		2mm	3	5	2	6.91	Serpentinite Infill

J	18.20	Pyro	1	3	82	22	1mm		3mm	3	5	2	7.49	Serpentinite
J	18.82	Pyro	1	3	80	28	1mm		2mm	3	5	2	5.00	Serpentinite Infill
J	20.27	Pyro	1	3	86	37	1mm		1mm	3	5	2	7.88	Serpentinite Infill
J	22.20	Pyro	1	3	82	28			5mm	3	6	2	6.25	No Infill
J	22.65	Pyro	1	3	5	55			1mm	3	6	2	4.06	No Infill
J	23.71	Pyro	1	3	80	67			1mm	3	6	2	3.38	No Infill
J	24.90	Pyro	1	3	85	65			2mm	3	6	2	3.34	No Infill
J	24.90	Pyro	1	3	90	5			2mm	3	6	2	4.37	No Infill
J	26.10	Pyro	1	3	85	21			1mm	3	6	2	3.87	No Infill
J	27.02	Pyro	1	3	87	26			3mm	3	6	2	5.92	No Infill
J	27.9	Pyro	1	3	72	52			1mm	3	6	2	4.06	No Infill
J	28.6	Pyro	1	3	85	34			2mm	3	6	2	5.92	No Infill
J	0.70	Pyro	1	3	70	65	1mm		1mm	3	6	2	5.10	Calcite Infill
J	0.97	Pyro	1	3	55	74			1mm	3	6	2	5.80	No infill
J	1.30	Pyro	1	3	80	69	1mm		1mm	3	5	2	4.70	Serpentinite Infill
J	1.56	Pyro	1	3	60	190	1mm		1mm	3	6	2	6.60	Calcite Infill
J	2.05	Pyro	1	3	85	130	1mm		2mm	3	6	2	5.80	Calcite Infill
J	3.37	Pyro	1	3	70	185	3mm		3mm	3	6	2	10.40	Calcite Infill
J	5.24	Pyro	1	3	76	188	1mm		1mm	3	5	2	7.80	Serpentinite Infill
J	6.30	Pyro	1	3	25	10	1mm		1mm	3	5	2	0.72	Serpentinite Infill
J	6.48	Pyro	1	3	95	20	1mm		1mm	3	5	2	3.60	Serpentinite
J	7.28	Pyro	1	3	65	60	1mm		1mm	3	5	2	4.90	Serpentinite Infill
J	8.28	Pyro	1	3	70	68	2mm		2mm	3	5	2	6.40	Serpentinite Infill
J	9.60	Pyro	1	3	45	65			1mm	3	6	2	4.70	No infill
J	10.00	Pyro	1	3	75	68	2mm		3mm	3	6	2	4.80	Calcite Infill
J	11.03	Pyro	1	3	85	57	1mm		1mm	3	6	2	6.50	Calcite Infill
J	12.15	Pyro	1	3	72	48	1mm		1mm	3	6	2	6.00	Calcite Infill
J	13.24	Pyro	1	3	75	225	1mm		1mm	3	6	2	6.10	Calcite Infill
J	14.76	Pyro	1	3	85	355	2mm		2mm	3	5	2	5.60	Serpentinite Infill
J	14.77	Pyro	1	3	85	194	1mm		1mm	3	5	2	5.60	Serpentinite Infill

Appendix B. Block Mapping Data

B.1 UG2 reef

KEYBLOCK SURVEY SHEET																
LOCALITY		15-53-3N&4N (UG2)														
RECORDED BY		Edgar and Jonas														
Location	Offset	Distance to Face	Blast/ Barring	Block Dimensions					Structural Properties							
				Block Shape	L	W	H	No.	Joint Structure	Dip	DipDr	Set	Jr	Ja	Jw	
21.80		3.3	Blast	T	0.88	0.56	0.19		J	90	252	J1	2	8	1	
									J	42	049	J1	2	8	1	
									J	80	053	J1	2	8	1	
21.30		2.9	Blast	T	0.33	0.29	0.9		J	85	101	J2	2	8	1	
									J	87	055	J1	2	8	1	
20.6		0	Blast	W	0.97	0.64	0.15		J	85	042		2	8	1	
									J	82	304		2	8	1	
20.75		3.5	Blast	W	0.69	0.49	0.29	2	J	55	084		2	8	1	
									J	72	194		3	1	1	
									J	87	162		3	1	1	
20.4		3.1	Blast	W	0.60	0.49	0.25	2	J	80	280		2	8	1	
									J	85	284		2	8	1	
19.5		1.7	Bar	W	0.41	0.24	0.14		J	75	257		2	8	1	
									J	86	301		2	8	1	
19.1		2.2	Blast	W	0.88	0.49	0.20	2	J	78	104		3	1	1	
									J	68	023		3	1	1	
18.73	4	0.44	Blast	T	0.29	0.18	0.14	1	J	80	280		2	8	1	
									J	27	186		2	8	1	
17.7		1.9	Blast	W	0.57	0.25	0.2	1	J	60	025		3	1	1	
									J	37	019		3	1	1	

17.4		0.0	Blast	W	0.46	0.41	0.17	2	J	90	278		2	8	1
									J	48	087		2	8	1
17.2		1.3	Blast	W	0.55	0.29	0.16	2	J	65	009		2	8	1
					0.35	0.85	0.22		J	40	052		2	8	1
15.1		1.4	Blast	W	0.41	0.51	0.13		J	68	275		3	1	1
									J	39	231		3	1	1
										82	277		3	1	
5.3		0.66	Bar	T	1.61	1.12	0.16		J	80	283		2	4	1
									J	85	125		3	2	1
6.0		1.1	Blast	W	0.39	0.29	0.11		J	75	144		2	4	1
									J	79	059		2	4	1
6.4		1.8	Blast	W	0.74	0.61	0.04		J	85	025		2	4	1
									J	87	205		3	2	1
									J	80	029		3	1	1
7.5		1.5	Bar	W	0.17	0.24	0.04		J	88	019		2	8	1
									J	85	005		2	8	1
7.5		1.2	Bar	W	0.32	0.29	0.11		J	80	213		2	4	1
									J	85	294		2	8	1
9.8		1.1	Blast	W	0.37	0.44	0.09		J	76	049		2	4	1
									J	88	040		2	8	1
11.76		1.1	Blast	W	0.26	0.44	0.12		J	80	296		2	4	1
									J	80	296		2	8	1
									J	85	036		2	4	1
15.8		1.0	Blast	W	0.38	0.44	0.10		J	75	040		2	4	1
									J	82	278		2	4	1
									J	50	106		2	4	1
18.2		1.5	Blast	W	0.37	0.56	0.13		J	63	056		2	4	1
									J	80	098		2	4	1

21.5		1.3	Blast	W	1.24	0.96	0.38		J	65	318		2	8	1
									J	88	043		3	1	1
22.7		2.24	Blast	W	0.38	0.41	0.19		J	75	306		2	8	1
									J	80	232		3	1	1
22.7		1.4	Blast	W	0.19	0.26	0.14		J	75	234		2	4	1
									J	89	035		3	2	1
4.50	0.7	2.5	Bar	W	0.38	1.72	2.11	2	J	78	115		3	2	1
									J	75	042		3	2	1
9.80	-0.21	1.9		W	0.36	0.49	0.11		J	80	044		3	1	1
									J	80	115		2	8	1
11.60	1.62	0.0	Blast	W	0.69	0.6	0.24		J	53	015		2	8	1
									J	30	202		3	1	1
12.50	1.05	0.0	Blast	W	0.64	0.79	0.32		J	60	010		2	8	1
									J	38	210		3	1	1
16,90	1.46	0.0	Blast	W	0.75	0.46	0.18		J	70	288		2	8	1
									J	75	234		2	8	1
16.90	0.78	1.1	Blast	T	0.38	0.44	0.16		J	70	191		1	4	1
									J	85	106		3	1	1
									J/D	30	061		2	8	1
18.60	-0.17	1.8	Blast	W	0.69	0.55	0.13		J	90	134		2	8	1
									J	82	314		2	8	1
21.10	-0.44	2.1	Blast	T	0.68	1.84	0.26		J	86	035		2	4	1
									J	66	295		2	8	1
5.2	-1.03	2.1	Bar	W	0.37	0.26	0.11		J	85	265		2	8	1
									J	85	118		2	4	1
									J	80	316		2	4	
7.8	-0.55	2.1	Blast	W	0.24	0.26	0.12		J	62	318		3	1	1

									J	85	118		3	1	1
9.27	-0.93	5.6	Blast	TP	0.42	0.35	0.11		J	85	103		2	4	1
									J	75	279		2	4	1
									J	85	103		3	1	1
9.6	0.81	0.61	Blast	TW	0.85	0.35	0.22		J	88	211		2	4	1
									J	65	275		3	1	1
11.6	0.73	0.0	Blast	W	0.42	0.16	0.15		J	65	011		2	8	1
									J	65	304		3	1	1
12.0	0.79	0.45	Blast	TP	0.47	0.16	0.15		J	55	005		2	4	1
									J	80	195		3	1	1
22.7	0.87	1.2	Bar	W	0.59	0.42	0.23		J	75	113		3	1	1
									J	85	232		2	4	1
									J	75	295		2	4	1
9.3	1.91	1.5	Blast	W	0.34	1.35	0.21		J	55	003		2	4	1
									J	30	240		3	1	1
11	1.31	1.8	Blast	W	0.46	1.09	0.3		J	55	012		2	8	1
									B/F	35	236		3	1	1
12	1.3	2.3	Blast	W					J	55	010		2	8	1
									B/F	35	218		3	1	1
13	1.7	2.4	Bar	TW	0.52	0.45	0.12		J	85	087		2	8	1
									J	85	087		3	4	1
									J	75	019		2	4	1
16.6	-0.93	4.7	Blast	TT	1.1	1.21	0.14		J	75	090		2	8	1
									J	55	327		2	4	1
									J	85	225		2	4	1
19.5	-1.6	5	Blast	W	1.11	0.98	0.24		J	85	035		2	4	1
									J	80	302		2	8	1
									J	80	302		2	4	1

									J	85	035		3	1	1
7.8	1.3	0.51	Blast	TW	0.26	1.03	0.16		J	80	013		2	4	1
									J	83	015		2	4	1
11	0.81	1.89	Blast	W	0.16	0.55	0.11		B/F	55	012		2	8	1
									J	90	027		2	4	1
16.3	1.03	1.7	Blast	W	0.25	0.26	0.18		J	85	027		2	4	1
									J	85	027		2	4	1
19									J	77	283		2	4	1
									J	77	283		3	1	1
22.9	-1.3	3.1	Blast	TW	0.68	0.2	0.17		J	82	107		3	1	1
									J	86	036		3	1	1
0.10	4.60	1.23	Blast	TP	0.69	0.31	0.11	4	J	50	221	J1	2	4	1
					0.64	0.27			J	90	133	R	2	4	1
				Average	0.67	0.29	0.11		J	62	213	J1	2	4	
									J	65	83	J2	2	4	1
0.55	5.03	0.63	Blast	W	0.36	0.44	0.12	3	J	65	130	R	2	4	1
									J	65	215	J1	2	4	1
									J	70	218	J1	2	4	1
1.40	4.45	1.45	Blast	T	0.30	0.34	0.1	3	J	85	313	R	2	4	1
									J	80	222	J1	2	4	1
									J	84	123	J2	3	1	1
1.70	4.81	1.07	Blast	T	0.45	0.17	0.14	3	BF	60	91	N/A	3	1	1
									J	44	153	R	2	4	1
									J	50	319	R	2	4	1
									J				3	1	1
1.80	1.80	-0.77	Bar	TP	1.20	0.35	0.13	3	J	85	136	R	2	4	1
									J	80	311	R	2	4	1
									J	15	33		3	1	1
									J	75	221	J1	2	4	
									J	55	224	J1	2	4	1

2.00	5.43	0.47	Blast	W	0.71	0.35	0.25	3	J	62	118	J2	2	4	1
									J	72	334	R	3	1	1
									J	68	195	J3	2	4	1
5.55	6.99	0.103	Blast	TP	0.58	0.18	0.11	3	J	80	140	R	2	4	1
									J	78	331	R	2	4	1
									J	50	224	J1	3	1	1
8.80	6.60	-1.15	Blast	TP	0.87	0.32	0.12	3	J	80	319	R	2	4	1
									J	75	36	J1	2	4	1
									J	80	130	R	2	4	1
12.30	5.00	0	Blast	W	0.50	5.00	0.25	3	J	32	220	J1	2	4	1
									J	80	62	J1	2	4	1
0.15	4.15	1.35	Blast	T	0.30	0.49	0.11	3	Joint	85	213	J1	2	4	1
									Joint	76	322	R	2	4	1
									Joint	80	147	R	2	4	1
0.25	3.70	1.62	Blast	T	0.26	0.47	0.09	3	Joint	88	222	J1	3	1	1
									Joint	70	292	R	3	2	1
									Joint	88	318	R	3	1	1
0.55	4.45	0.85	Blast	TT	0.69	0.23	0.09	3	Joint	80	226	J1	3	2	1
									Joint	70	322	R	2	4	1
									Joint	60	121	J2	3	2	1
0.61	3.99	1.30	Blast	TT	0.47	0.36	0.09	4	Top Surf	35	58	J1	2	4	1
									Joint	85	42	J1	2	4	1
									Joint	80	325	R	2	4	1
									Joint	80	230	J1	3	1	1
									Joint				3	1	1
0.84	4.31	1.02	Blast	T	0.23	0.23	0.11	3	Joint	90	236	J1	2	4	1
									Joint	75	332	R	2	4	1
									Joint	15	33		3	1	1
									Top Surf	30	344	N/A	3	1	1

1.10	5.03	0.25	Blast	T/D	0.77	0.28	0.16	3	Joint	65	215	J1	2	4	1
									Joint	85	317	R	3	1	1
									Joint	78	347	J3	3	1	1
									Top Surf	20	356	N/A	2	4	1
2.05	2.47	2.97	Bar	TT	0.36	0.53	0.13	3	Joint	80	65	J1	2	4	1
									Joint	52	336	R	3	2	1
									Joint	65	150	R	3	1	1
2.10	2.69	2.60	Blast	W	0.77	0.50	0.18	4	Joint	40	332	R	2	4	1
									Joint	50	141	R	2	4	1
									Joint	75	240	J1	3	1	1
									Joint	84	310	R	3	2	1
2.90	1.18	3.63	Blast	W	1.90	1.10	0.43	4	Joint	62	136	R	3	1	1
									Top Surf	30	4	N/A	2	4	1
									Joint	78	224	J1	2	4	1
									Joint	80	51	J1	3	1	1
									BF	80	318	N/A	3	1	1
4.34	3.85	0.92	Blast	TT	0.60	0.98	0.15	3	Joint	70	210	J1	2	4	1
									Joint	70	358	R	3	2	1
									Joint	80	328	R	3	2	1
5.71	3.48	1.64	Blast	T	0.98	1.42	0.32	3	Joint	80	225	J1	3	1	1
									Joint	38	167	J3	3	2	1
									Joint	75	336	R	3	1	1
11.90	4.39	1.30	Blast	T	0.44	0.50	0.16	3	Joint	71	10	J3	3	1	1
									Joint	52	227	J1	2	4	1
									Joint	56	90	J2	3	1	1
13.60	3.84	1.95	Blast	TP	0.95	0.3	0.21	4	Joint	80	322	R	2	4	1
					0.87	0.25			Joint	70	318	R	2	4	1
				Average	0.91	0.275	0.21		Joint	45	224	J1	3	1	1
									Joint	58	238	J1	3	2	1
19.85	4.11	2.70	Blast	TP	1.00	0.39	0.095	4	Joint	42	290	J2	3	2	1
									Joint	75	170	J3	3	2	1

									Joint	68	97	J2	2	4	1
									Joint	80	213	J1	2	4	1

B.2 Merensky reef

KEYBLOCK SURVEY SHEET															
LOCALITY		23_42 1S													
				Block Dimensions					Structural Properties						
Location	Distance to face	Offset	Blast/ Barring	Block Shape Shape	L	W	H	No.	Joint Structure	Dip	DipDr		Jr	Ja	Jw
10.57	2.13	-0.13	Barring	W	0.83	1.14	0.35	1	Joint	85	244	J1	3	1	1
									Joint	85	66	J1	3	1	1
11.14	1.48	0.52	Blast	W	0.37	0.37	0.18	1	Joint	88	155	J2	3	1	1
									Joint	10	343	R	3	1	1
12.74	1.81	0.19	Barring	W	0.42	0.32	0.28	1	Joint	89	236	J1	3	1	1
									Joint	35	59	J1	3	1	1
12.61	1.88	0.12	Barring	W	0.4	0.29	0.24	1	Joint	75	28	R	3	2	1
									Joint	75	355	J3	3	1	1
12.96	1.47	0.53	Blast	W	0.47	0.21	0.21	1	Joint	85	356	R	3	2	1
									Joint	30	172	J3	3	1	1
									Blast Fracture	55	36	N/A	3	2	1
									Joint	65	107	J2	3	1	1
13.58	1.52	0.48	Barring	W	0.48	0.57	0.21	2	Joint	85	358	J3	2	4	1
									Joint	85	32	R	3	1	1
									Joint	70	170	J3	3	1	1
															1
13.82	2.08	-0.08	Blast	P	0.39	0.44	0.22	1	Joint	85	27	R	3	2	1
									Joint	40	122	J2	3	1	1
									Joint	80	217	J1	3	1	1
									Joint	65	312	R	3	2	1
14.1	2.02	-0.02	Blast	TP	0.58	0.61	0.26	1	Joint	85	34	R	3	2	1
									Joint	85	121	J2	2	4	1

									Joint	65	217	J1	3	1	1
									Blast Fracture	70	322	R	3	1	1
14.8	1.91	0.09	Barring	TP	0.72	0.57	0.23	1	Joint	70	20	J3	3	1	1
									Joint	85	113	J2	3	1	1
									Joint	65	307	R	3	2	1
									Joint	72	224	J1	3	1	1
17.1	2.35	-0.35	Blast	TP	0.34	0.41	0.24	1	Joint	80	190	J3	3	2	1
									Joint	74	277	J2	3	1	1
									Joint	85	93	J2	3	1	1
									Blast Fracture	50	28	N/A	3	2	1
21.29	0.61	0.39	Barring	TP	0.95	0.39	0.06	1	Joint	75	333	R	3	1	1
									Joint	70	241	J1	3	2	1
									Joint	60	159	R	3	2	1
									Joint	65	66	J1	2	4	1
19.9	1.17	-0.17	Blast	W	0.32	0.29	0.11	1	Joint	85	341	R	2	4	1
									Joint	10	257	J2	3	2	1
									Joint	75	163	J3	3	1	1
									B/F	80	71	J1	3	1	1
19.8	0.52	0.48	Blast	W	0.22	0.21	0.1	1	Joint	65	329	R	3	1	1
									Joint	80	234	J1	3	1	1
									Joint	85	160	J3	3	2	1
									B/F	85	66	N/A	2	4	1
19.2	0.7	0.3	Blast	W	0.4	0.22	0.14	1	Joint	60	336	R	3	1	1
									Joint	15	154	R	3	2	1
18.5	1.36	-0.36	Blast	W	0.78	0.49	0.25	1	Joint	80	346	J3	3	1	1
									Joint	10	168	J3	3	2	1
									Joint	75	77	J2	3	2	1
									B/F	83	25	N/A	3	1	1
18.8	2.34	-1.34	Barring	W	0.48	0.57	0.21	1	Joint	65	340	J3	2	4	1
									B/F	30	72	N/A	3	1	1
									Joint	85	255	J1	2	4	1
									Joint	80	163	J3	3	2	1
17.2	1.35	-0.35	Blast	W	0.94	0.63	0.21	1	Joint	88	190	R	3	2	1
									Joint	10	346	J3	3	1	1
									B/F	77	14	N/A	3	1	1

									Joint	85	107	J2			
17	2.04	-1.04	Blast	TW	0.54	0.51	0.23	1	Joint	70	314	R	3	1	1
									Joint	60	255	J1	3	1	1
									B/F	20	94	N/A	3	2	1
									Joint	80	170	J3	3	1	1
16.2	0.41	0.59	Blast	W	1.1	0.95	0.18	1	Joint	69	25	J3	3	1	1
									Joint	45	117	J2	3	1	1
									Joint	80	210	J1	3	1	1
									Joint	85	322	R	3	2	1
15.4	0.73	0.27	Blast	W	0.97	0.71	0.21	1	Joint	65	346	J3	3	2	1
									B/F	25	18	N/A	3	1	1
									Joint	85	262	J2	3	2	1
									Joint	70	167	J3	3	1	1
12.64	0.58	0.42	Blast	W	0.59	0.54	0.12	1	Joint	85	119	J2	3	2	1
									B/F	15	32	N/A	3	1	1
11.2	0.71	0.29	Blast	W	0.53	0.41	0.15	1	Joint	85	138	R	3	1	1
									B/F	25	38	J1	3	1	1
									Joint	84	222	J1	3	2	1
									Joint	65	331	R	3	1	1
10.96	0.81	0.19	Barring	TW	0.1	0.72	0.11	1	Joint	80	111	J2	3	1	1
									B/F	20	44	N/A	3	2	1
									Joint	55	201	J3	3	2	1
									Joint	85	342	J2	3	1	1
7.5	2	2.2	Blast	W	0.58	1.00	0.32	2	Joint	75	355	R	3	1	1
									Joint	72	177	J3	3	1	1
									Joint	65	89	J2	3	2	1
									B/F	10	254	N/A	3	1	1
12.1	1.6	2.6	Blast	TP	0.52	0.94	0.39	1	Joint	70	20	J3	2	4	1
					0.40	0.72			Joint	55	111	J2	3	1	1
				Average	0.46	0.83	0.39		Joint	84	207	J3	3	1	1
									B/F	80	306	N/A	3	1	1
13.6	2.5	1.7	Barring	TP	1.00	0.49	0.31	1	Joint	70	313	R	3	2	1
					0.76	0.32			Joint	85	215	J1	2	4	1
				Average	0.88	0.405	0.31		Joint	70	116	J2	3	2	1
									B/F	55	10	N/A	3	1	1

14.1	1.7	2.5	Blast	W	0.36	0.53	0.24	2	Joint	60	336	R	3	1	1
									Joint	74	201	J3	3	2	1
									Joint	85	107	J2	3	1	1
									B/F	30	13	N/A	3	1	1
14.8	2.29	1.91	Unknown	TP	0.51	0.69	0.33	1	Joint	80	323	R	3	1	1
									Joint	85	229	J1	3	2	1
									Joint	75	128	J2	3	1	1
									Joint	15	33	J1	3	1	1
15.8	2.00	2.2	Barring	TP	0.34	0.33	0.19	1	Joint	75	301	J2	3	1	1
					0.29	0.25			Joint	65	213	J1	3	1	1
				Average	0.32	0.29	0.19		Joint	85	117	J2	3	2	1
									Joint	70	25	J3	3	1	1
16.2	2.9	1.3	Unknown	W	1.10	0.46	0.12	1	Joint	88	322	R	3	1	1
									Joint	10	215	J1	3	1	1
									Joint	85	118	J2	3	2	1
									B/F	30	21	N/A	3	1	1
16.3	2	2.2	Blast	W	0.95	0.56	0.24	1	Joint	10	57	J1	3	1	1
									Joint	80	152	R	3	1	1
									Joint	85	247	J1	3	2	1
									Joint	80	341	J3	3	1	1
17.3	0.86	3.34	Barring	W	0.49	0.29	0.18	1	Joint	75	50	J1	3	2	1
									Joint	35	148	R	3	1	1
									Joint	77	240	J1	3	1	1
									Joint	85	328	J2	3	2	1
17.5	1.36	2.84	Blast	W	0.50	0.27	0.11	1	Joint	70	55	J1	3	1	1
									Joint	35	128	J2	3	1	1
									Joint	77	224	J1	3	1	1
									Joint	90	324	R	3	1	1
19.2	1.61	2.59	Barring	TP	0.31	0.24	0.11	1	Joint	60	45	J1	3	1	1
									Joint	80	137	R	3	2	1
									Joint	75	322	R	3	1	1
									Joint	85	235	J1	2	4	1
19.8	0.70	3.5	Blast	W	0.23	0.27	0.19	1	Joint	85	352	R	3	1	1
									Joint	30	50	J1	2	4	1
									Joint	80	268	J2	2	4	1

									Joint	65	141	R	2	4	1
20.1	0.97	3.23	Blast	TP	0.26	0.32	0.14	1	Joint	85	22	J3	2	4	1
					0.20	0.25			Joint	78	117	J2	2	4	1
				Average	0.23	0.285	0.14		Joint	80	214	J1	3	2	1
									Joint	85	311	R	3	1	1
20.8	0.70	3.50	Blast	W	0.41	0.32	0.20	1	B/F	75	4	N/A	3	1	1
									Joint	80	101	J2	3	2	1
									Joint	55	198	J3	3	2	1
									Joint	76	302	J2	3	1	1
21.6	1.34	2.86	Barring	W	0.84	0.29	0.19	2	Joint	75	62	J1	3	1	1
									Joint	85	157	R	3	2	1
									Joint	45	250	J1	2	4	1
									Joint	85	342	J3	3	1	1
21.61	0.98	3.22	Blast	T	1.73	0.42	0.25	1	Joint	35	57	J1	3	1	1
									Joint	85	152	R	3	1	1
									Joint	75	248	J1	3	2	1
6.1	0.94	3.26	Blast	TW	1.59	0.99	0.52	1	Joint	80	263	J2	3	1	1
					1.38	0.80			Joint	45	172	J3	3	1	1
				Average	1.49	0.90	0.52		Joint	85	89	J2	3	2	1
									Joint	75	352	R	3	2	1
6.9	1.74	2.46	Blast	T	0.62	0.49	0.14	1	Joint	88	291	J2	3	1	1
					0.40	0.72			Joint	25	111	J2	3	2	1
				Average	0.51	0.61	0.14		B/F	62	25	J3	3	1	1
									Joint	85	205	J3	3	1	1
7.7	1.75	2.45	Barring	TP	0.73	0.44	0.19	1	Joint	80	345	J3	3	2	1
					0.76	0.32			Joint	65	277	J2	3	1	1
				Average	0.75	0.38	0.19		Joint	32	178	J3	3	2	1
									Joint	75	79	J2	3	1	1
									B/F	DR	DDR	N/A	3	1	1
8.3	1.4	2.8	Blast	T	0.26	0.11	0.09	2	Joint	35	338	R	3	1	1
									Joint	75	160	J3	3	1	1
									Joint	52	252	J1	3	1	1
9.01	1.78	2.42	Blast	TW	0.66	0.45	0.15	2	Joint	80	331	R	2	4	1
					0.60	0.39			Joint	45	242	J1	2	4	1
				Average	0.63	0.42	0.15		Joint	60	155	J2	3	1	1

11.8	1.86	2.34	Blast	W	0.66	0.44	0.09	1	Joint	85	340	J3	3	1	1
									Joint	40	164	J3	3	2	1
									Joint	75	253	J2	3	1	1
									Joint	65	87	J2	3	1	1
13.63	1.65	2.55	Barring	W	0.69	0.36	0.21	1	Joint	85	160	J3	2	4	1
									Joint	5	75	J2	3	1	1
									Joint	55	343	J3	3	1	1
									Joint	65	252	J1	3	1	1
13.8	1.57	2.63	Blast	TW	0.39	0.35	0.21	1	Joint	85	235	J1	3	1	1
									Joint	45	342	J3	3	1	1
									Joint	75	160	J3	3	2	1
									Joint	63	78	J2	3	1	1
17.35	1.81	2.39	Blast	TP	0.39	0.45	0.19	1	Joint	85	335	R	3	1	1
									Joint	20	245	J1	3	1	1
									Joint	70	60	J1	3	2	1
									Joint	80	152	R	3	1	1
									B/F	DR	DDR	N/A	3	1	1
19.4	3.83	0.37	Barring	TP	0.68	0.4	0.18	2	B/F	80	55	J1	3	1	1
									Joint	45	148	R	3	2	1
									Joint	63	239	J1	3	1	1
									Joint	85	332	R	3	1	1
22.0	2.42	1.78	Unknown	TW	0.31	0.68	0.22	1	Joint	85	45	J1	3	1	1
									Joint	45	312	R	2	4	1
									Joint	65	225	J1	3	1	1
									Joint	70	138	R	3	2	1
1.5	4.12	-0.12	Barring	T	0.59	0.85	0.1	1	Joint	80	50	J1	3	2	1
									Joint	40	250	J1	3	2	1
									Joint	75	5	J3	3	2	1
									B/F	10	36	J1	3	1	1
1.55	5.05	-1.05	Unkown	TT	0.45	0.34	0.09	1	Joint	80	215	J1	3	2	1
					0.32	0.21			Joint	55	308	R	3	2	1
				Average	0.39	0.28	0.09		B/F	10	40	J1	3	1	1
2.3	4.3	-0.3	Unknown	TT	0.32	0.58	0.07	1	Joint	75	328	R	3	2	1
					0.21	0.5			Joint	80	218	J1	3	2	1
				Average	0.27	0.54	0.07		Joint	85	110	J2	3	1	1

2.33	3.6	0.4	Barring	TP	0.55	0.4	0.17	3	Joint	75	358	R	3	2	1
			3 small		0.50	0.36			Joint	60	275	J2	3	1	1
				Average	0.53	0.38	0.17		Joint	20	190	J3	3	1	1
									Joint	55	88	J2	3	1	1
7.6	3.25	0.75	Barring	W	0.62	0.24	0.16	2	Joint	85	9	J3	2	4	1
			2 small						Joint	65	95	J2	2	4	1
									Joint	74	188	J3	3	1	1
									Joint	48	272	J2	2	4	1
8.1	3.14	0.86	Barring	W	0.41	0.24	0.16	1	Joint	80	40	J1	3	1	1
									Joint	55	101	J2	2	4	1
									Joint	65	179	J3	3	2	1
									Joint	60	258	J2	3	1	1
10.05	5.4	-1.4	Barring	T	0.41	0.25	0.17	3	Joint	70	46	J1	3	2	1
									Joint	85	160	J3	3	2	1
									Joint	60	220	J1	3	2	1
18.05	3.3	0.7	Unknown	W	0.75	0.53	0.15		Joint	55	37	J1	3	2	1
									Joint	65	125	J2	2	4	1
									Joint	85	212	J1	3	2	1
									Joint	73	299	J2	3	1	1
0.9	5.39	-0.47	Unknown	TP	0.8	0.55	0.22	3	Joint	85	160	J3	3	1	1
									Joint	70	175	J3	3	1	1
									Joint	80	238	J1	3	1	1
									B/F	10	036	J1	3	1	1
3	5.42	-0.11	Unknown	TT	0.59	0.32	0.14	2	Joint	70	313	R	3	2	1
					0.50	0.27			Joint	90	172	J3	3	2	1
				Average	0.55	0.295	0.14		B/F	10	36	J1	3	1	1
4.5	4.14	1.38	Barring	W	1.15	0.28	0.22	2	Joint	35	126	J2	3	2	1
									Joint	80	345	J3	3	1	1
4.9	5.32	0.16	Unknown	W	1.13	0.41	0.33	3	Joint	85	324	R	2	4	1
									Joint	85	53	J1	2	4	1
									Joint	20	135	R	3	1	1
									Dome Surf			N/A	3	1	1
6	4.94	0.55	Barring	W	0.89	0.56	0.9	2	Joint	30	3	J3	3	2	1
									Joint	25	122	J2	3	1	1

									Joint	48	272	J2	2	4	1
6.32	4.20	1.26	Barring	W	0.84	0.47	0.18	4	Joint	60	294	J2	3	2	1
									Joint	80	357	J3	3	1	1
									Joint	85	242	J1	3	2	1
									Joint	30	109	J2	3	1	1
7.9	5.11	0.6	Unknown	TP	0.92	0.43	0.21	3	Joint	85	350	J3	3	1	1
					0.82	0.39			Joint	30	73	J1	3	2	1
				Average	0.87	0.41	0.21		Joint	85	157	R	3	2	1
11.4	4.97	1.25	Barring	W	0.57	0.38	0.15	2	Joint	80	33	J1	3	1	1
									Joint	48	140	R	3	1	1
15.2	4.8	0.47	Barring	W	1	0.62	0.18	2	Joint	25	66	J1	3	1	1
									Joint	85	180	J3	2	4	1
4.59	4.15	-0.39	Unknown	W	0.24	0.32	0.08	3	BF	20	141	R	3	1	1
									Joint	70	300	J2	3	1	1
									Joint	85	49	J1	3	1	1
4.7	3.8	0.25	Unknown	TP	0.2	0.51	0.11	3	Joint	81	42	J1	3	1	1
									Joint	45	38	J1	3	1	1
									Joint	49	238	J1	3	1	1
5.79	4.67	-0.62	Bar	T	0.15	0.22	0.05	3	BF	20	145	R	3	1	1
									Joint	80	213	J1	3	2	1
									Joint	70	320	R	3	1	1
6.54	3.87	0.43	Unknown	W	0.77	0.25	0.14	3	BF	30	357	J3	3	1	1
									Joint	85	323	R	3	2	1
									Joint	85	196	J3	3	1	1
7.44	3.77	0.54	Unknown	TP	0.45	0.38	0.14	3	Joint	75	160	J3	3	1	1
									Joint	75	217	J1	2	4	1
									BF	35	170	J3	3	1	1
7.99	4.56	-0.43	Bar	W	0.67	0.31	0.1	3	BF	35	130	R	3	2	1
									J/C	72	137	R	3	1	1
									Joint	90	208	J3	3	2	1
8.84	3.23	1.04	Bar	TT	0.31	0.24	0.09	3	Joint	85	205	J3	2	4	1
					0.28	0.2			BF	25	40	J1	3	1	1
				Average	0.3	0.22	0.09		Joint	80	151	R	3	1	1

10.34	3.72	0.8	Unknown	W	0.55	0.19	0.1	3	Joint	75	357	R	3	1	1
									BF	35	100	J2	3	1	1
									Joint	90	131	R	3	2	1
13.33	2.67	2.06	Unknown	TP	0.63	0.43	0.19	3	Joint	76	174	J3	3	2	1
									Joint	45	249	J1	3	2	1
									Joint	85	42	J1	3	2	1
14.64	2.94	1.55	Unknown	W	0.5	0.15	0.05	2	Joint	90	172	J3	2	4	1
									Joint	45	117	J2	3	1	1
15.1	3.29	1.35	Unknown	W	0.65	0.29	0.11	3	Joint	80	177	J3	3	2	1
									Joint	50	65	J1	3	1	1
									BF	45	148	R	3	1	1
17.32	3.42	1.96	Unknown	TT	0.54	0.32	0.14	3	BF	40	100	J2	3	1	1
									Joint	90	161	J3	3	1	1
									Joint	45	56	J1	3	1	1
17.77	3.11	1.9	Unknown	T	0.48	0.32	0.13	3	Joint	90	271	J2	3	1	1
									Joint	85	358	R	3	1	1
									Joint	62	112	J2	3	1	1
19.31	2.6	2.55	Bar	W	0.95	0.9	0.12	3	Joint	40	142	R	3	2	1
										65	228	J1	3	1	1
									Joint	85	177	J3	3	2	1
0.5	1.45	-0.25	Blast	W	0.53	0.57	0.42	1	Joint	85	40	J1	3	2	1
									Joint	75	218	J1	3	2	1
									B/F	55	306	J2	3	1	1
1.03	1.99	-0.79	Blast	W	0.44	0.39	0.19	1	Joint	80	309	R	2	4	1
									Joint	65	220	J1	2	4	1
									B/F	73	40	N/A	3	1	1
1.7	1.98	-0.78	Barring	TP	0.57	0.44	0.16	1	Joint	85	65	J1	3	2	1
					0.44	0.38			B/F	25	234	N/A	3	1	1
				Average	0.51	0.41	0.16								
1.7	0.93	0.27	Barring	TW	0.84	0.67	0.18	1	Joint	55	355	R	3	1	1
					0.75	0.61			Joint	75	41	J1	3	2	1
				Average	0.8	0.64	0.18		B/F	10	210	N/A	3	1	1

3.5	2.11	-0.91	Barring	T	0.32	0.24	0.11	1	Joint	10	212	J1	2	4	1
									Joint	85	132	R	2	4	1
									Joint	80	45	J1	3	1	1
4.44	1.81	-0.61	Blast	TT	0.32	0.25	0.12	1	Joint	75	95	J2	3	1	1
					0.24	0.17			Joint	65	254	R	3	1	1
				Average	0.28	0.21	0.12								
6.20	1.46	-0.26	Blast	T	1.01	0.52	0.17	1	Joint	85	324	R	3	2	1
									Joint	55	223	J1	3	1	1
									Joint	40	42	J1	3	1	1
6.50	0.8	0.4	Blast	W	0.55	0.28	0.12	1	Joint	40	48	J1	3	1	1
									Joint	85	190	J3	3	2	1
									Joint	65	277	J2	3	1	1
6.60	0.61	0.59	Barring	W	0.52	0.88	0.18	1	Joint	65	47	J1	3	1	1
									Joint	73	210	J3	3	2	1
									Joint	54	132	R	3	2	1
7.10	1.26	-0.06	Blast	TW	0.77	0.56	0.26	1	Joint	65	36	J1	3	1	1
					0.67	0.50			Joint	75	118	J2	3	2	1
				Average	0.72	0.53	0.26		Joint	55	175	J3	3	2	1
									Joint	85	272	J2	3	1	1
8.10	1.78	-0.58	Blast	W	0.31	0.24	0.11	1	Joint	65	44	J1	2	4	1
									Joint	55	226	J1	3	1	1
									Joint	85	320	R	2	4	1
9.70	0.77	0.43	Barring	P	0.67	0.39	0.17	1	B/F	45	41	N/A	3	1	1
									Joint	80	92	J2	2	4	1
									Joint	85	178	J3	2	4	1
									Joint	80	262	J2	2	4	1
10.80	2.00	-0.80	Blast	TP	0.56	0.32	0.14	1	Joint	85	337	R	3	2	1
					0.50	0.25			Joint	80	243	J1	3	2	1
				Average	0.53	0.285	0.14		Joint	65	70	J1	3	1	1
11.30	0.80	0.40	Blast	W	0.40	0.32	0.16	1	Joint	75	262	J2	3	2	1
									Joint	66	77	J2	3	1	1
14.80	1.56	-0.36	Barring	T	0.31	0.33	0.24	2	Joint	80	250	J1	3	1	1
									Joint	65	162	J3	3	1	1
									Joint	15	75	J1	3	2	1

2.4	2.88	-0.88	Unknown	P	0.53	0.32	0.14	1	Joint	85	231	J1	3	1	1
									Joint	80	150	R	3	1	1
									Joint	55	58	J1	3	2	1
									Joint	60	318	R	3	1	1
2.51	0.5	1.5	Blast	TW	0.62	0.5	0.28	1	Joint	75	214	J1	2	4	1
					0.57	0.44			Joint	65	357	R	2	4	1
				Average	0.6	0.47	0.28		Joint	73	40	J1	3	1	1
3.09	2.76	-0.76	Barring	TP	0.53	0.32	0.14	1	Joint	88	231	J1	2	4	1
					0.45	0.36			Joint	65	323	R	2	4	1
				Average	0.49	0.34	0.14		B/F	57	52	N/A	3	1	1
7.46	3.29	-1.29	Unknown	T	0.61	0.4	0.22	1	Joint	70	62	J1	3	2	1
									Joint	75	243	J2	3	1	1
									Joint	55	322	R	3	1	1
9.95	1.88	0.12	Blast	TP	0.48	0.70	0.14	1	Joint	20	255	J2	2	4	1
									Joint	75	342	J3	2	4	1
									B/F	10	36	N/A	3	1	1
10.9	1.11	0.89	Barring	W	0.21	0.69	0.18	1	Joint	75	358	R	3	1	1
									Joint	25	270	J2	2	4	1
									Joint	67	88	J2	3	1	1
13.40	1.6	0.4	Blast	W	0.16	0.28	0.08	1	Joint	50	328	R	3	1	1
									Joint	69	252	J1	3	1	1
									Joint	85	63	J1	2	4	1
13.82	1.07	0.93	Blast	W	0.54	0.46	0.15	1	Joint	40	98	J2	3	1	1
									Joint	77	190	J3	3	2	1
									B/F	65	275	N/A	3	1	1
14.74	1.15	0.85	Barring	TP	0.43	0.28	0.12	1	Joint	46	356	J3	3	1	1
					0.38	0.22			Joint	55	272	J2	3	2	1
				Average	0.41	0.25	0.12		Joint	79	89	J2	2	4	1
16.25	1.70	0.3	Blast	T	0.52	0.71	0.11	1	Joint	70	348	R	2	4	1
									Joint	45	260	J2	2	4	1
									Joint	66	94	J2	3	1	1
20.20	2.04	-0.04	Barring	W	0.55	0.26	0.19	1	Joint	85	340	R	2	4	1
									Joint	55	93	J2	3	1	1

									Joint	77	261	J2	2	4	1
2.50	3.26	0.04	Unknown	T	0.7	0.28	0.12	1	Joint	60	135	R	3	1	1
									Joint	75	225	J1	3	1	1
									Joint	70	345	J3	3	2	1
4.00	3.96	-0.66	Unknown	TT	0.5	0.36	0.09	1	Joint	85	242	J1	3	1	1
					0.40	0.3			Joint	80	150	R	2	4	1
				Average	0.45	0.33	0.09		Joint	45	333	R	3	1	1
									B/F	12	36	N/A	3	1	1
5.55	3.41	-0.11	Barring	P	1.39	0.43	0.22	2	Joint	85	60	J1	3	2	1
									Joint	65	162	J3	3	2	1
									Joint	75	240	J1	3	1	1
									Joint	85	344	J3	3	1	1
									B/F	12	36	N/A	3	1	1
7.82	4.15	-0.85	Barring	T	1.19	0.35	0.21	1	Joint	75	47	J1	2	4	1
									Joint	89	283	J2	3	1	1
									Joint	45	132	R	3	2	1
									Joint	72	356	J3	3	1	1
7.84	2.65	0.65	Barring	W	0.21	0.67	0.10	1	Joint	65	327	R	3	2	1
									Joint	85	245	J1	3	2	1
									Joint	77	166	J3	3	1	1
									B/F	12	36	N/A	3	1	1
9.4	3.07	0.23	Barring	T	0.55	0.41	0.11	1	Joint	88	165	J3	3	2	1
									Joint	85	228	J1	3	1	1
									Joint	15	155	R	3	1	1
10.90	3.66	-0.36	Barring	T	0.76	0.25	0.22	1	Joint	80	304	J2	3	2	1
									Joint	85	357	J3	3	2	1
									Joint	45	150	R	3	1	1
11.83	3.21	0.09	Unknown	W	0.68	0.27	0.19	1	Joint	40	158	R	3	1	1
									Joint	75	316	R	3	1	1
									Joint	85	355	J3	3	2	1
14.40	3.05	0.25	Barring	W	0.6	0.32	0.11	1	Joint	60	171	J3	3	2	1
									Joint	70	243	J1	3	2	1
									Joint	85	358	J3	3	2	1
0.84	5.98	-1.14	Barring	W	0.49	0.38	0.15	3	Joint	85	233	J1	2	4	1
									Joint	70	136	R	3	2	1

									Joint	20	57	J1	3	1	1
1.60	4.49	-0.18	Barring	TW	0.52	0.39	0.12	3	Joint	75	218	J1	3	2	1
					0.46	0.32			Joint	70	320	R	3	2	1
				Average	0.49	0.355	0.12		Joint	25	42	J1	3	1	1
2.3	6.14	-1.14	Unknown	W	0.44	0.39	0.09	3	Joint	75	213	J1	3	2	1
									Joint	80	125	J2	2	4	1
									Joint	20	52	J1	3	1	1
3.05	5	0.25	Unknown	W	0.59	0.44	0.13	3	Joint	85	142	R	2	4	1
									Joint	85	115	J2	3	2	1
									B/F	15	94	J2	3	1	1
4.23	4.83	0.3	Barring	W	0.53	0.26	0.12	3	Joint	90	185	J3	3	1	1
									Joint	40	134	R	2	4	1
									Joint	80	350	J3	3	1	1
4.55	5.49	-0.41	Barring	TT	0.71	0.42	0.12	3	Joint	30	128	R	3	1	1
									Joint	70	125	J2	3	2	1
									Joint	75	48	J1	2	4	1
7.53	5.81	-0.42	Barring	TP	0.52	0.33	0.09	4	B/F	25	117	J2	3	1	1
									Joint	83	3	J3	3	1	1
									Joint	65	184	J3	3	2	1
									Joint	90	232	J1	3	1	1
7.63	3.68	1.52	Unknown	W	0.69	0.39	0.22	2	Joint	45	131	R	3	1	1
									Joint	85	27	J3	3	1	1
8.13	6.66	-1.45	Unknown	W	0.35	0.22	0.14	3	Joint	25	22	J3	3	2	1
									Joint	55	128	R	3	2	1
									Joint	75	15	J3	3	1	1
8.55	5.43	-0.34	Barring	TT	0.62	0.38	0.13	3	Joint	55	159	J3	3	2	1
									Joint	90	235	J1	3	1	1
									Joint	35	176	J3	3	1	1
10.07	4.24	1.27	Unknown	W	0.54	0.57	0.16	2	Joint	55	36	J1	3	2	1
									Joint	65	291	J2	3	1	1
10.83	4.03	1.46	Blast	W	0.84	0.2	0.11	2	Joint	25	89	J2	3	2	1
									Joint	90	150	R	3	2	1

11.83	4.12	1.36	Unknown	W	1.1	0.56	0.2	3	Joint	32	98	J2	3	2	1
									Joint	68	44	J1	3	1	1
									Joint	70	141	R	3	2	1
13.23	4.25	1.05	Barring	W	0.92	0.26	0.16	3	Joint	10	152	R	2	4	1
									Joint	50	160	J3	2	4	1
									Joint	80	355	J3	3	1	1
13.83	5.8	-0.85	Barring	W	0.81	0.3	0.17	2	Joint	50	122	J2	3	2	1
									Joint	80	344	J3	3	1	1
13.88	5.8	-0.21	Unknown	TW	0.7	0.36	0.19		Joint	70	91	J2	3	1	1
									Joint	70	232	J1	3	1	1
									Joint	62	337	R	3	2	1
14.14	3.73	1.44	Barring	W	0.78	0.24	0.11	3	Joint	72	115	J2	3	1	1
									Joint	80	347	J3	3	1	1
									B/F			N/A	3	1	1
18.83	3.08	2.65	Barring	W	0.29	0.43	0.15	3	Joint	80	28	J3	3	2	1
									Joint	48	138	R	3	2	1
									Joint	55	140	R	3	1	1
21.13	4.59	1.23	Barring	W	0.22	0.28	0.17	2	Joint	80	36	J1	3	1	1
									Joint	80	131	R	3	1	1
									B/F			N/A	3	1	1
21.58	5.51	0.3	Unknown	TP	0.41	0.93	0.14	4	Joint	55	240	J1	3	2	1
									Joint	85	160	J3	3	1	1
									Joint	85	237	J1	3	1	1
									Joint	38	147	R	3	1	1

Appendix C. Friction angle graphs

C.1 UG2 reef - Case Study 1

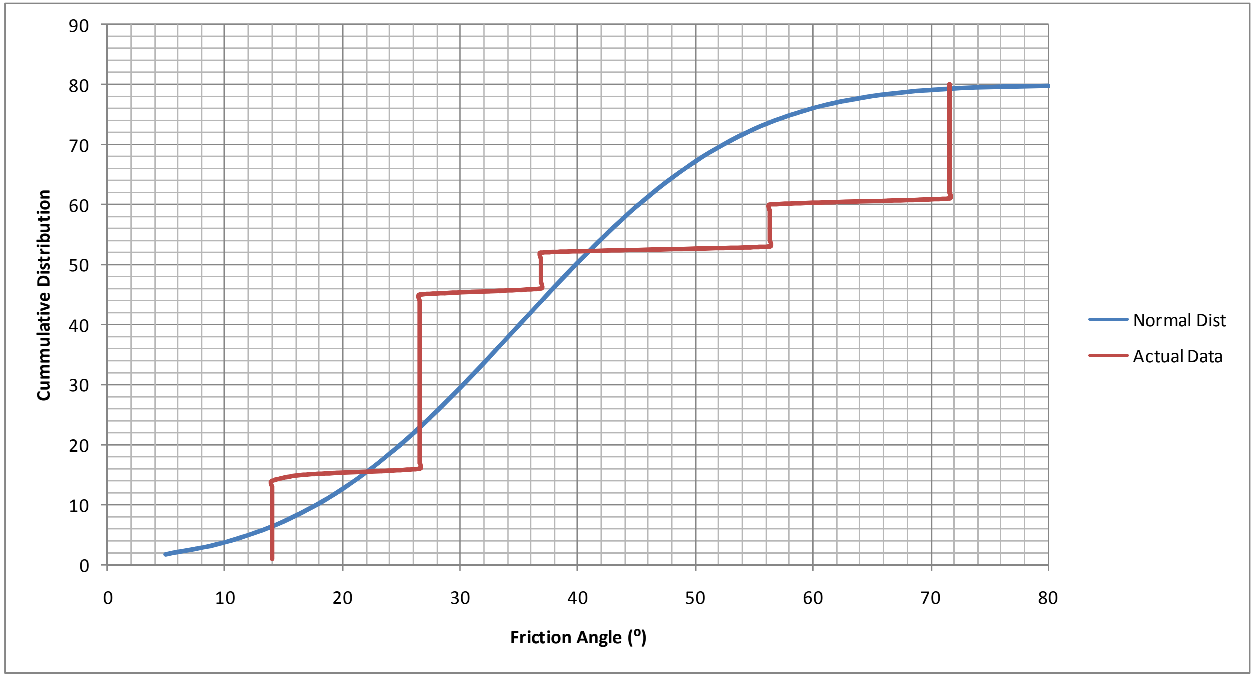

Figure 7-1: UG2 J1 set

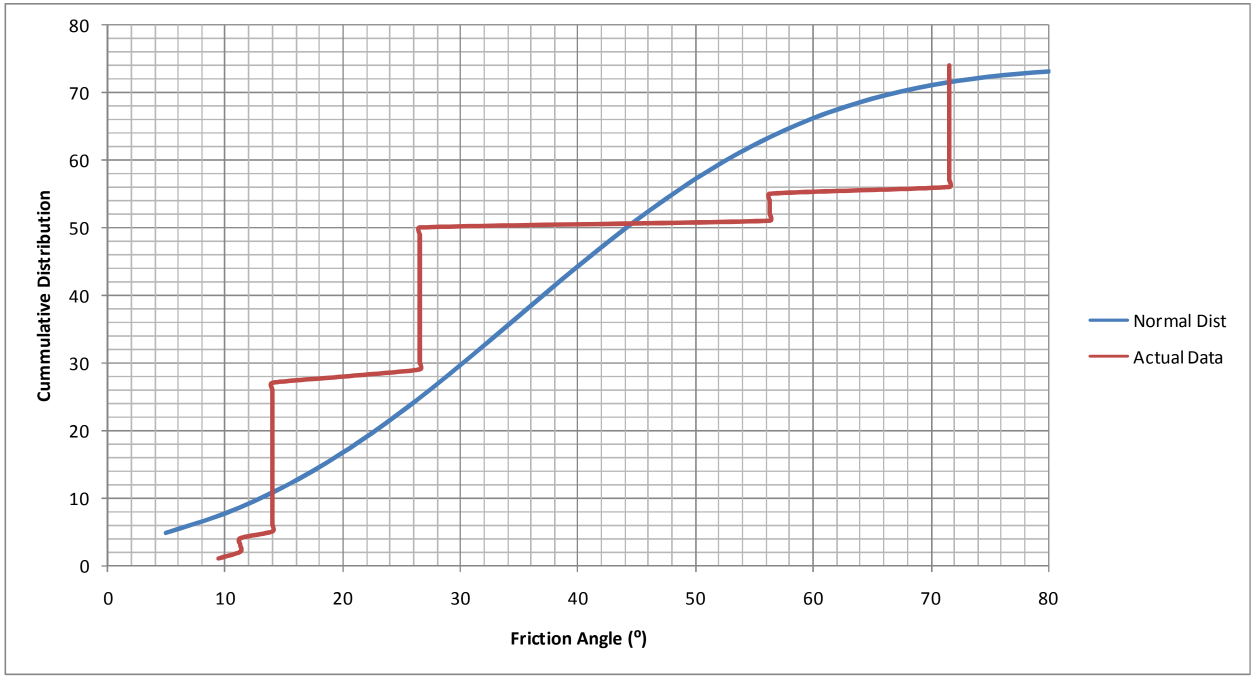

Figure 7-2: UG2 J2 set

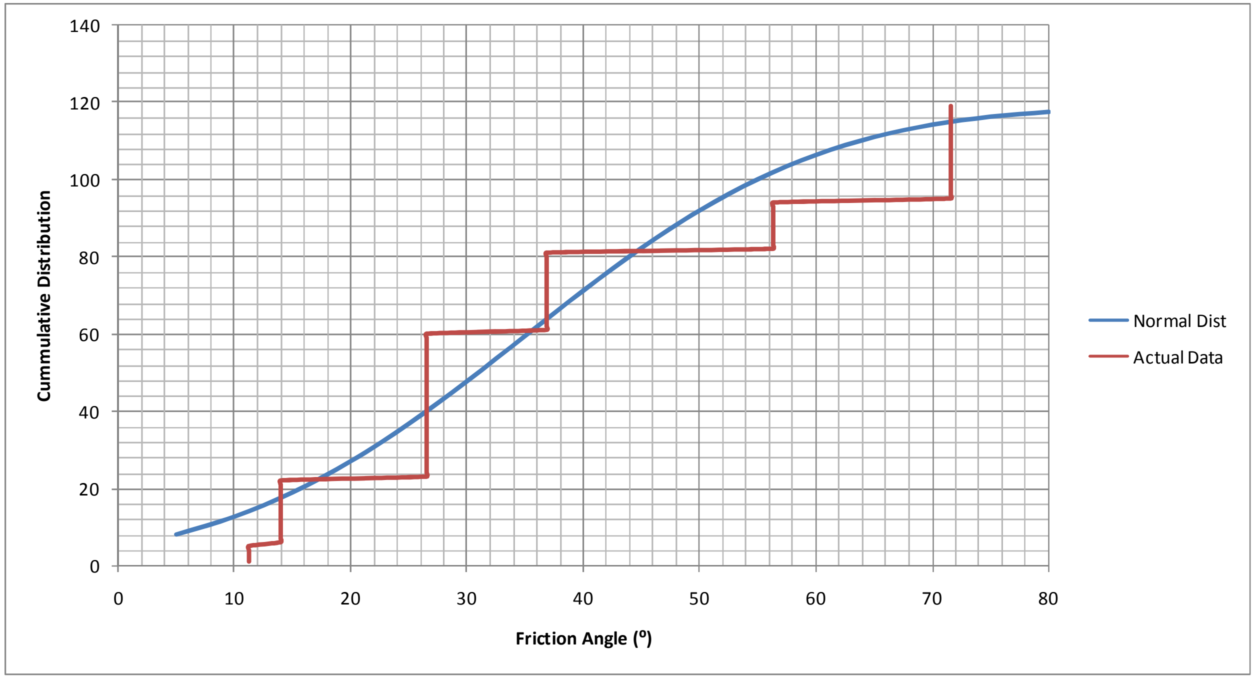

Figure 7-3: UG2 JR set

C.2 Merensky reef - Case Study 2

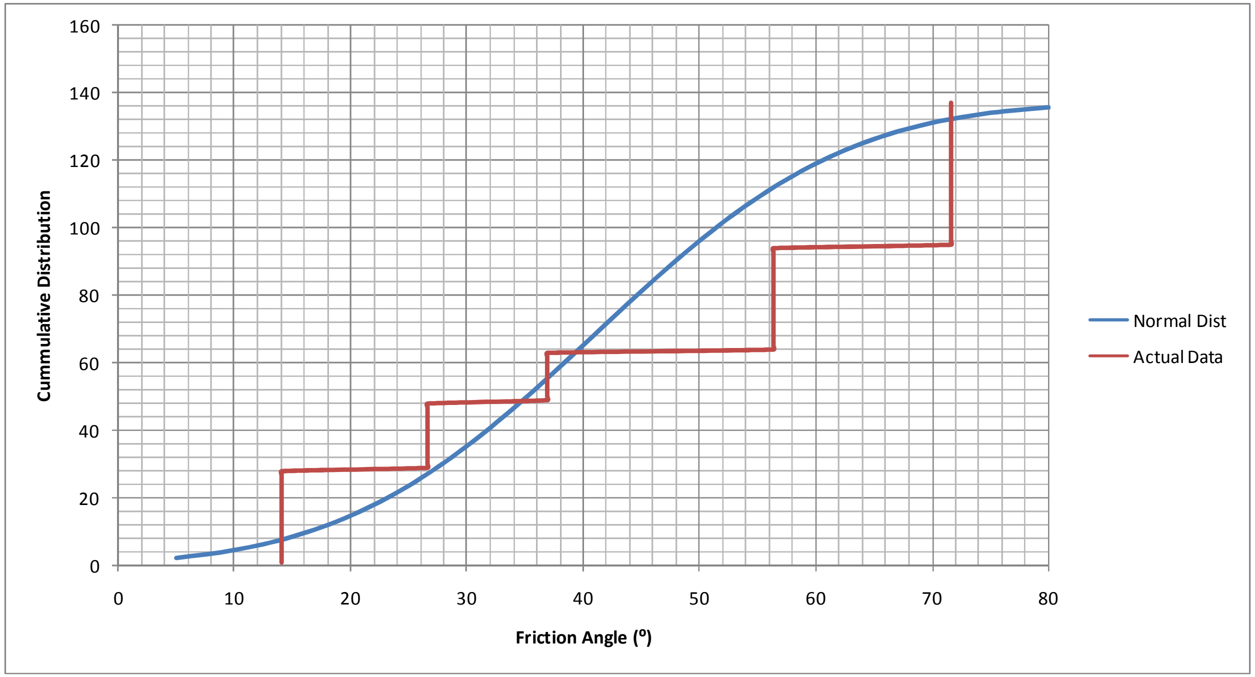

Figure 7-4: Merensky J1 set

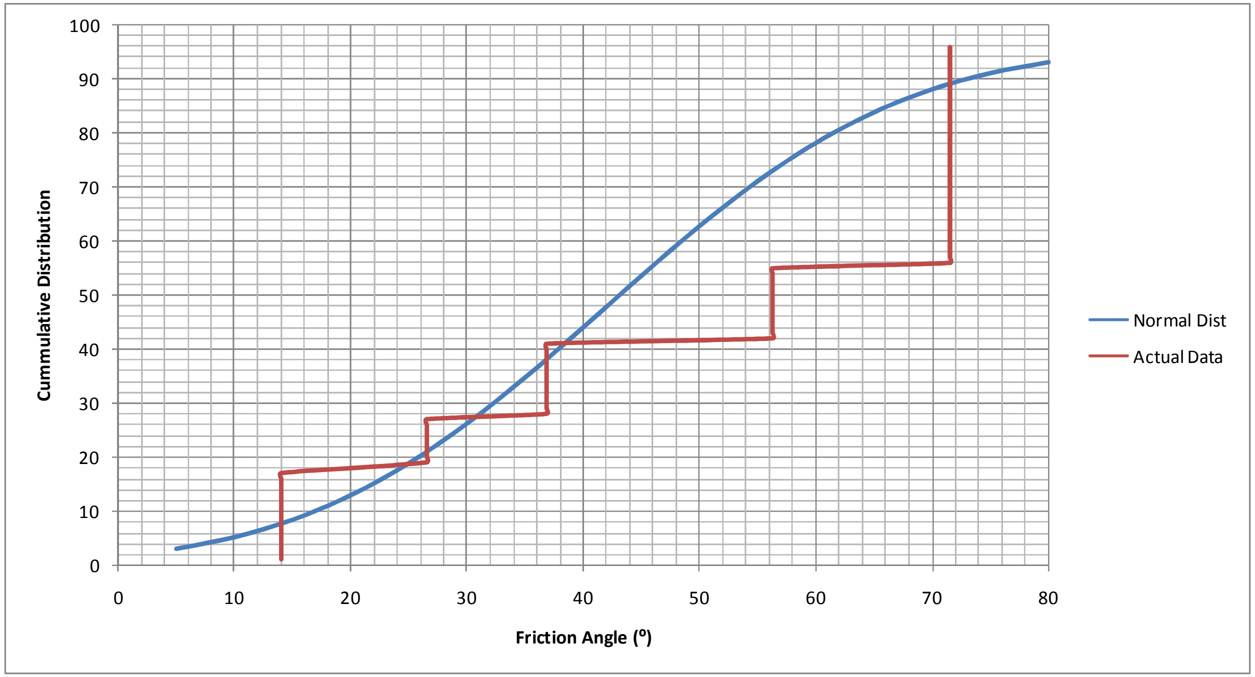

Figure 7-5: Merensky J2 set

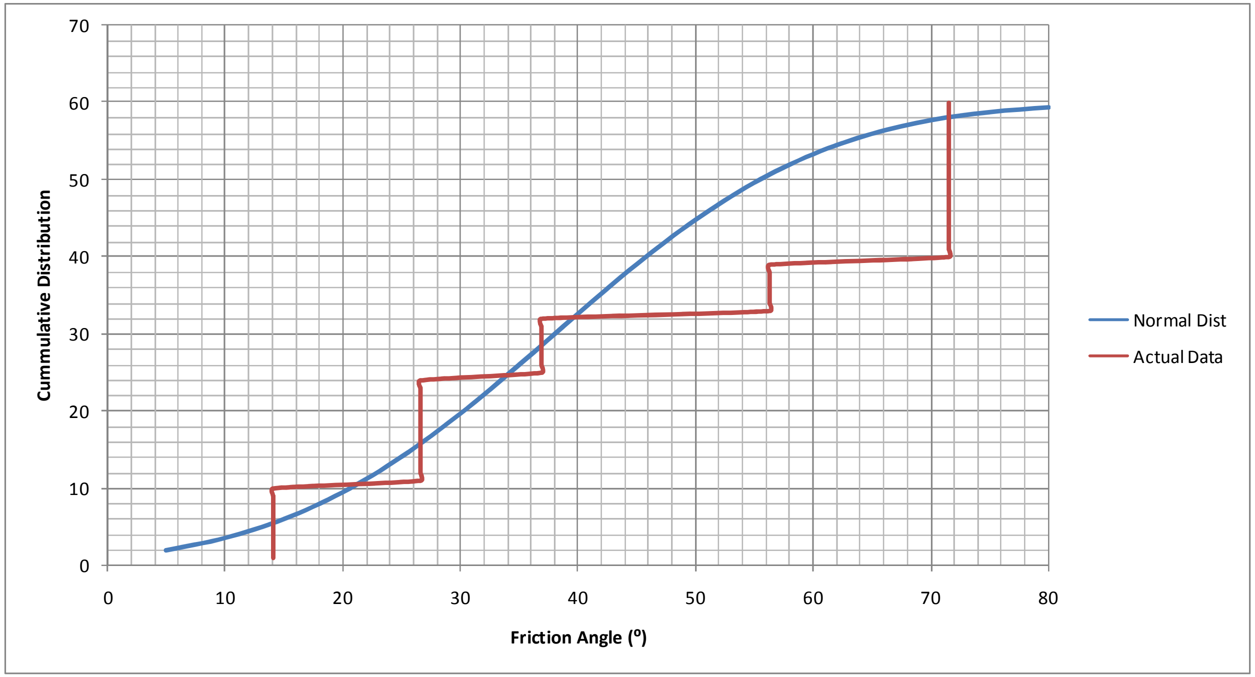

Figure 7-6: Merensky JR

C.3 Merensky reef - Case study 3

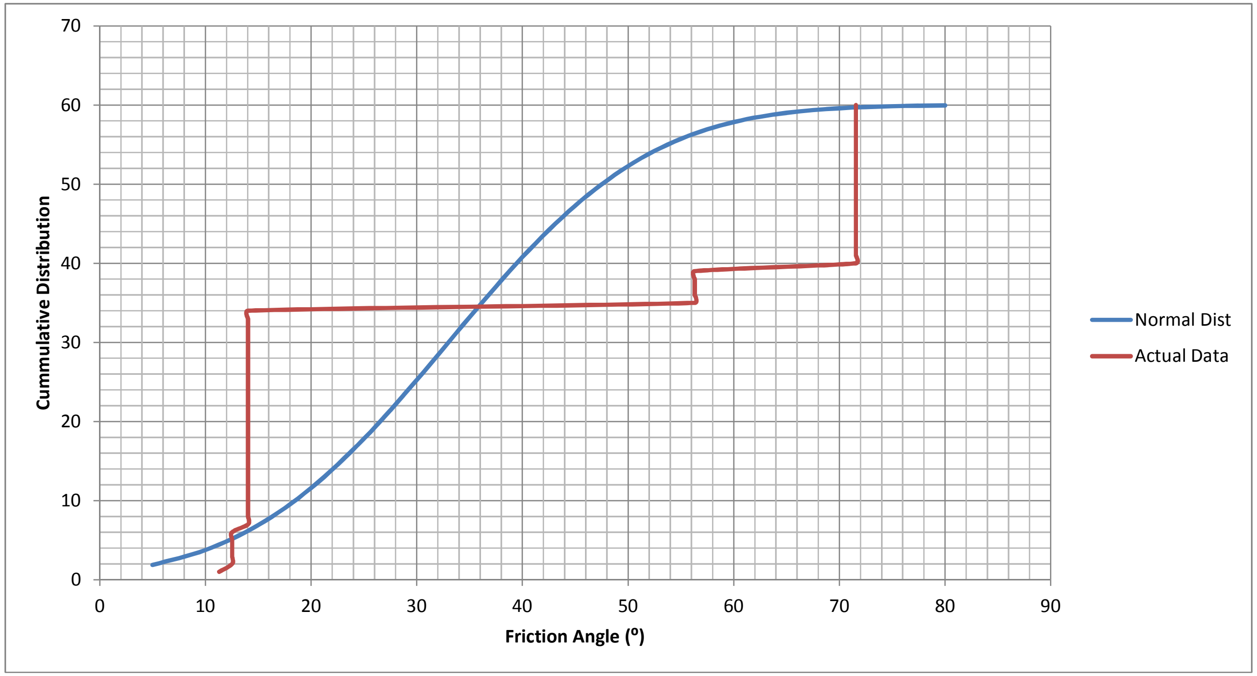

Figure 7-7: Case study 3 J1 set

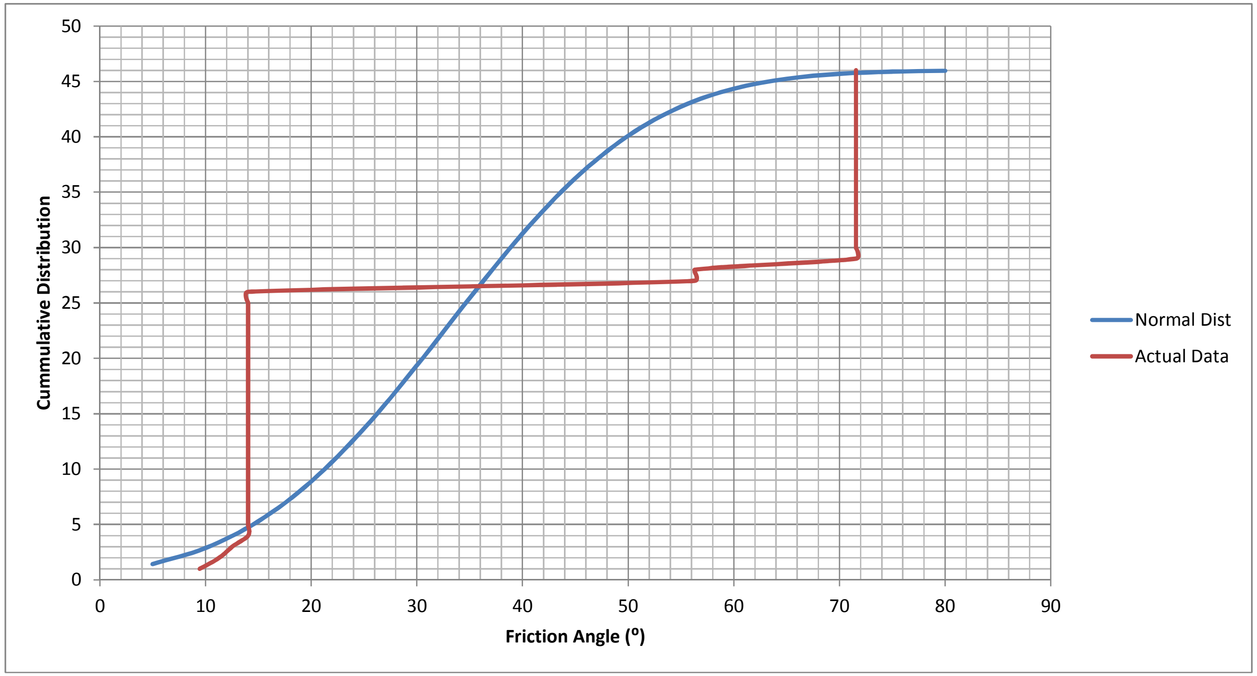

Figure 7-8: Case study3 J2 set

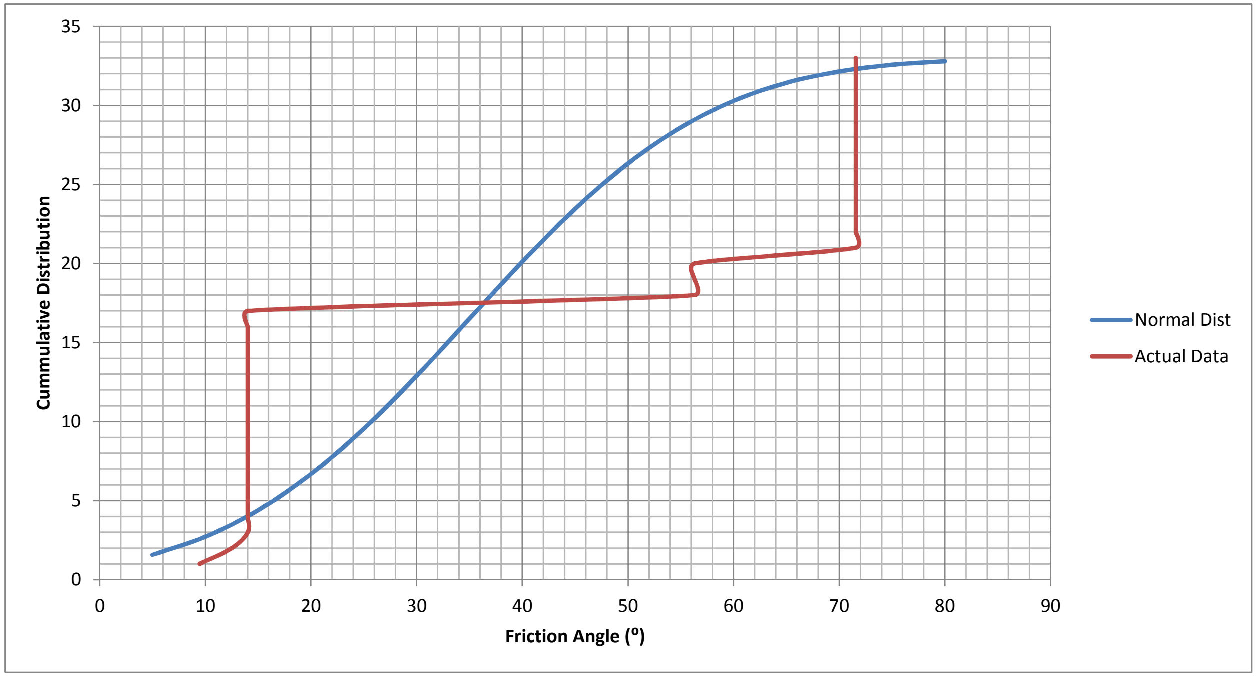

Figure 7-9: Case study 3 J3 set

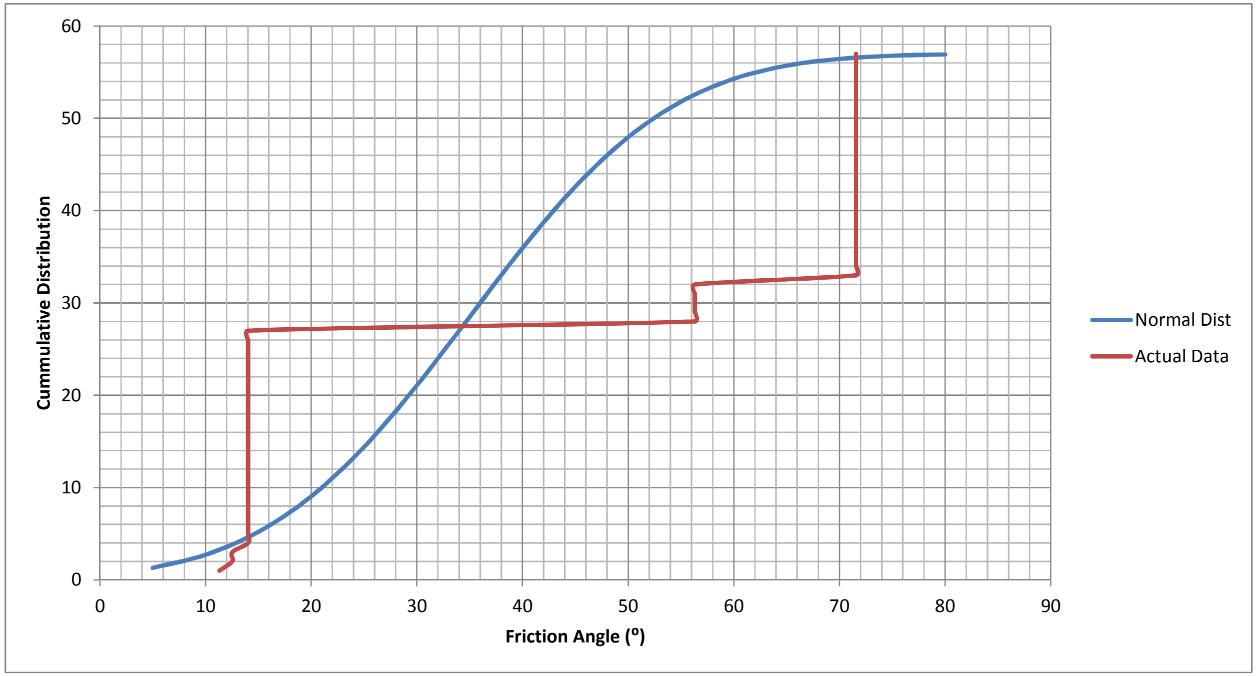

Figure 7-10: Case study 3 J4 set

Appendix D. Parameters for case study 1 (UG2 reef at Mine A)

D.1 JBlock Parameters

D.1.1 Mine Pole Support system

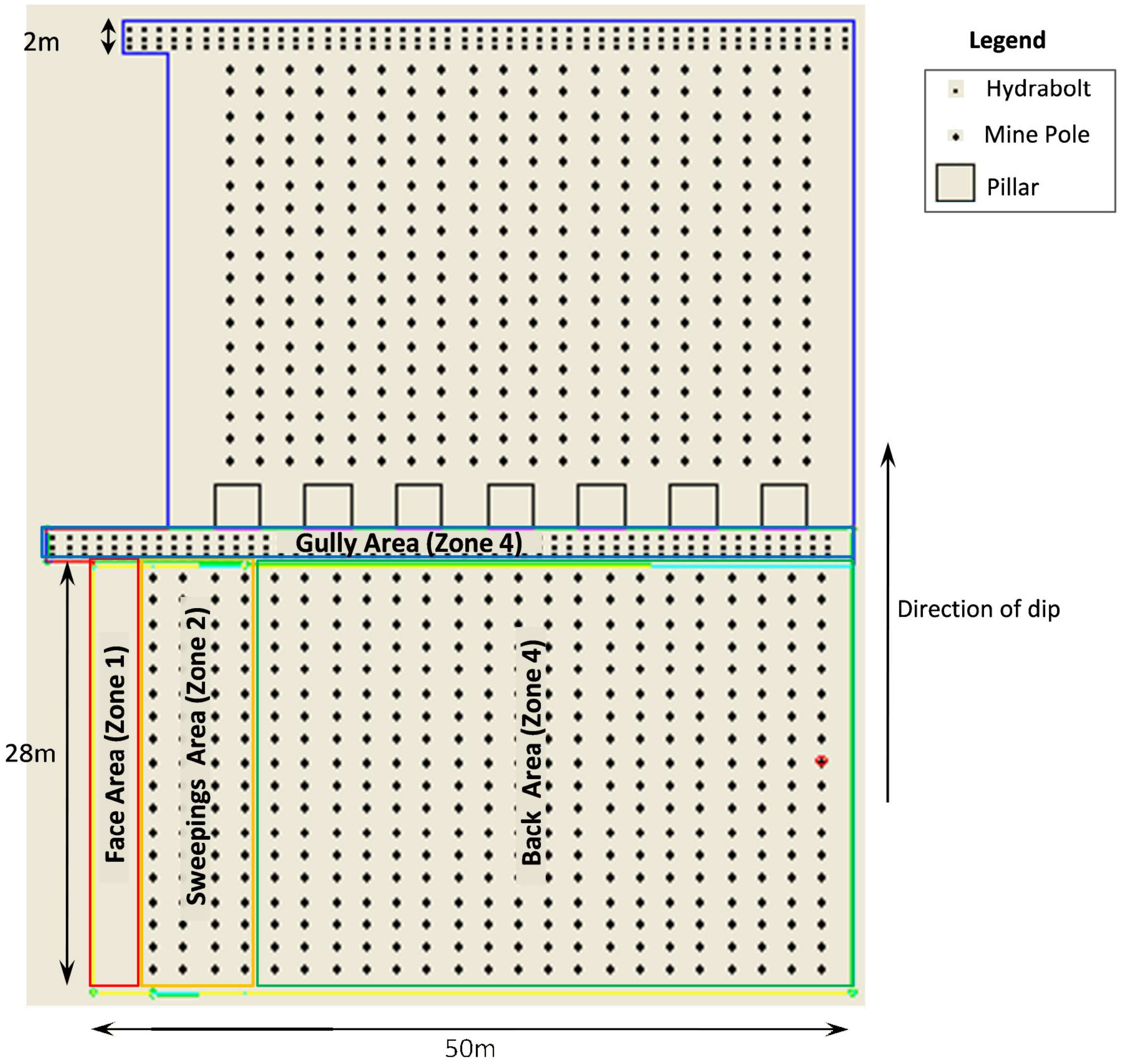

Figure 7-11: JBlock support layout for UG2 reef at mine A

Hydrabolts

Strength: 10t
Grout bond strength: 320kN/m
Length: 1.5 m, 2 m, 2.5 m, 3 m, 3.5 m, 4 m
Spacing (Gully): 0.5 m x 1 m

Mine Poles

Peak Strength: 250kN
Spacing: 1.8 m x 1 m

D.1.2 Mine poles with either 10T 1.2 m, 1.5 m and 1.8 m hydrabolts or 25T 1.5 m and 1.8 m cable bolt support system

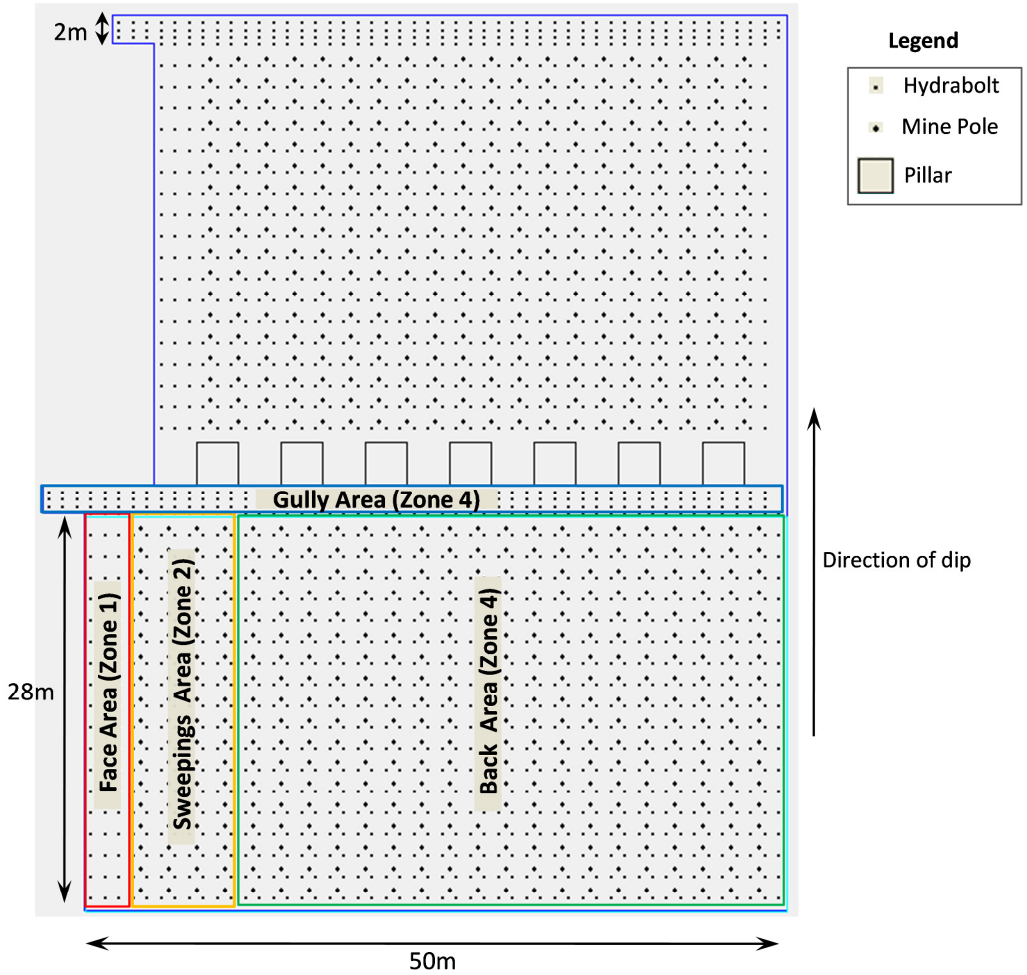

Figure 7-12: JBlock support layout for either 1.2 m, 1.5 m, and 1.8 m Hydrabolts or 1.5 m and 2 m cable anchors used with mine poles for UG2 reef at mine A

Hydrabolts

Strength: 10t
Grout bond strength: 320kN/m
Length: 1.2 m, 1.5 m, 1.8 m
Spacing (Gully): 0.5 m x 1 m
Spacing (Panel): 1.5 m x 1 m

Cablebolts

End anchored
Strength: 25t
Length: 1.5 m, 2 m
Spacing (Gully): 0.5 m x 1 m
Spacing (Panel): 1.5 m x 1 m

Mine Poles

Peak Strength: 250kN
Spacing: 2 m x 1.5 m

D.2 RiskEval Parameters

Maximum aspect ratio =2

Geometry

Face Length = 30 m

Advance per blast = 1 m

Stope height = 1 m

Rockmass

Ore density = 4 t/m^3

Hangingwall density = 3.2 t/m^3

Sweepings density = 2.5 t/m^3 assuming a swell factor of 1.6

Sweepings height = 0.2 m

General

Re-support area factor = 1.5

Sweepings area factor = 1.2

Working days per month = 23

Blast per month = 12

Table 7-1: Support scenario costing for case study 1

Support Scenario	Cost/unit	Spacing	Cost/m2	Total Cost/m2
Mine Poles	R 67.49	2m x 1.5m	R 22	R 22
1.2m Hydrabolt + Mine Poles	R 66.80	1m x 1.5m	R 45	R 67
1.5m Hydrabolt + Mine Poles	R 76.21	1m x 1.5m	R 51	R 73
1.8m Hydrabolt + Mine Poles	R 85.57	1m x 1.5m	R 57	R 80
1.5m Cable Bolt + Mine Poles	R 119.30	1m x 1.5m	R 80	R 102
2.0m Cable Bolt + Mine Poles	R 126.61	1m x 1.5m	R 84	R 107
Mine Pole + Safety Net	R 67.49	2m x 1.5m	R 22	R 22

Table 7-2: Worker cartegory exposure in different zones

			Exposure Hrs per day				Exposure	
Category	Shift	No of	Zone 1	Zone 2	Zone 3	Zone 4	Blast	Barring
Stope Driller	Day	3	4.0	1.5	0.5	0.0	0.65	0.9
Gully Driller	Day	1	0.0	1.5	4.5	0.0	0.65	0.9
Stope Timber	Day	2	2.0	2.5	1.5	0.0	0.65	0.9
Winch Driver	Day	2	2.0	2.0	2.0	0.0	0.65	0.9
Team leader	Day	1	4.0	1.0	1.0	0.0	0.65	0.4
Winch Driver	Night	2	2.0	2.0	2.0	0.0	0.65	0.2
Team leader	Night	1	3.0	2.0	1.0	0.0	0.65	0.1

Table 7-3: Revenue Calculation for UG2 reef at Mine A

Merensky reef grade		3.49g/t
1 oz = 31.10348 g		
Grade Distribution		
Platinum	47.9%	
Palladium	25.8%	
Rhodium	25.6%	
Gold	0.6%	
Long Term Price $/oz		
Platinum		1400
Palladium		450
Rhodium		1400
Gold		900
Long exchange rate $1 = R 7.80		
Recovery		85%
Mining Grade Loss		75%
Mine Call Factor		97%
Revenue/t		$ 79.83
		R 622.66
Total Cost/t ore		R 670.00
Variable Costs = 30% of total cost/t		
Dilution = 20% of total cost/t		
Variable Cost/t		R 201.00
Dilution Cost/t		R 134.00
Production Loss		**R 421.66**
Sweepings Loss		**R 488.66**

Injury ratio:

LTI = 0.55

Serious = 0.43

Fatalities = 0.02

Section 54:

Days Lost = 5

Nummber of panels affected = 100

Consultant and legal fees = R 3 000 000

Days Lost:

LTI = 7 days

Serious = 28 days

Fatality = 6 000 days

SIMRAC Levy = R 3.14/day lost

Medical Costs:

Per Injury = R 10 018

Per Fatality = R1 465

Wages and Compensation:

Per Injury = R 7 527

Per Fatality = R 26 583

Rehabilitation:

Pillar width = 3 m

Pillar safety distance = 1 m

Re-establish gully width = 6 m

Re-establish raise width = 2 m

Raise advance = 2 m per blast

Gully advance = 2 m per blast

Spare panel = 0

Blasting efficiency = 0.7

Appendix E. Parameters for case study 2 (Merensky reef at mine A)

E.1 JBlock Parameters

E.1.1 Mine poles with either 10T 1.2 m,1.5 m, 1.8 m Hydrabolts or 25T 1.5 m and 2 m cable bolts

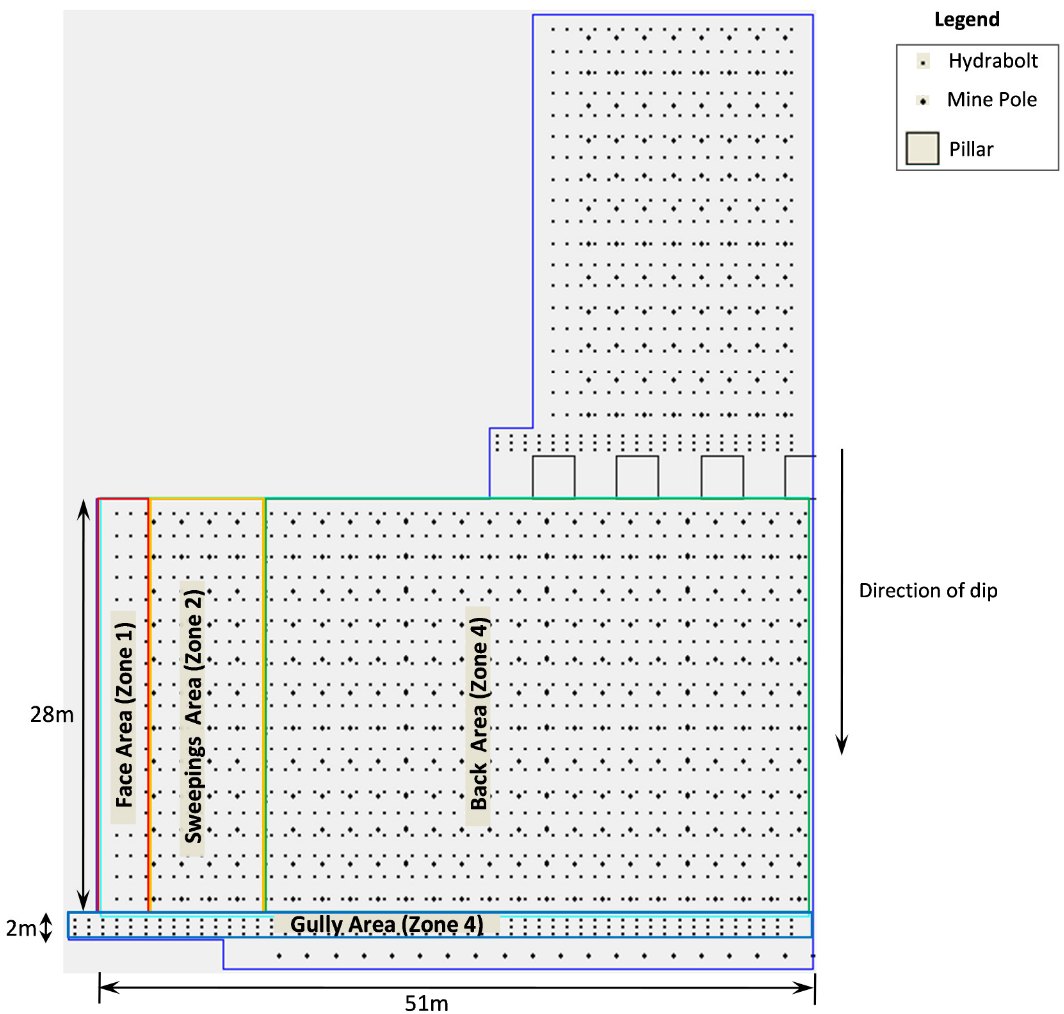

Figure 7-13: JBlock support layout for either 1.2 m, 1.5 m, and 1.8 m Hydrabolts or 1.5 m and 2 m cable anchors used with mine poles forMerensky reef at mine A

Hydrabolts

Strength: 10t
Grout bond strength: 320kN/m
Length: 1.2 m, 1.5 m, 1.8 m
Spacing (Gully): 0.5 m x 1 m
Spacing (Panel): 1.5 m x 1 m

Cablebolts

End anchored
Strength: 25t
Length: 1.5 m, 2 m
Spacing (Gully): 0.5 m x 1 m
Spacing (Panel): 1.5 m x 1 m

Mine Poles

Peak Strength: 250kN
Spacing: 2 m x 2.4 m

E.2 RiskEval Parameters

Maximum aspect ratio =2

Geometry

Face Length = 30 m

Advance per blast = 1 m

Stope height = 1.2 m

Rockmass

Ore density = 3.2 t/m^3

Hangingwall density = 3.2 t/m^3

Sweepings density = 2 t/m^3 assuming a swell factor of 1.6

Sweepings height = 0.2 m

General

Re-support area factor = 1.5

Sweepings area factor = 1.2

Working days per month = 23

Blast per month = 12

Table 7-4: Support scenario costing for case study 2

Support Scenario	Cost/unit	Spacing	Cost/m^2	Total cost/m^2
Mine Poles	R 67.49	2m x 2.4m	**R 14**	R 14
1.2m Hydrabolt + Mine Poles	R 66.80	1m x 1.5m	**R 45**	**R 59**
1.5m Hydrabolt + Mine Poles	R 76.21	1m x 1.5m	**R 51**	**R 65**
1.8m Hydrabolt + Mine Poles	R 85.57	1m x 1.5m	**R 57**	**R 71**
1.5m Cable Bolt + Mine Poles	R 119.30	1m x 1.5m	**R 80**	**R 94**
2.0m Cable Bolt + Mine Poles	R 126.61	1m x 1.5m	**R 84**	**R 98**
1.2m Hydrabolt + Mine Poles + Safety Net	R 66.80	1m x 1.5m	**R 45**	**R 59**

Table 7-5: Worker cartegory exposure in different zones

			Exposure Hrs per day				Exposure	
Category	Shift	No of	Zone 1	Zone 2	Zone 3	Zone 4	Blast	Barring
Stope Driller	Day	3	4.0	1.5	0.5	0.0	0.65	0.9
Gully Driller	Day	1	0.0	1.5	4.5	0.0	0.65	0.9
Stope Timber	Day	2	2.0	2.5	1.5	0.0	0.65	0.9
Winch Driver	Day	2	2.0	2.0	2.0	0.0	0.65	0.9
Team leader	Day	1	4.0	1.0	1.0	0.0	0.65	0.4
Winch Driver	Night	2	2.0	2.0	2.0	0.0	0.65	0.2
Team leader	Night	1	3.0	2.0	1.0	0.0	0.65	0.1

Table 7-6: Revenue Calculation for case study 2

Merensky reef grade		3.92g/t
1 oz = 31.10348 g		
Grade Distribution		
Platinum	56.7%	
Palladium	24.9%	
Rhodium	14.8%	
Gold	3.6%	
Long Term Price $/oz		
Platinum		1400
Palladium		450
Rhodium		1400
Gold		900
Long exchange rate $1 = R 7.80		
Recovery		85%
Mining Grade Loss		75%
Mine Call Factor		97%
Revenue/t		$ 89.27
		R 696.31
Total Cost/t ore		R 670.00
Variable Costs = 30% of total cost/t		
Dilution = 20% of total cost/t		
Variable Cost/t		R 201.00
Dilution Cost/t		R 134.00
Production Loss		**R 495.31**
Sweepings Loss		**R 562.31**

Injury ratio:

LTI = 0.55

Serious = 0.43

Fatalities = 0.02

Section 54:

Days Lost = 5

Nummber of panels affected = 100

Consultant and legal fees = R 3 000 000

Days Lost:

LTI = 7 days

Serious = 28 days

Fatality = 6 000 days

SIMRAC Levy = R 3.14/day lost

Medical Costs:

Per Injury = R 10 018

Per Fatality = R1 465

Wages and Compensation:

Per Injury = R 7 527

Per Fatality = R 26 583

Rehabilitation:

Pillar width = 3 m

Pillar safety distance = 1 m

Re-establish gully width = 6 m

Re-establish raise width = 2 m

Raise advance = 2 m per blast

Gully advance = 2 m per blast

Spare panel = 0

Blasting efficiency = 0.7

Appendix F. Parameters for case study 3 (Merensky reef at mine B)

F.1 JBlock Parameters

F.1.1 :25T Cable anchor only support system

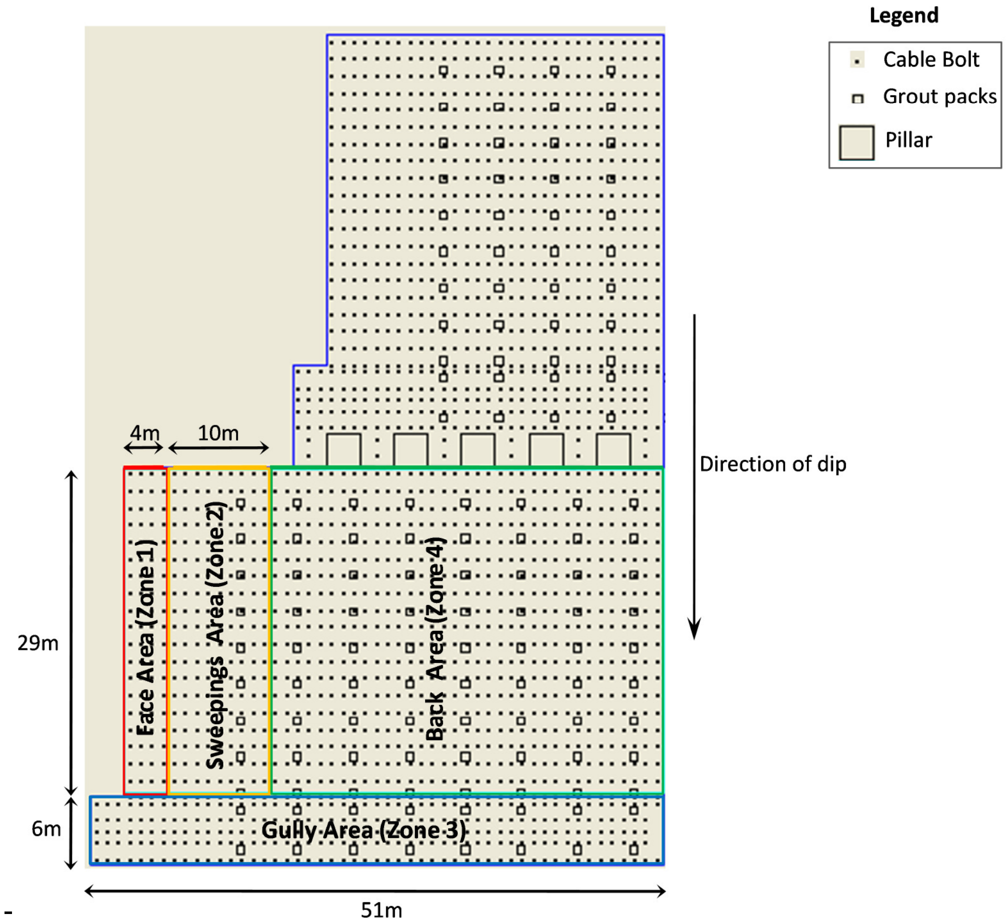

Figure 7-14: JBlock support layout for 25T 1.5 m, 2 m, 2.5 m, 3 m, 3.5 m and 4 m cable anchors

Cable Bolts

End anchored
Strength: 25t
Length: 1.5 m, 2 m, 2.5 m, 3 m, 3.5 m, 4 m
Spacing (Gully): 1 m x 1 m
Spacing (Panel): 1 m x 1.5 m

Grout Packs

Peak strength: 2 500kN
Width: 0.66m
Length: 0.66m
Spacing: 5 m x 3.2 m

F.1.2 :12T cable anchor and mine pole support system

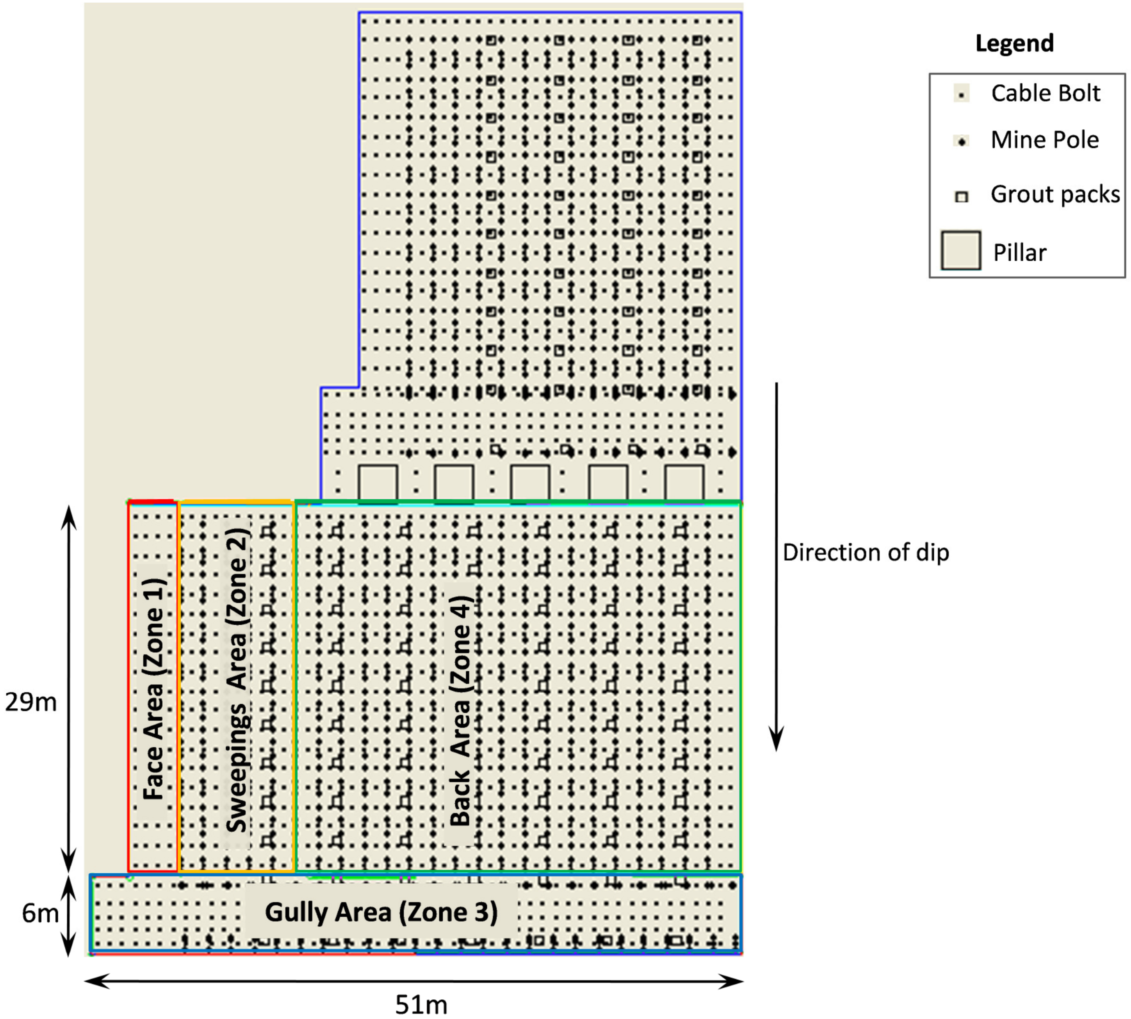

Figure 7-15: JBlock support layout for 12T 1.5m cable anchors and mine poles support layout

Cable Bolts

End anchored
Strength: 12t
Length: 1.5 m, 2 m, 2.5 m, 3 m, 3.5 m, 4 m
Spacing (Gully): 0.9 m x 1 m
Spacing (Panel): 0.9 m x 1.5 m

Mine Poles

Peak Strength: 250kN
Spacing: 1.8 m x 1 m

Grout Packs

Peak strength: 2 500kN
Width: 0.66m
Length: 0.66m
Spacing: 5.4 m x 3 m

F.2 RiskEval Parameters

Maximum aspect ratio =2

Geometry

Face Length = 30 m

Advance per blast = 1 m

Stope height = 1.2 m

Rockmass

Ore density = 3.2 t/m^3

Hangingwall density = 3.2 t/m^3

Sweepings density = 2 t/m^3 assuming a swell factor of 1.6

Sweepings height = 0.2 m

General

Re-support area factor = 1.5

Sweepings area factor = 1.2

Working days per month = 23

Blast per month = 12

Table 7-7: Support scenario costing for mine B

Support Scenario	Cable Anchors			Timber			Total
	Cost /unit	Spacing	Cost/m^2	Cost /unit	Spacing	Cost/ m^2	Cost/m^2
1.5m(25T)	R 119.30	1m x 1.5m	R 80	-	-	-	R 80
2.0m(25T)	R 126.61	1m x 1.5m	R 84	-	-	-	R 84
2.5m(25T)	R 133.93	1m x 1.5m	R 89	-	-	-	R 89
3.0m(25T)	R 141.25	1m x 1.5m	R 94	-	-	-	R 94
3.5m(25T)	R 148.56	1m x 1.5m	R 99	-	-	-	R 99
4.0m(25T)	R 155.88	1m x 1.5m	R 104	-	-	-	R 104
1.5m(12T) + Mine Poles	R 114.50	0.9m x 1.5m	R 85	R 65.00	1m x 1.8m	R 36	R 121

Table 7-8: Worker cartegory exposure in different zones

			Exposure Hrs per day				Exposure	
Category	Shift	No of	Zone 1	Zone 2	Zone 3	Zone 4	Blast	Barring
Stope Driller	Day	3	4.0	1.5	0.5	0.0	0.65	0.9
Gully Driller	Day	1	0.0	1.5	4.5	0.0	0.65	0.9
Stope Timber	Day	2	2.0	2.5	1.5	0.0	0.65	0.9
Winch Driver	Day	2	2.0	2.0	2.0	0.0	0.65	0.9
Team leader	Day	1	4.0	1.0	1.0	0.0	0.65	0.4
Winch Driver	Night	2	2.0	2.0	2.0	0.0	0.65	0.2
Team leader	Night	1	3.0	2.0	1.0	0.0	0.65	0.1

Table 7-9: Revenue calculation for mine B

Merensky reef grade		5.5g/t
1 oz = 31.10348 g		
Grade Distribution		
Platinum	63%	
Palladium	25%	
Rhodium	10%	
Gold	2%	
Long Term Price $/oz		
Platinum		1400
Palladium		450
Rhodium		1400
Gold		900
Long exchange rate $1 = R 7.80		
Recovery		85%
Mining Grade Loss		75%
Mine Call Factor		97%
Revenue/t		$ 126.02
		R 982.97
Total Cost/t ore		R 670.00
Variable Costs = 30% of total cost/t		
Dilution = 20% of total cost/t		
Variable Cost/t		R 201.00
Dilution Cost/t		R 134.00
Production Loss		**R 781.97**
Sweepings Loss		**R 848.97**

Injury ratio:

LTI = 0.55

Serious = 0.43

Fatalities = 0.02

Section 54:

Days Lost = 5

Nummber of panels affected = 100

Consultant and legal fees = R 3 000 000

Days Lost:

LTI = 7 days

Serious = 28 days

Fatality = 6 000 days

SIMRAC Levy = R 3.14/day lost

Medical Costs:

Per Injury = R 10 018

Per Fatality = R1 465

Wages and Compensation:

Per Injury = R 7 527

Per Fatality = R 26 583

Rehabilitation:

Pillar width = 3 m

Pillar safety distance = 1 m

Re-establish gully width = 6 m

Re-establish raise width = 2 m

Raise advance = 2 m per blast

Gully advance = 2 m per blast

Spare panel = 0

Blasting efficiency = 0.7